CIVIL & ENVIRONMENTAL ENGINEERING

RESEARCH REPORT

Development and Validation of Deterioration Models for Concrete Bridge Decks

Phase 2: Mechanics-based Degradation Models

by

Nan Hu

Syed W. Haider

Rigoberto Burgueño

Report No. CEE-RR – 2013/02

June 2013

Research Report for MDOT under Contract No. 2009-0746/Z2
SPR No. 107451

Department of Civil and Environmental Engineering
Michigan State University
East Lansing, Michigan

Technical Report Documentation Page

1. Report No.	2. Government Accession No.	3. MDOT Project Manager
RC-1587b	N/A	Peter Jansson

4. Title and Subtitle	5. Report Date
DEVELOPMENT AND VALIDATION OF DETERIORATION MODELS FOR CONCRETE BRIDGE DECKS – Phase 2: Mechanics-based Degradation Models	6/11/2013
	6. Performing Organization Code N/A
7. Author(s) Nan Hu, Syed W. Haider and Rigoberto Burgueño	**8. Performing Org. Report No.** N/A
9. Performing Organization Name and Address Michigan State University 3546 Engineering Building East Lansing, MI 48824-1226	**10. Work Unit No. (TRAIS)** N/A
	11. Contract No. 2009-0746
	11(a). Authorization No. Z2
12. Sponsoring Agency Name and Address Michigan Department of Transportation Research Administration 8885 Ricks Rd. P.O. Box 30049 Lansing MI 48909	**13. Type of Report & Period Covered** Final Report 10/20/2009 – 9/30/2012
	14. Sponsoring Agency Code N/A

15. Supplementary Notes

16. Abstract

This report summarizes a research project aimed at developing degradation models for bridge decks in the state of Michigan based on durability mechanics. A probabilistic framework to implement local-level mechanistic-based models for predicting the chloride-induced corrosion of the RC deck was developed. The methodology is a two-level strategy: a three-phase corrosion process was modeled at a local (unit cell) level to predict the time of surface cracking while a Monte Carlo simulation (MCS) approach was implemented on a representative number of cells to predict global (bridge deck) level degradation by estimating cumulative damage of a complete deck. The predicted damage severity and extent over the deck domain was mapped to the structural condition rating scale prescribed by the National Bridge Inventory (NBI). The influence of multiple effects was investigated by implementing a carbonation induced corrosion deterministic model. By utilizing realistic and site-specific model inputs, the statistics-based framework is capable of estimating the service states of RC decks for comparison with field data at the project level. Predicted results showed that different surface cracking time can be identified by the local deterministic model due to the variation of material and environmental properties based on probability distributions. Bridges from different regions in Michigan were used to validate the prediction model and the results show a good match between observed and predicted bridge condition ratings. A parametric study was carried out to calibrate the influence of key material properties and environmental parameters on service life prediction and facilitate use of the model. A computer program with a user-friendly interface was developed for degradation modeling due to chloride induced corrosion.

17. Key Words	18. Distribution Statement
Bridge deck; Chloride; corrosion; Predictions; Structural reliability; Monte Carlo method; NBI Rating.	No restrictions. This document is available to the public through the Michigan Department of Transportation.

19. Security Classification - report	20. Security Classification - page	21. No. of Pages	22. Price
Unclassified	Unclassified	131	N/A

Report No. CEE-RR – 2013/02

DEVELOPMENT AND VALIDATION OF DETERIORATION MODELS FOR CONCRETE BRIDGE DECKS

PHASE 2: MECHANICS-BASED DEGRADATION MODELS

by

Nan Hu
Graduate Research Assistant

Syed Waqar Haider, Ph.D., P.E.
Assistant Professor

Rigoberto Burgueño, Ph.D.
Associate Professor of Structural Engineering

Research Report to Michigan DOT under Contract No. 2009-0746/Z2
SPR No. 107451

Department of Civil and Environmental Engineering
Michigan State University
East Lansing, MI 48824-1226

June 2013

DISCLAIMER

The opinions, findings, conclusions and recommendations presented in this report are those of the authors alone and do not necessarily represent the views and opinions of Michigan State University or the Michigan Department of Transportation.

ABSTRACT

The deterioration of reinforced concrete bridge decks is one of the major concerns for highway agencies and accurate prediction of their deterioration process and assessment of their remaining service life is essential for the effective management and preservation of bridge infrastructure. This report presents the second phase of a research project aimed at developing degradation mechanisms for bridge decks in the state of Michigan. The research focus was to develop and validate degradation models based on durability mechanics. A probabilistic framework to implement local-level mechanistic-based models for predicting the chloride-induced corrosion of the RC deck was developed. The methodology is a two-level strategy: a three-phase corrosion process was modeled at a local (unit cell) level to predict the time of surface cracking while a Monte Carlo simulation (MCS) approach was implemented on a representative number of cells to predict global (bridge deck) level degradation by estimating cumulative damage of a complete deck. The predicted damage severity and extent over the deck domain was mapped to the structural condition rating scale prescribed by the National Bridge Inventory (NBI). The influence of multiple effects was investigated by implementing a carbonation induced corrosion deterministic model. The carbonation degradation process was assumed to be decoupled from chloride induced corrosion such that the controlling effect to the initiation of corrosion would dictate the initiation period, with the propagation and crack to surface periods being modeled equally. By utilizing realistic and site-specific model inputs, the statistics-based framework is capable to estimate the service states of the RC deck and compare with field data at the project level. Predicted results showed that different surface cracking time can be identified by the local deterministic model due to the variation of material and environmental properties based on probability distributions. Bridges from different regions in Michigan were used to validate the prediction model and the results show a good match between observed and predicted bridge condition ratings. A parametric study was carried out to calibrate the influence of key material properties and environmental parameters on service life prediction and facilitate use of the model. A computer program with a user-friendly interface was developed for degradation modeling due to chloride induced corrosion. The program can be used to evaluate the performance of Michigan highway bridges or generic new designs.

ACKNOWLEDGMENTS

The research described in this report was carried out under funding from the Michigan Department of Transportation, Contract 2009-0746/Z2, SPR No. 107451, with Mr. Peter Jansson as project manager. The financial support of MDOT and the coordination of Mr. Jansson throughout the execution of the experimental program are gratefully acknowledged.

The authors also thankfully acknowledge the assistance of Dr. Ioannis Balafas from the University of Cyprus and Prof. Chris Burgoyne from the University of Cambridge who shared their work and experience on the deterministic model for chloride-induced corrosion.

TABLE OF CONTENTS

LIST OF FIGURES

LIST OF TABLES

1 INTRODUCTION

1.1 Background and Motivation

The deterioration of reinforced concrete (RC) bridge decks has been investigated considerably over the past few decades as concerns with their performance has increasingly become a major infrastructure maintenance issue since the 1970s (Russell 2004). The general approach for infrastructure maintenance can be summarized in three aspects: deterioration model, cost model, and decision models (Estes and Frangopol 2001, Frangopol et al. 2004). This report deals with deterioration modeling. The approaches to degradation modeling of reinforced concrete elements may be grouped in five categories: statistical models, probabilistic models, soft-computing models (e.g., artificial neural networks, support vector machines, etc.), numerical methods, and mechanics-based methods. Clearly, several sub-classifications can be made in each of the noted categories. Of the noted methods, statistical, probabilistic, and soft-computing methods rely on the use of data to infer relationships and predict behavior. For modeling the deterioration of infrastructure the data has typically been that from visual inspections and evaluating the fundamental mechanisms behind the degradation process is not possible. A variety of options is available to simulate degradation through numerical simulations; however, the models tend to be complex and are generally difficult to modify for multiple structures or generalize for a network. Mechanics-based models, both theory-based and experiment-based (or phenomenological) model degradation based on the fundamental physico-chemical processes by using basic material properties and a diverse set of mechanics, thermodynamics and chemical models. Purely analytical models have been proposed but most mechanics-based models are calibrated (to different degrees) with laboratory-scale experiments. Mechanics-based models offer the best way to simulate and understand the degradation process based on fundamental material properties and thermo-mechano-chemical processes. However, the models can be quite complex, typically relying on numerical solutions, and models for combined degradation effects (e.g., corrosion together with freeze-thaw effect) are very limited. No withstanding these limitations, mechanics-based models are the best way to not only model degradation of infrastructure elements but to also understand the fundamental environmental, material and design parameters that affect the degradation process.

The degradation of reinforced concrete decks is complex since it has many sources. A classification of the different damage bridge decks and its source in is presented in Table 1 (TRB, 2006). It can be seen that at any given time the damage that may be observed in a bridge deck may be caused by multiple simultaneous factors.

Table 1. The classification of crack types, its factors and time (TRB 2006)

Type of Cracking	Form of Crack	Primary Cause	Time of Appearance
Plastic settlement	Over and aligned with reinforcement, subsidence under reinforcing bars	Poor mixture design leading to excessive bleeding, excessive vibrations	10 min to 3 h
Plastic shrinkage	Diagonal or random	Excessive early evaporation	30 min to 6 h
Thermal expansion and contraction	Transverse	Excessive heat generation, excessive temperature gradients	1 day to 2–3 weeks
Drying shrinkage	Transverse, pattern or map cracking	Excessive mixture water, inefficient joints, large joint spacings	Weeks to months
Freezing and thawing	Parallel to the surface of concrete	Lack of proper air-void system, non durable coarse aggregate	After one or more winters
Corrosion of reinforcement	Over reinforcement	Inadequate cover, ingress of sufficient chloride	More than 2 years
Alkali–aggregate reaction	Pattern and longitudinal cracks parallel to the least restrained side	Reactive aggregate plus alkali hydroxides plus moisture	Typically more than 5 years, but weeks with a highly reactive material
Sulfate attack	Pattern	Internal or external sulfates promoting the formation of ettringite	1 to 5 years

Common crack types that appear before and after hardening are shown in Figure 1. While early age cracking can be controlled through the improvement in concrete mixture design, material placement and curing; the issue of deck deterioration in the medium- to long-term is associated with cracks after concrete hardening. However, it is impossible and impractical to discuss the influence of all these factors on surface cracking.

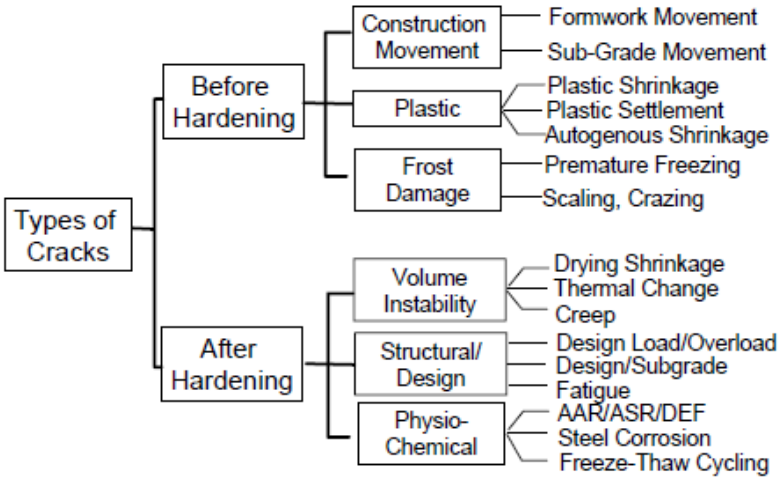

Figure 1: Common causes for cracking in concrete structures (TRB 2006)

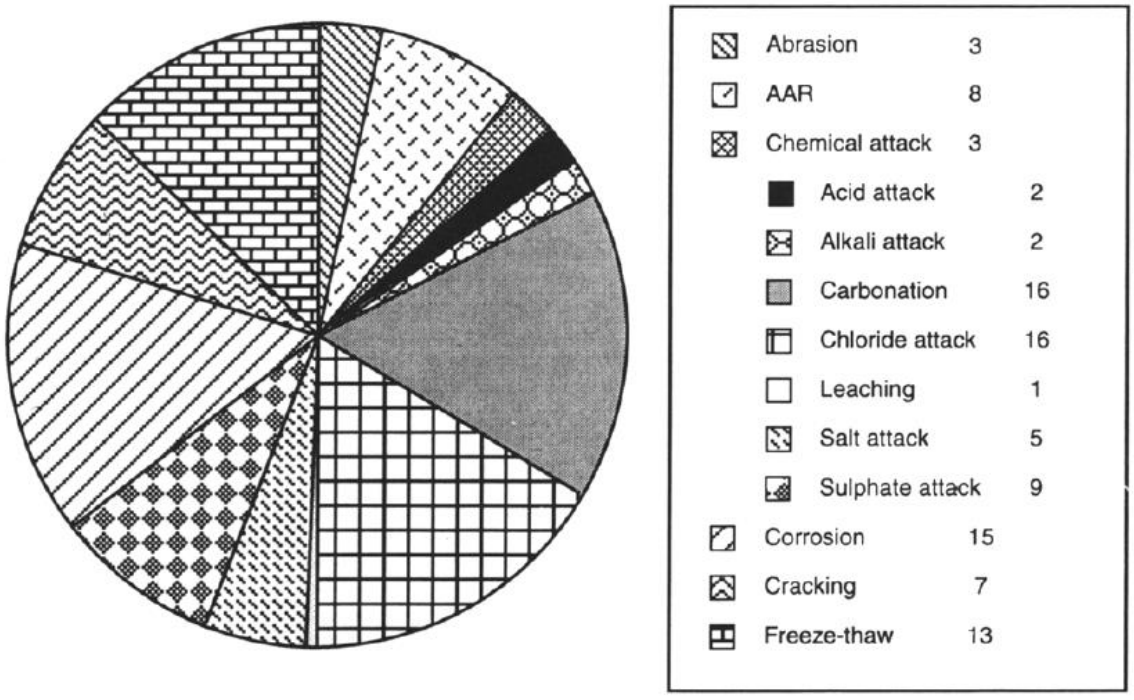

Figure 2: Various mechanisms affecting the durability of concrete (Basheer et al. 1996)

Basheer et al. (1996) reviewed of more than 400 published documents on the deterioration of concrete and categorized the deterioration mechanism in concrete after hardening into physical and chemical processes. The study concluded that the three most important environmental factors affecting RC deck deterioration are chloride induced corrosion, carbonation and freeze-

thaw. The first two mechanisms are due to a chemical-mechanical coupling process while third one is due to a physical-mechanical process. The most reported cause of deterioration is attributed to corrosion of the reinforcing bar due to chloride ingress from deicing salts or sea water. It is well known that cracking and/or scaling will propagate to the deck surface because of the reinforcing bar corrosion process.

In spite of the well-known fact that several degradation mechanisms act simultaneously, consideration of multiple effects is difficult and studies of coupled degradation effects is considerably limited. A recent example is the study by Bastidas-Arteaga, et al. (2009) who considered the coupled effect of corrosion-fatigue on RC structures.

The focus of this report is on the development of a framework to implement a mechanics-based model for predicting the life-time degradation of bridge decks due to chloride-induced corrosion. Two other mechanicsms were also considered, namely, carbonation-induced corrosion and freeze-thaw effects. However, studies on these two factors were less comprehensive. The objective was to obtain an appropriate deterioration model that can offer a prediction of the service condition of reinforced concrete bridge decks based on the simulation of the fundamental degradation process.

There are two major ways to model concrete damage from environmental effects. One way is to model the corrosion process at a local level or characteristic reinforced prism. This follows from the typical experimental methods on small-scale samples used to calibrate analytical and phenomenological models. Detailed literature review on this approach is presented in Chapter 2. However, a reinforced prism cannot represent the real condition of a bridge deck. The second approach to simulate degradation is based on reliability and probability analyses of service life prediction. Several contributions have been made on this type of modeling approach by Enright and Frangopol (1998), Steward and Rosowsky (1998), Vu and Steward (2000), Steward and Mullard (2007) and Marsh and Frangopol (2008). However, most of the noted works involved the assessment of ultimate limit states of elements, such as structural strength resistance, flexural failure, etc. There are also a number of investigations (Lounis and Amleh 2003, Lounis and Daigle 2008) that have focused on service limit states, such as cracking, spalling, etc., but these mechanistic models are too simple for describing the complicated concrete deterioration process. While several commercial programs for concrete service life prediction have recently emerged,

careful examination of their underlying theory (see Chapter 2) shows the need for improvement in the service-life deterioration modeling of concrete elements. Degradation modeling of large structures based on mechanistic considerations is thus an ongoing area of research with still many gaps to be overcome.

1.2 Proposed Framework

This research project combined previous works on the deterioration of concrete decks to develop a probabilistic-based framework for practical application of mechanics-based deterioration models. A similar work by Firouzi and Rahai (2011) investigated the likelihood of degradation due to chloride ingress by random sampling on a hypothetical deck but they did not validate the prediction with actual decks. The methodology in this research project is a two-level strategy, as shown in Figure 3.

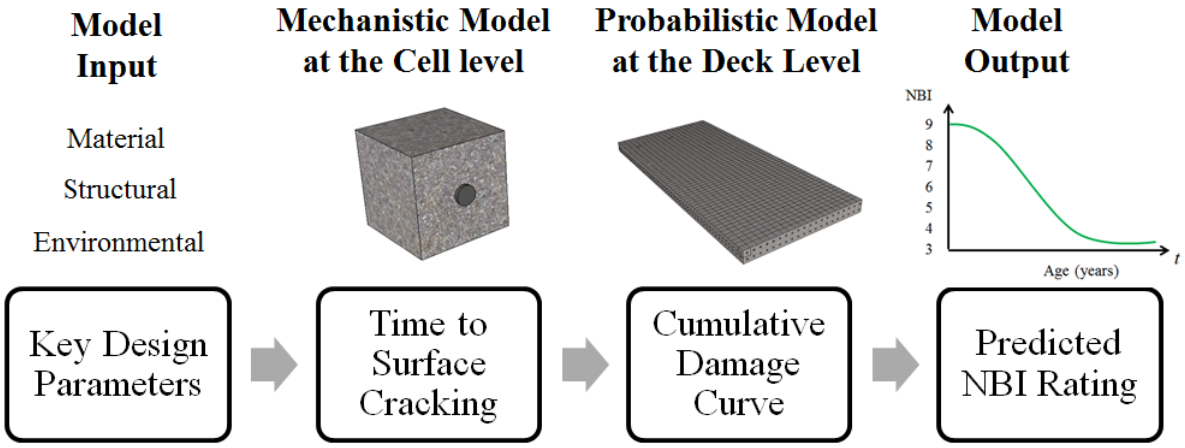

Figure 3: Proposed framework for deck deterioration modeling

The framework of deck deterioration modeling is as follows:

1. Random values of the parameters of interest (such as chloride concentration at the concrete surface, concrete compressive strength, diffusion coefficient of concrete, threshold value for chloride concentration at the steel level, corrosion rate, concrete cover depth, etc.) are generated and assigned to different cells, so that these values will form sets of parameter combinations.

2. At a local level (unit cell), the corrosion process was modeled by employing mechanistic models that can predict the time for reinforcement bar corrosion to manifest in surface cracking. To overcome the limitations of current methods and commercial programs for concrete service-life prediction, existing models from different aspects of the degradation process were selected to provide a relatively accurate prediction. The selected models were chosen to have the following desired features: (1) consider multi-mechanisms; (2) use a more sophisticated model for corrosion process; and (3) take uncertainty of key parameters into account. Each parameter combination is adopted for the deterministic local-level analysis and the major results (such as time to surface cracking and crack width over time at the concrete surface) is obtained and recorded.
3. At the global level (bridge deck), a probabilistic approach is implemented on a representative number of cells from the deck domain. To account for the uncertainty of environmental conditions and material properties, statistical analyses, namely, Monte Carlo simulations (MCS) are adopted into the prediction of concrete service life. Properties at the local/cell level are varied based on probability distributions. The predicted results of the cell-level deterministic analysis are collected for the entire bridge deck and a cumulative damage index (CDI) curve of the deck is calculated based on the predicted time to surface cracking from all the unit cells. A CDI bound is then calculated by taking into account different input data combinations, as shown in Figure 4(a).
4. Final major step in this proposed framework is to the damage severity of the deck is mapped to the National Bridge Inventory (NBI) rating, a conventional bridge rating system used by highway agencies, as shown in Figure 4(b). The overall condition of the bridge deck will be determined based on the results of the sub-analyses. Therefore, the CDI bound is mapped into an NBI rating bound. The MCS provides a worst scenario and best scenario in the CDI curve and corresponding NBI rating curve. Finally, a mean value curve is obtained for the CDI curve and NBI rating curve.

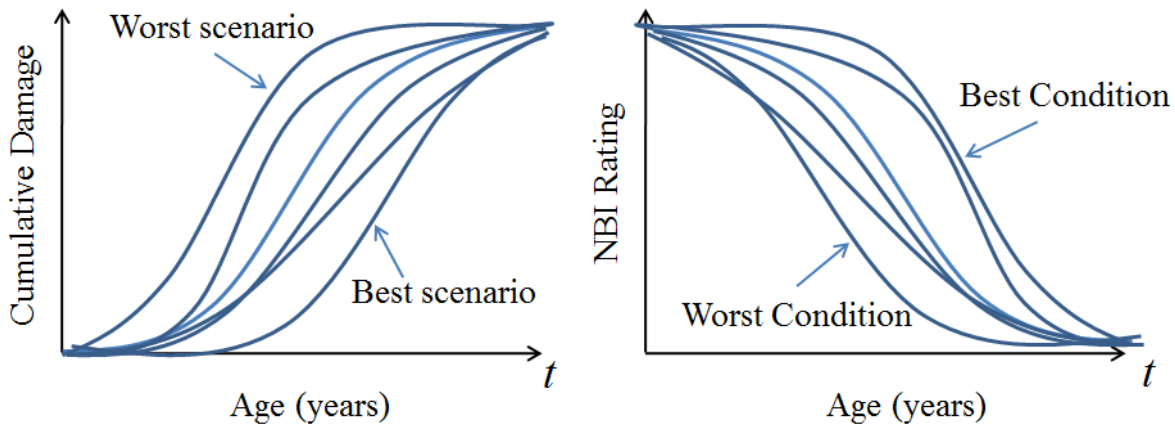

Figure 4 Expected prediction results through the Monte Carlo Simulation

The core of Monte Carlo simulation is based on numerous sub-analyses and the accuracy of the results clearly depends on the number of analyses. Thus, it can be predicted that the primary limitation of the proposed approach is the computational demand. It is essential to determine the minimum number of analyses needed for a reliable result. On the other hand, the sophistication level of the model adopted for each mechanism will also be limited by computational demand in order to be feasible. The advantage of Monte Carlo simulations is that it allows the prediction of the most possible behavior of the structure while taking into account for the uncertainty of the input parameters. If only the extreme scenarios are evaluated, the prediction will be provided as a wide band between the extreme scenarios, which is much less informative.

1.3 Report Organization

This report is organized to highlight the results of the proposed statistical-based framework for predicting the degradation of reinforced concrete decks in Michigan highway bridges. A literature review is presented in Chapter 2 to outline the state-of-the-art on service-life prediction in reinforced concrete decks due to chloride corrosion, carbonation and freeze-thaw. Based on a summary of the shortcomings of analytical solutions and currently available commercial software, Chapter 3 documents a three-phase corrosion process assembled from existing mechanistic models that can predict the time for reinforcement bar corrosion to manifest in surface cracking. Chapter 4 discusses the implementation of the Monte Carlo simulation (MCS) approach as well as the

prediction results of the MCS. Chapter 5 presents a series of validations of the proposed mechanistic-based framework, both at the project level, and at the network level. A parametric study is also presented to investigate the influence of key parameters on deck degradation. Further, a series of reference charts documenting the effect of different parameters on deck deterioration were established for quick consultation. Chapter 6 presents and discusses deck deterioration due to multiple mechanisms. Finally, a summary, conclusions and recommendations are given in Chapter 7.

2 LITERATURE REVIEW

2.1 Chloride-induced Corrosion

2.1.1 Analytical Models

Corrosion of metals in aqueous environments develops via electrochemical mechanisms that includes an exchange of electrons. The process of corrosion in metals can be described by the following two half-cell reactions:

$$Fe \rightarrow Fe^{2+} + 2e^{-} \text{ (Anodic reaction)} \quad (2\text{-}1)$$

$$O_2 + 2H_2O + 4e^{-} \rightarrow 4OH^{-} \text{ (Catholic reaction)} \quad (2\text{-}2)$$

Chloride-induced corrosion of reinforcement bars in concrete is a serious problem due to two reasons: i) corrosion will lead to reduction of the effective area of a reinforcing bar and the corresponding flexural strength of the concrete element; ii) the concrete surrounding a corroding bar is subjected to internal pressure that may cause cracking and spalling, since the volume of the corrosion products is higher than the volume of the initial steel. The main reactions that generate corrosion products are shown in the following:

$$Fe^{2+} + 2OH^{-} \rightarrow Fe(OH)_2 \quad (2\text{-}3)$$

$$4Fe(OH)_2 + 2H_2O + O_2 \rightarrow 4Fe(OH)_3 \quad (2\text{-}4)$$

$$2Fe(OH)_3 \rightarrow 2H_2O + Fe_2O_3 \cdot H_2O \quad (2\text{-}5)$$

The entire corrosion process is typically divided into different phases. Tutti's two-stage model, namely initiation period and propagation period is a widely-accepted definition approach for corrosion modeling. Generally, the initiation period is much longer than the propagation period. Ervin (2007) reported that the prediction from several models showed that, on average, the initiation period is six and a half times longer than the propagation period. That is why in some prediction models a constant value is given to the propagation period. However, research has shown that propagation can also take a very long time. Therefore, several approaches have considered a detailed definition of the service life phase (Suwito and Xi 2008, Li et al. 2008), as shown in Figure 5 and Figure 6.

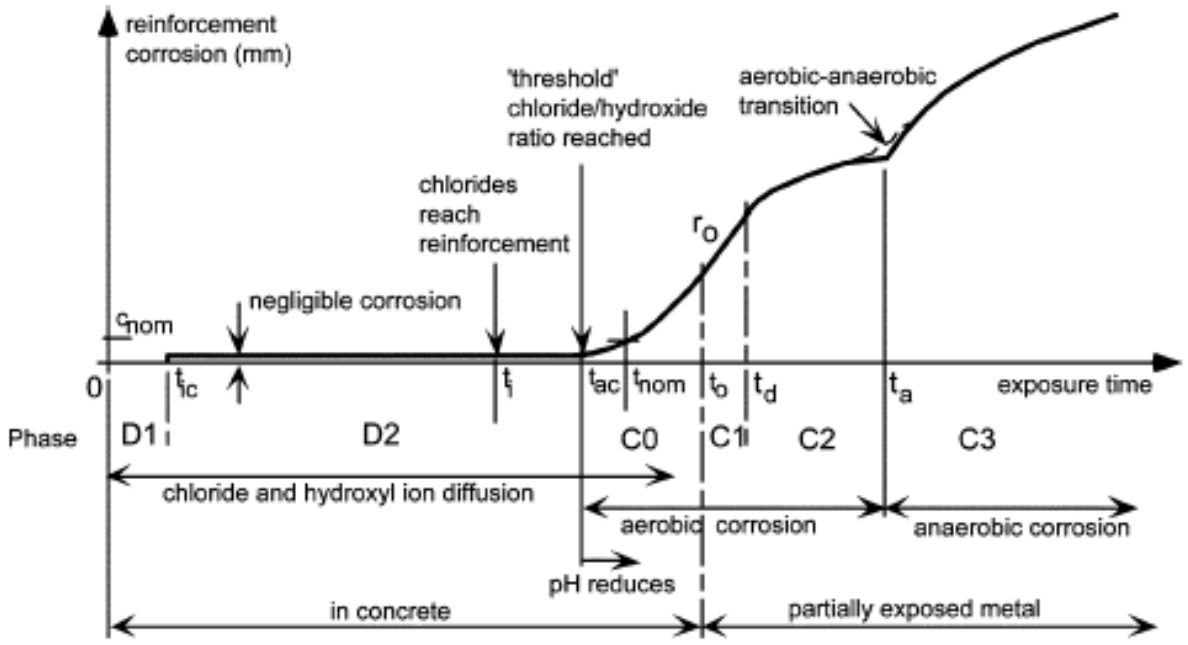

Figure 5 Phenomenological modeling for steel corrosion in concrete (Li et al 2008)

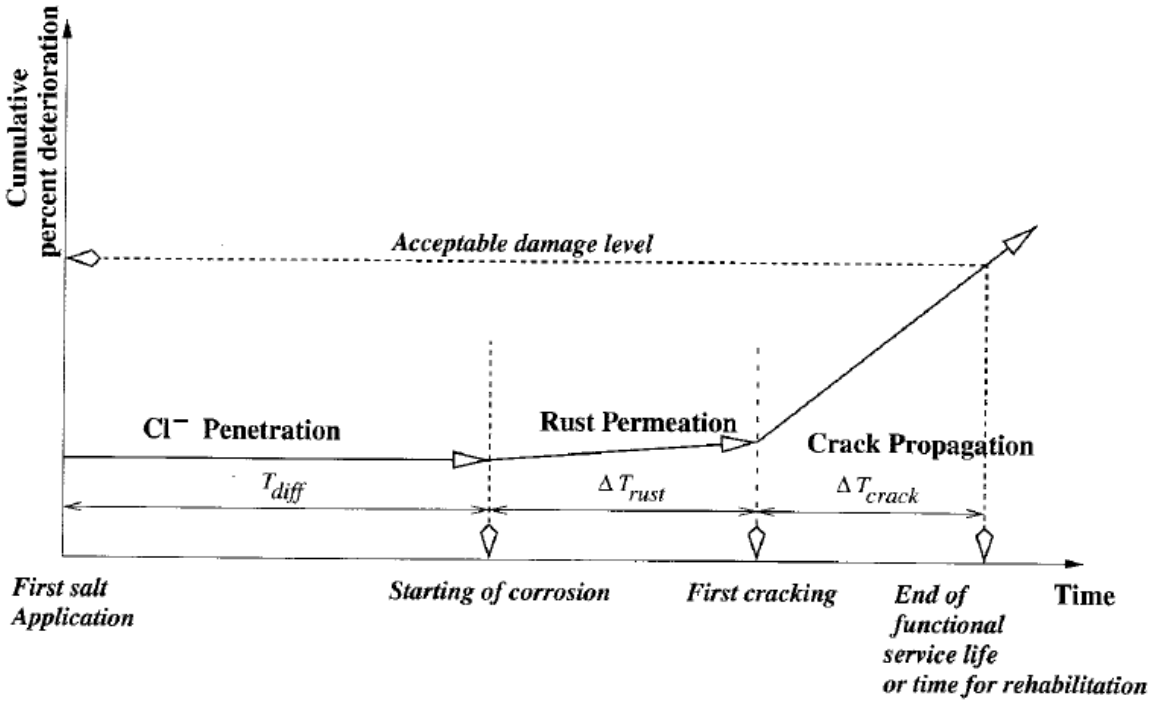

Figure 6 Periods in the service life of RC structures (Suwito and Xi 2008)

In this project a three-phrase corrosion process that includes diffusion, rust accumulation and crack propagation was identified and implemented. There is a vast amount of literature on the modeling of these three periods. A review is presented here in order to compare different models and justify the suitable selection of modeling approaches for this project.

2.1.1.1 Diffusion Process

In the first period, the diffusion process, Fick's second law, which is a rather simple approach, is still the most computationally convenient way to determine the time to corrosion initiation, even though there is extensive evidence on the complexity of the process of chloride ion penetration into concrete. In principle, Fick's second law is only a linear approximation to the process of chloride ingress. In some sense, the real nonlinear behavior on a bridge deck can be regarded as perturbations from this linear model. Therefore, while Fick's second law cannot provide the complete answer it can capture the central part for the theory (Poulsen and Mejlbro 2006). To improve Fick's second law, Mangat and Molloy (1994) pointed out that the diffusion coefficient is dependent on time (decrease with time) and proposed an empirical model between the diffusion coefficient and the exposure time. Basheer et al. (1996) also present the same model for chloride concentration, which is derived from the principle of mass conservation but ignoring the evaporable water. Boddy et al. (1999) consider the multi-mechanism effect on chloride transfer and present models for each effect, but there was no experimental data to verify the proposed model. Que (2007) summarized and compared several available diffusion models. Suwito and Xi (2008) presented a couple processes between the chloride and moisture diffusion. Marchand and Samson (2009) discussed the limitations of determine the transfer of chloride ions into concrete with Fick's second law and pointed out that the assumptions behind the simplified model can rarely be satisfied. Lin et al. (2010) established a comprehensive thermal-hydro-mechanical model in which the transport model of chloride ions was predicted more accurately. The model accounted for the moisture transport during drying-wetting cycles (non-saturated concrete), fluctuation of external environment, and the interaction between mass transport and decay of RC structural performance.

2.1.1.2 Rust Accumulation

In the second period, rust accumulation, the chloride ions (Cl^-) reach the reinforcement surface and an electrochemical reaction will be ready to start, followed by a reduction in bar

diameter and then the accumulation of rust products around the bar. Otieno et al. (2011) provide a comprehesive review on current models of corrosion rate (i_{corr}). They show that i_{corr} can be determined empirically from statistical analyses on experimental data or mathematically from electrochemical principles. Obviously, i_{corr} is also an uncertain time-dependent parameter, which is affected by many factors, including chloride concentration, pre-corrosion cracks, etc. Due to the porosity at the concrete/rebar interface, there is a free-expansion time period of rust into this zone before the initiation of the cracks propagation process. It is reported that the volume of rust products could be 4 to 6 times larger than that of the rebar diameter. Three types of corrosion product are found at steel/concrete interface, at the corrosion-induced crack as well as the edges of cracks: Fe_3O_4, β-FeO(OH) and Fe_2O_3 (Zhao et al. 2012). An important finding is that rust does not penetrate into the corrosion-induced cracks before the cracks reach the concrete surface. Furthermore, very little rust has been observed in the internal cracks between neighboring reinforcement. The difference between external and internal cracks is because of the ingress of outer solution. Therefore, there are two phases for rust diffusion: the time to completely fill the voids and the time to initiate cracks in the surrounding concrete.

2.1.1.3 Crack Propagation

In the last period, crack propagation, both empirical and analytical models are available for predicting the time for cracks to reach the concrete cover surface. The recent review by Chernin and Val (2010) pointed out that an empirical model derived from experimental data cannot provide sufficient and accurate information. Thus, models based on the analysis of a thick-walled concrete cylinder with a concentric hole (representing the space occupied by the rebar) have been proposed to simulate the chloride-induced cracking process on steel reinforced concrete decks. Two well-established analytical models are shown in Figure 7(a) a thick-walled uniform cylinder model and Figure 7(b) a partially cracked thick-walled cylinder model (Chernin and Val 2010). Before discussing these models it needs to be mentioned that external loading effects are not taken into account, even though researchers have pointed out the effects of sustained loads on corrosion rate and crack propagation (Malunbela et al. 2009).

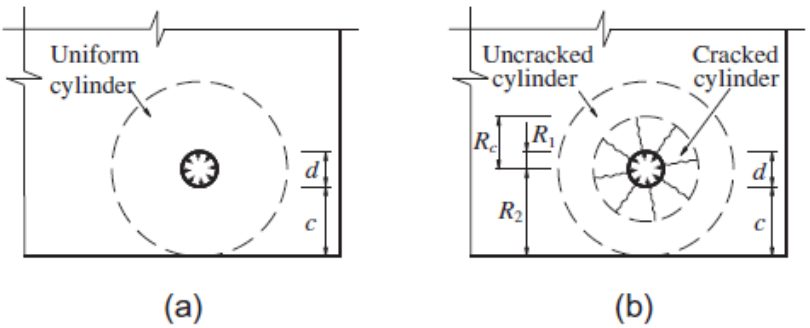

Figure 7 Two modeling approaches for crack propagation from corrosion

The uniform cylinder model proposed by Bazant (1979) is based on several assumptions, including the consideration of concrete as a homogeneous linear material, a constant value of rust production, etc. Liu and Weyers (1998b) modified this model with the consideration of a porous zone between the concrete and rebar. However, the model underestimates the mass loss of the rebar and does not take into account nonlinear behavior at the concrete/rebar interface. Recent studies have also noted that uniform steel corrosion in concrete structures will underestimate the maximum pressure applied by the corrosion products and hence overestimate the time for cracking of the cover concrete (Malumbela et al. 2011).

A double-cylinder model has been proposed on the basis of a partition between a cracked inner cylinder and an un-cracked outer layer. Modifications of this concept have been proposed by many researchers. Pantazopoulou and Papoulia (2001) considered that cover concrete maintains residual strength even after its tensile strength is reached and that rust products deposit into the concrete cracks. Li et al (2006) modeled the inner cracked cylinder as an orthotropic material with a modulus reduction. Ervin (2007) recommended a combined model for service life evaluation during the propagation period and used the model by Pantazopoulou and Papoulia before cracking in the concrete cover appears. Conversely, Wang and Liu's model was applied after crack initiation. Chernin et al. (2010) improved the compatibility in both stress and strain at the concrete/rebar interface.

An interesting comparison between the uniform and double cylinder models mentioned above shows that the former model is better to describe crack growth for cover-to-diameter (c/d) ratios smaller than 2.5, whereas the latter one is more appropriate for c/d ratios between 2.5 to 4.0

(Chernin et al. 2010). Therefore, the double-cylinder model seems to be more realistic for the current investigation.

Basheer et al. (1996) pointed out that permeability and fracture strength are the dominant factors for concrete durability. A number of recent investigations have used energy-based methods to predict the time to cracking of the concrete cover and crack propagation (Balafas and Burgoyne 2010, Zhong et al. 2010). Balafas and Burgoyne (2010) used the thick-wall cylinder theory but established the time to cracking on the basis of fracture mechanics and strain energy. This model was selected for concrete cracking prediction in this project. The criteria is that g(t) $=G_R-G_F$, where G_R is the total energy release rate in the concrete ring; and G_F is the fracture energy of concrete (0.12 Gpa). When g(t) is larger than G_R, the crack is assumed to immediately reach the top of the concrete element and thus the time to surface failure can be determined.

2.1.1.4 Post-cracking Process

Estimating the crack width at the surface is the most important issue after the crack propagates to the top. Cracks always propagate along the shortest path from the rebar to the free surface. Obviously, crack widths keep increasing after the onset of hairline cracking at the surface. Zhao et al. (2012) report that the crack width increases slightly at the concrete surface compared to that at the concrete/rebar interface. Thus, after cracking at concrete surface, the crack shape is assumed to be trapezoidal as shown in Figure 8(c). The post cracking process found in the review paper by Chernin et al. (2012) has been investigated in various ways, including analytical, experimental and numerical models.

For analytical solutions, the prediction of crack widths as a function of tangential strain proposed by Li et al (2006) has been recommended by many previous works, but a decisive stiffness reduction coefficient (α) is not easy to determine because it is related to specific material properties of concrete. In addition, the double-ring concrete cylinder was considered as a plane stress problem, while a plane strain solution is more reasonable for this investigation. Despite difficulty in defining the stiffness reduction coefficient, this analytical solution is still worth comparing with the results from experimental regression functions.

Many regression functions have been derived from accelerated experiments or long-term field testing. For example, Zhao et al. (2012) reported a linear variation of crack width with the ratio of cross-section loss to original bar size. However, it has been documented that the

prediction from this function did not provide a reasonable result in Monte Carlo Simulations. Chernin et al. (2012) summarized recent empirical functions and compared the predictions with their experimental tests. Some models underestimated the crack width while the others overestimated it significantly. It seems hard to conclude which one best fits their testing.

Finally, it was determined that numerical analysis was not suitable for our research purpose. Chemin et al. (2012) also pointed out that most of the numerical results overestimate crack widths compared to experimental data because the real corrosion process is typically simplified by this kind of modeling, especially neglecting the nature of rust growth and distribution in the porous concrete.

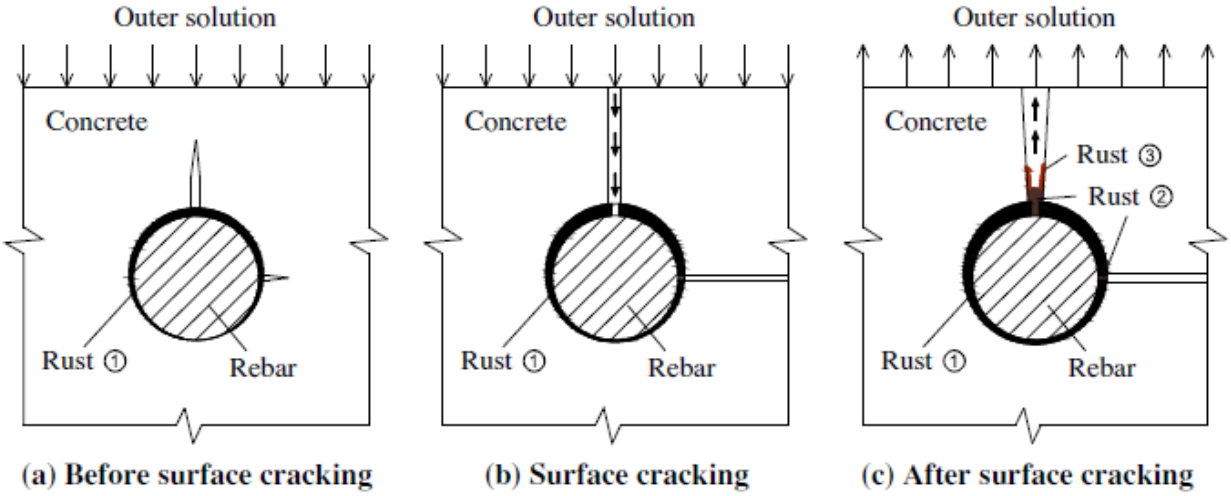

Figure 8 Crack propagation and rust production (Zhao et al. 2012)

2.1.2 Commercial Software

In order to have a better idea of the existing knowledge about service life prediction of concrete structures and to identify current limitations (gaps), several commercial programs for concrete durability modeling were reviewed, as shown in Table 2 to Table 4..

All programs basically have a library of different concrete materials, whose properties were generally obtained experimentally. The necessary input for these programs is basically the structure geometry, type of concrete, and the location (or exposure condition/environmental

condition). The output is the chloride concentration profile in space domain or time domain. As mentioned before, the initiation period of the corrosion process is assumed to be the time when the concentration of chloride ions at the reinforcement level reaches the threshold value, which is a default or user defined value. The estimated service life of the concrete structure is assumed to be the initiation period of the corrosion process (STADIUM) or the initiation period plus propagation period (LIFE-365). However, the propagation period is simply assumed to be 6 or 20 (for epoxy coated rebar) years.

Table 2. Features of the STADIUM program

STADIUM (SIMCO)	
Year	**2011 (latest version 2.99)**
Capability	**Chloride induced corrosion**
Description	STADIUM is powerful software developed to predict the service life of a concrete structure.
Advantages	It can take into account the effect of concrete and reinforcement type, exposure condition, repair history and is able to evaluate the performance of a concrete structure by estimating the transport of chloride ions based on experimentally obtained (or user provided) parameters. It uses advanced models to estimate the transfer of chloride ions, which can account for the interaction of multiple ions (Nernst-Planck equation), water movement, and temperature.
Disadvantages	Degradation is assessed purely as a mass transfer problem and the mechanical characteristics of concrete are not taken into account. The influence of concrete material deterioration on the chloride ion transfer process is not considered. The propagation period is neglected, which may be inaccurate and impractical.
Comment	This program can be very useful if the service life of the concrete structure of interest to account only for the initiation period of corrosion. However, if the propagation period needs to be considered additional work/estimations need to be conducted, which is beyond the capacity of the program.

Table 3. Features of the Life-365 program

Life-365	
Year	**2009 (latest version 2.0.1)**
Capability	**Chloride induced corrosion**
Description	Life-365 is a program used to predict the service life of concrete structures. The service life is assumed to be the sum of the initiation period of corrosion process and the propagation period. The initiation period is estimated by solving Fick's second law using the finite difference method while assuming the diffusion coefficient of concrete to be a function of both time and temperature. The propagation period is assumed to be constant (6 or 20 yrs.).
Advantages	The program can take into account the effect of silica fume, fly ash, slag, corrosion inhibitors, membranes and sealers, epoxy-coated steel and stainless steel. Most of the estimation parameters are based on experimental data or simple assumptions.
Disadvantages	Life-365 claims that it can predict the entire service life of a concrete structure (initiation period and propagation period.) However, the length of propagation period is assumed to be constant (6 or 20 yrs.), which may be too simplified. The estimate of the initiation period only considers the diffusion of chloride ions using Fick's second law. In other words, the concrete is evaluated as saturated and un-cracked. More complex modeling is necessary (not a capability of the program) to take into account the moisture transport during drying and wetting, and the interaction between diffusion coefficient and deterioration of concrete material.
Comment	The program uses a simple model for the initiation period and a poor estimate for the propagation period.

Table 4. Features of the CONLIFE program

CONLIFE	
Year	**2002**
Capability	**Sulfate attack and freeze thaw**
Description	CONLIFE is a program developed by Bentz et al. (2002) that can be used to predict the service life of concrete structures due to sulfate attack and freeze thaw effects. It assumes that sorption is the primary transport mechanism in concrete. A test method for sorptivity is proposed.
Advantages	The program's model is based on a relatively less popular transport mechanism (sorption). A time of wetness model (Bentz et al. 2002) was developed that can predict the wetting event based on data of temperature and relative humidity. This model is used to predict the "filling" process of air voids in concrete.
Disadvantages	Sorption is assumed to be the only transport mechanism, which may not be accurate. Other mechanism such as diffusion may need to be taken into account. Concrete is assumed to be damaged when the air void in concrete is saturated to a certain level. However, the actual cracking process is not considered in the material behavior after damage occurs. Multi-mechanisms and the interactions were not considered and the material is assumed to be homogenous.
Comment	Similar model of wetness may be adopted but other mechanisms need to be introduced; including the uncertainty of input parameters.

2.2 Carbonation

Carbonation is another chemical attack that can lead to the corrosion of reinforcement in RC deck structures, especially in urban and industrial areas. Keller (2004) reported that carbonation is usually slow on bridge decks, especially for good quality concretes. Carbonation rates are dependent on humidity, with a high rate near 50% relative humidity (RH) but the process nearly nearly stops at 0 and 100% relative humidity. Zhong et al. (2010) pointed out that a notable difference between chloride-induced and carbonation-induced corrosion is that the former

exhibits localized cracking and spalling on the concrete surface while the latter causes a widespread and uniform cracking pattern.

As another major chemical attack that initiates the degradation of RC decks, carbonation-induced corrosion received less attention than chloride-induced corrosion before the year 2000. Most of the developed models are empirical or semi-empirical. Similarly to the prediction of chloride-induced corrosion, the carbonation models are also based on many assumptions. Early analytical models are simply estimated by Equation 2-6 from Fick's first law, which describes the carbonation depth as a function of concrete age and the carbonation rate coefficient K.

$$x = K\sqrt{t} \tag{2-6}$$

where, x is the carbonation depth (mm) and K is the carbonation rate coefficient (mm/year$^{-1/2}$). K is equal to $[(2 \cdot D_{CO2} \cdot C_{CO2})/\alpha]^{1/2}$, where D_{CO2} is CO_2 diffusion coefficient (cm^2s^{-1}), C_{CO2} is atmospheric CO_2 concentration (g cm^{-3}), α is an amount of CO_2 for complete carbonation, and t is the exposure time to CO_2 (years).

It is reported that the carbonation coefficient is dependent on the environment and the material properties of concrete. Humidity is the most important factor among all the environmental parameters. Carbonation rate would be lower if the structure is subject to periodic wetting. Several previous works have reported that the chemical process of carbonation is highest near a relative humidity (RH) of 50 to 70%. It also mentioned that RH below 50% is insufficient to trigger the carbonation reactions. Stewart et al. (2011) pointed out that, conservatively, the carbonation front stops if RH is less than 40%. The RH range in Michigan is between 58 and 80%, which indicates that carbonation corrosion is an issue for the durability of RC decks. As for the material properties, the concrete water/cement (w/c) ratio plays an essential role on the diffusion of carbon dioxide. Previous research has shown that a lower ratio slows down the penetration of carbonation. In turn, the carbonation process results in changes of the mechanical properties and durability of concrete. Chi et al. (2002) noted that the compressive strength of carbonated concrete is slightly larger than that of non-carbonated concrete.

Some recent research (Isgor and Razaqpur, 2004; Saetta et al. 2004) has led to the development of mathematical-numerical models to simulate the carbonation process in RC structures by considering the combination of moisture, heat and agent flows through concrete.

Isgor and Razaqpur (2004) present the governing equations of the important phenomena that affect carbonation and then solved them through numerical methods. Song et al. (2006) developed an analytical technique for carbonation prediction in early-aged cracked concrete wby considering both CO_2 diffusion of pore water in sound concrete and in cracked concrete. Marques and Costa (2010) presented a performance-based methodology as regards carbonation-induced corrosion of RC structure. In spite of their comprehensive nature, the noted models are not easily implemented into the conceptualized framework for degradation modeling in this project.

2.3 Freeze-thaw Effect

Freeze-thaw damage is one of the most well-recognized damage sources for bridge decks. The concrete freeze-thaw durability is usually evaluated by conducting accelerated tests in the laboratory or exposure tests in the actual environment. Most of the experiment and research focus on the relationship between the dynamic elastic modulus of concrete material and freeze-thaw cycles. A series of experimental studies on deterioration induced by scaling in the early 1950s confirmed that the presence of deicing salts accelerates the deterioration of concrete under freeze-thaw cycles. It is widely accepted that the presence of deicing chemicals will increase freeze-thaw damage, at least in the surface layer. The experimental findings by Macinnis and Whiting (1979) proved that deicing salts increase the damage caused by frost action. Similar conclusions were also drawn by Mu et al. (2002) and Sun et al. (2002) based on their experiments. The higher the salt concentration in the solution, the higher was the degree of saturation retained in the concrete. Chung et al. (2010) also found that concrete can have higher chloride coefficient of diffusion under freeze-thaw cycles.

The deterioration of concrete due to the freeze-thaw cycles is a complex physical phenomenon. Water contained in the concrete pores freezes at low temperatures increasing in volume by by 9%. Freeze-thaw damage begins with the pressure developed within the void system of the cement paste and aggregates. A large number of freeze-thaw cycles can eventually lead to deterioration of the deck surface. The concrete cover may loss up to 3 to 10 mm of depth because of the exposure of repeated cycles (Fabbri et al. 2008). The most reported types of freeze-thaw damage are internal cracking and surface scaling. Both of these failure modes are progressive phenomena (Rønning 2001). Wang and Song (2010) explained that internal damage

mainly results from changes in the physical properties (the mass loss and decline of dynamic elastic modulus, etc.) and mechanical properties (flexural strength, compressive strength, etc.).

Air-entrained concrete, developed in the late 1930s, has been confirmed as an effective way to improve the frost resistance of concrete by adding proper volume and void spacing. Bazant et al. (1988) commented that use of air entrainment is not a perfect choice because the addition of pores causes a reduction in concrete strength and fracture toughness. Sabir (1997) found that the use of silica fume can improve compressive strength and reduce the rate of weight loss. Tanesi and Meininger (2006) investigated the freeze-thaw resistance of concrete with marginal air content. They showed that the type of air-entraining admixture played a major role in performance. Penttala (2006) reported that the need for air-entrainment is determined by surface scaling damage in low-strength concrete and by internal cracking in high strength concrete. Shang et al. (2009) carried out an experiment of air-entrained concrete subjected to different freeze-thaw cycles. The results showed that the dynamic modulus of elasticity, tensile strength, and compressive strength decreased as freeze-thaw cycles were repeated. In their tests, the compressive strength decreased 14% from its initial value after 300 cycles, but it dropped quickly to 54% of the initial value after 400 cycles. It is interesting to note that the influence of freeze-thaw on tensile strength is larger than compressive strength, dropping to 37% of the initial strength. In addition, the relative dynamic modulus decreased to 77% and concrete weight loss was 2% from its initial value after 400 cycles.

Water-cement ratio is associated with the porosity of the cement. It is reported that dense concrete of low w/c ratio has higher frost resistance, as shown in Figure 9**Error! Reference source not found.**. If the w/c ratio is very low, the concrete is frost-resistant even without air-entrainment. Air-entrained concrete could have very small and uniform bubbles inside the cement paste, but it requires that the distances between the bubbles be less than 0.1 to 0.2 mm. Even a low w/c ratio cannot guarantee frost resistance. There are many factors that could have a significant influence, such as the concrete age, the type of binder, the pre-treatment, minimum temperature during the test, etc. (Fagerlund 1995). The experiments by Ghafoori and Mathis's (1995) also proved that low w/c ratio improves the resistance to freezing and thawing by reducing the amount of freezable water initially in the paste. Those specimens with high cement content withstood a greater number of freezing and thawing cycles and reduced the rate of crack propagation.

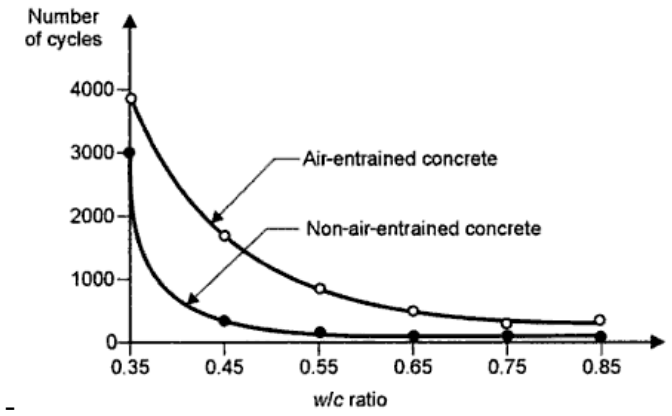

Figure 9 Number of freeze-thaw cycles vs. w/c ratio (Bertolini et al. 2004)

It is known that concrete is a complex multi-scale material. Concrete itself has a microclimate, which is still not fully understood. Hydraulic pressure theory is the most widespread explanation for frost deterioration. In this theory concrete damage is caused by pore pressure due to the expulsion of water during the freezing process (Bazant et al. 1988). The pore water is considered to move from frozen part to others, but this theory does not seem to work for high quality concrete and is valid only in very saturated conditions (Penttala 2006). Later, osmotic pressure theory was proposed to describe the movement of pore water. The water movement is caused by the dissolved substances that are not included in the formed ice structures. Recent findings reported by Fabbri et al. (2008) note that the mechanical response of a saturated or partially saturated porous material at freezing temperatures is caused by the volumetric increase of water during its solidification, the transport of unfrozen liquid water and the thermo-mechanical properties of all the concrete phases.

Fagerlund (1995) investigated the damage mechanisms at the micro-scale level, such as the pressure by the frozen water in the air content. However, our research project only deals with concrete damage at the macro-scale level, i.e., considering the concrete as a continuum material. Nevertheless, analytical solutions can be very useful to show the frost resistance of concrete. For example, it has been shown that very low air content is needed to protect a low-porosity concrete. The required air space is about 0.8% in normal concrete and 0.2% in high performance concrete. Rønning (2001) presented equations of mass loss due to the contraction of air voids, to the contraction of pore solution and to the thermally induced flow, etc. Bertolini et al. (2004)

reported that the degree of saturation of the pores has a critical value (80% to 90% of the total porous volume is water filled) for the frost resistance of concrete. Below this value, the concrete is able to withstand a high number of freeze-thaw cycles, while a few cycles may cause the damage to concrete above the critical value.

Other aspects addressed in the existing literature include the macro-scale behavior of concrete under freeze thaw actions like the loss of strength, modulus, mass, etc. Janssen and Snyder (1994) carried out a comprehensive experimental study on the freeze-thaw resistance of concrete. The results provided the basis for determining the potential benefits of using concrete sealers to mitigate or prevent the development of D-cracking in concrete pavements constructed using nondurable aggregates. Liu and Wang (2012) also studied the stress-strain relationship of the concrete undergoing repeated cycles of freeze-thaw. However, many important questions still have yet to be answered. Further, most of these works provide only qualitative knowledge. The experimental works by Amini and Tehrani (2011) investigated the combined effect of water flow and salt on deterioration of concrete under freeze-thaw cycles. Weight change and compressive strength were measured and regression functions for these specimens are given by Equation 2-7 and 2-8:

$$W_{loss} = 0.887 \cdot N + 479.379 \cdot W + 26.122 \cdot S - 216.111 (R^2 = 0.693) \quad (2\text{-}7)$$

$$CSL = 1.148 \cdot N + 682.144 \cdot W + 23.951 \cdot S - 299.019 (R^2 = 0.728) \quad (2\text{-}8)$$

where: N is the number of cycles; W is the water-cement ratio; and S is the nominal value of the presence of saltwater (0.586 for W_{loss} and 0.375 for CSL). Results show that the presence of water flow and saltwater increased the deterioration of concrete, resulting in larger compressive strength loss.

Jia et al. (2010) obtained several regression functions (Equations 2-9 to 2-11) for concrete in a a laboratory environment, including compressive strength, tensile strength, and elastic modulus. They also reported that the ratio of the number of cycles in the laboratory and the real environment is between 1/10 and 1/15. The mean average is about 1/12.5, which means that one freeze-thaw cycle in an accelerated test is equal to 12.5 cycles in real conditions. Thus, if the freeze-thaw cycles in Michigan is 150 per year, the number of cycles in a laboratory study is 12 (150/12.5=12). For a given year of t, the number of cycles in a laboratory environment (N) is equal to 12×t.

$$f_c(t) = 47.583e^{-0.002N} \tag{2-9}$$

$$f_t(t) = 3.5145e^{-0.0016N} \tag{2-10}$$

$$E_c(t) = 89.75e^{-0.0037N} \tag{2-11}$$

Note: N is the number of cycle in the lab environment, assuming equal to 12×t in Michigan.

In spite of the literature review just presented, the regression functions from the noted studies are not suitable for direct use in our project because of the difference in material properties and environmental conditions. Numerical methods to investigate freeze-thaw effect have also been proposed, but they cannot be used in the proposed framework. The best way for implementing freeze-thaw deterioration models within the framework develop in this project is to get regression functions for each region in Michigan so that the changes in concrete at the macro level can be described, like the decrease in compressive strength, elastic modulus, etc. Then, those material properties can be updated yearly by the model. Another recently proposed model for predicting freeze-thaw effects as also recently proposed by Cho (2007). However, the model is not suitable for the proposed framework

Another difficulty in finding general functions for the response of concrete under freeze-thaw actions is that there are too many different types of concrete. Kelly and Murphy (2010) studied the influence of different mix designs on the freeze-thaw resistance of concrete. Existing literature on freeze-thaw action contains high strength concrete (Jacobsen and Sellevold 1995), recycled aggregated concrete (Zaharieva et al. 2004), concrete with different pore liners (Basheer and Cleland 2006), air-entrained concrete (Shang et al. 2009) and alkali-activated slag concrete (Fu et al. 2011), etc. Thus, even if functions that described the macro-scale behavior due to freeze-thaw effects they could still not be used in a general way for the purpose of multi-modal degradation prediction in the framework developed under this study.

2.4 Summary

A literature review on the deterioration mechanisms and modeling approaches thereof of RC structures was presented. Three major causes of deterioration in RC decks were recognized, including chloride induced corrosion, carbonation and freeze thaw. It was noted that chloride corrosion is the major cause. Carbonation will be considered as another effect in the current

study but freeze-thaw effects will be not incorporated into degradation modeling scheme. Existing analytical models for these three mechanisms were highlighted and compared. A review of existing programs developed for concrete durability modeling was conducted and their advantages and disadvantages were summarized. From this review, perceived limitations were identified in order to choose suitable models and to improve the accuracy of service life prediction. Therefore, the selection of mechanistic models for degradation was being aimed at: (i) considering multi-mechanisms, and (ii) improved modeling of carbonation and chloride corrosion. The selected mechanistic models are presented in detail in the next chapter.

3 LOCAL-LEVEL MECHANISTIC DEGRADATION MODELING

3.1 Selected Mechanistic Models

The mechanistic models chosen for the prediction of chloride-induced corrosion at the local/cell level are based on a representative volume element consisting of a thick-wall concrete ring that encapsulates a reinforcement bar. The model geometry only approximates the real stress conditions. However, it can be regarded as a critical section in a bridge deck domain because cracks always propagate along the shortest path from the rebar to the free surface. The selected deterioration model at the local/cell level improves on the noted shortcomings of analytical models and commercial software that summarized in Chapter 2 in the following ways:

(a) Fick's second law is still used to estimate the corrosion initiation time due to its convenience. Time-dependent effects on key parameters (surface chloride content, diffusion coefficient, etc.) were taken into account to improve accuracy.

(b) The propagation period is divided into two sub phases, rust production and crack propagation. An improved thick-wall cylinder model, proposed by Balafas and Burgoyne (2010), was used. Three new aspects of this models are (1) a new formulation to estimate rust production and consumed mass by combining two well accepted theories (Faraday's Law and Liu-Weyers formula); (2) a new volume compatibility condition is used to determine the pressure due to rust accumulation; and (3) a fracture mechanics approach and strain energy estimates are applied to determine the time required to produce surface cracking;

(c) The thick-walled cylinder model also takes into account the nonlinear behavior of concrete as proposed by Pantazopoulou and Papoulia (2001). Two important assumptions in this model are that the concrete cover retains residual strength after its tensile strength is reached and that rust products are deposited into the concrete cracks;

(d) Post-cracking behavior is considered by estimating the crack width on the concrete surface. Nevertheless, most of the analytical and empirical functions confirm a linear relation between the loss section of rebar and the propagation of crack width.

Although the omission of some factors can result in a poor estimate of service life, it should be emphasized that no model is perfect, since they are all based on a set of assumptions. It is obvious that it is very difficult to incorporate all of the factors in the chloride-induced corrosion process. Therefore, the analytical models were chosen with consideration of ease of implementation in a framework for life-time prediction and durability modeling. The key model parameters are given as shown in Figure 10: (1) T1: the time of corrosion initiation at the rebar surface; (2) T2: the time to cracking initiation at the interface between concrete and rebar; and (3) T3: the time for cracking to propagate to the concrete surface.

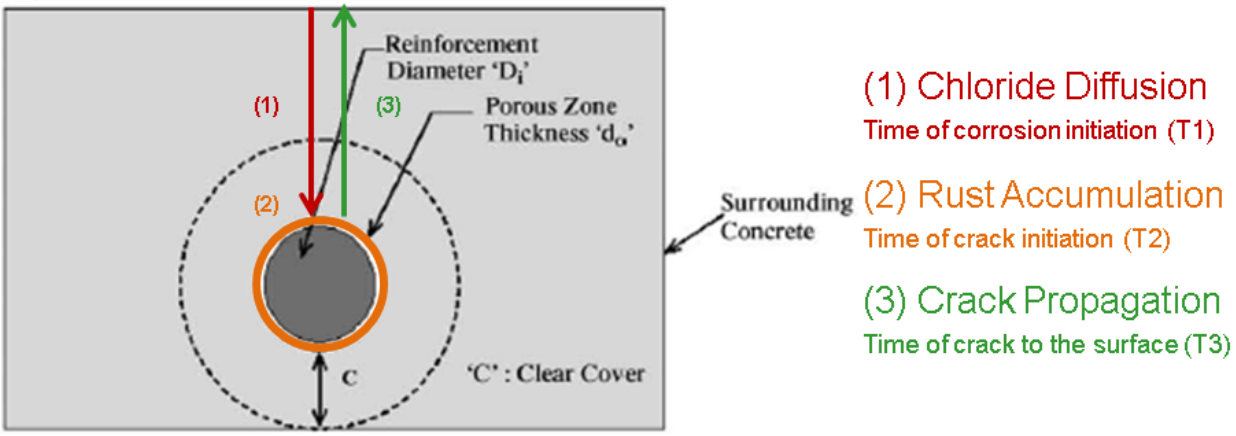

Figure 10 Concrete ring model and three-phase corrosion process at a local/cell level

3.2 Flow-chart of Cell-level Modeling and Key Parameters

The simulation process for chloride-induced corrosion is summarized as a flow chart in Figure 11. The input for the model is listed at the top right corner, mainly concerning the material properties of concrete and reinforcing steel. The model is able to provide time-dependent information on the chloride concentration at the bar surface, the mass change (consumed in bar and accumulated in rust, changing volume (in concrete, bar and rust), the pressure generated at the concrete/rebar interface, the strain energy in the concrete ring, the crack width, etc. The simulation was implemented in a computer program written in Matlab (MathWorks 2011). The output consists of the three significant times (T1, T2, and T3, see Figure 10) along the service life before first repair.

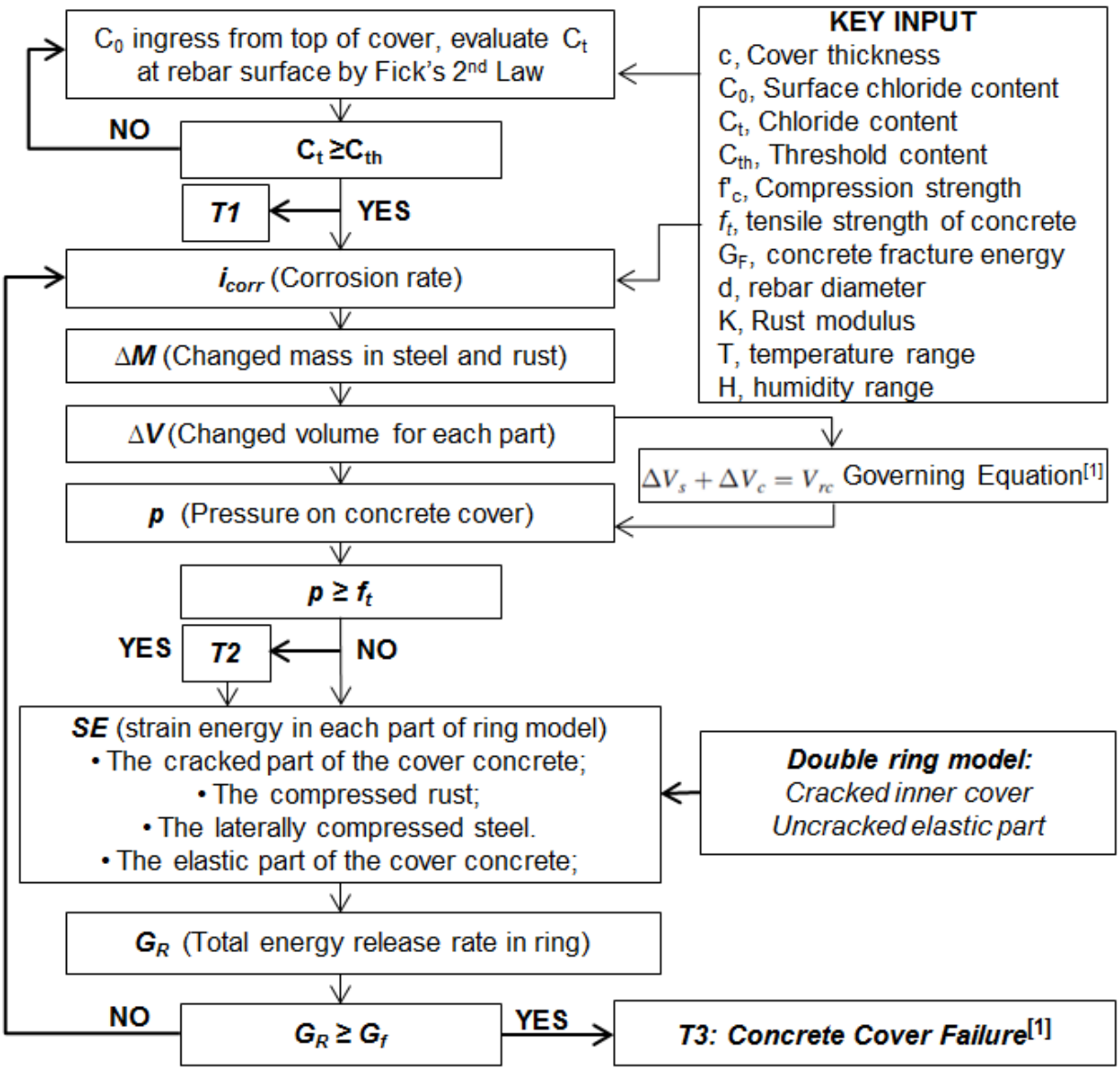

[1] Balafas, I., and Burgoyne, C. J. (2011). "Modeling the Structural Effects of Rust in Concrete Cover", *ASCE J. Eng. Mech.* 137(3), 175-185.

Figure 11 Flow-chart for service life prediction due to chloride-induced corrosion

The time of the corrosion initiation (T1) is determined by Fick's 2nd law with corrosion assumed to initiate at the rebar surface when the chloride content reaches a threshold level. Concrete cover acts as a physical barrier that prevents direct exposure of the reinforcement to the surrounding environment, including the negative effects of deicing salt, seawater, etc. Since

diffusion is regarded the primary governing mechanism, Fick's second law is applied to estimate the corrosion initiation period by Equation 3-1.

$$C(x,t) = C_0(1 - \text{erf}\left(\frac{x}{2\sqrt{Dt}}\right) \quad (3\text{-}1)$$

Note that C_0 = surface chloride concentration; D = chloride diffusion coefficient; and x = certain depth into the concrete cover. Corrosion in the reinforcement bar will initiate when the chloride concentration at its surface reaches a threshold level. By solving Fick's second law in an inverse manner the time T1 can be determined from Equation 3-2:

$$t_1 = \frac{c \cdot erf^{-1}\left(1 - \frac{C_{th}}{C_0}\right)^{-2}}{4D} \quad (3\text{-}2)$$

Note that c = depth of concrete cover; and C_{th} = threshold level of chloride concentration

However, it should be noted that the use of Fick's second law assumes that concrete has a constant diffusion coefficient and a constant surface chloride concentration over time. The drawbacks of this simplified approach can be curtailed by considering those key factors as time-dependent variables.

Surface Chloride Concentrations (C_0)

The surface chloride concentration (C_0) was considered to be dependent on the concrete mixture and the exposure condition (Song et al. 2009). Kassir and Ghosn (2002) reported that the data collected by Liu and Weyers (1998a) clearly showed that C_0 increases with time. Clearly, C_0 should be a time-dependent variable because a concrete deck is cyclically exposed to deicing salts over a given year. An early suggestion to consider surface concentration as a time-dependent parameter is to express it as proportional to the square root of time.

A general accepted knowledge is that the maximum chloride concentration is not at the concrete surface but at a certain depth below the concrete cover, typically 0.5 inches (13 mm) below the concrete surface (Fanous and Wu 2005). Chloride concentration content refers to the amount of free chloride ions in pore solution. It is not accurate to consider surface chloride content as a constant; however, chloride concentration reaches a maximum value at a certain concrete depth such that it can be assumed quasi-constant after exposure.

Chloride Diffusion Coefficient (D)

The diffusion coefficient (D) is another key parameter for accurate modeling of chloride transport. Many investigations have proved that D is time dependent, as it varies with both material and environmental factors. For example, Lin et al. (2010) present a definition of D by a multifactor law that accounts for the dependence on the temperature level T, the age t of the concrete structure, the moisture saturation degree θ, the decay d of concrete structural performance, etc. However, environmental data is hard to measure for all bridges. On the other hand, many research works also describe D as a constant in function of material properties due to the lack of field data at the referred conditions. Song et al. (2009) noted that the diffusion coefficient of concrete is different for the original and repair materials. Therefore, Equation 3-3 and 3-4 are applied in the prediction model.

$$D(t) = D_{w/c} \cdot \left(\frac{tr}{t}\right)^{0.2}, \quad when\ t \leq 30\ years \tag{3-3}$$

$$D(t) = D_{w/c} \cdot \left(\frac{tr}{tlim}\right)^{0.2}, when\ t > 30\ years \tag{3-4}$$

where Dw/c is the diffusion coefficient at a reference time tr (equal to 28 days), which is a function of water to cement ratio w/c (Vu and Stewart 2000); $Dw/c=10^{(-12.06+2.4*w/c)}$; tr is 28 days and the t limit is 30 years.

Chloride Threshold Level (C_{th})

Previous research has recommended that the critical chloride content to initiate corrosion can be taken as a constant. However, the recommended value has a wide range: from 0.2% to 1.5% by weight of cement. For example, Song et al. (2009) used 1.2 kg/m^3 and 2.0 kg/m^3 as the critical value for black steel bars. Zemajtis (1998) reported that concentrations of less than 1.42 kg/m^3 are acceptable for bridge decks, while replacement of the deck should occur when the chloride content reaches 2.8 kg/m^3. Other researchers (Kirkpatrick et al. 2002, Fanous and Wu 2005) have have determined chloride threshold levels for epoxy-coated reinforcing (ECR) bars with typical values ranging from 0.7 to 2.2 kg/m^3.

Corrosion Rate (I_{corr})

After the chloride ions (Cl-) reach the reinforcement surface an electrochemical reaction starts, followed by a reduction in bar diameter and then the accumulation of rust product around

the bar. The time to crack initiation (T2) is determined when the pressure at the interface of concrete cover and rebar reach the concrete tensile strength. I_{corr} ($\mu A/cm^2$) is one of the most important parameters for modeling the rust diffusion process and the key factor to determine the T2. The most frequently used empirical function for I_{corr} is the one proposed by Liu and Weyers (1998a) in which corrosion rate is dependent on chloride content, temperature and resistance of the concrete cover, see Equation 3-5 and 3-6. Balafas and Burgoyne (2010) examined the environmental effect on concrete cover cracking due to chloride corrosion and reported that I_{corr} is lowest at mid-summer and highest at end of autumn and the beginning of spring.

$$i_{cor} = 0.0092 \exp(8.37 + 0.168 \ln(1.69\, C_{th}) - \frac{3034}{T} - 0.000105 R_{c,res} + 2.35\, t^{-0.125} \quad (3\text{-}5)$$

$$R_{c,res} = 90.537 \cdot h^{-7.2548} [1 + \exp(5 - 50(1 - h))] \quad (3\text{-}6)$$

Note that i_{corr} = the corrosion rate (A/m^2), C_{th} = the critical chloride content (kg/m^3), T = temperature at the depth of the steel surface (K), t = the time from initiation of corrosion (years); and $R_{c,res}$ = the ohmic resistance of the cover concrete (ohms) as a function of relative humidity (h).

Change of Mass in Rebar (M_s)

The consumption of rebar mass during the corrosion process has been determined in two ways. The first is a constant rate of rust production according to Faraday's Law. However, it is known that Faraday's Law underestimates gravimetric mass loss at low corrosion levels (≤5%) and overestimates the loss at large corrosion levels (≥10%). The second method is a non-constant rate consideration as proposed by Liu and Weyers (1998a). A recent investigation by Balafas and Burgoyne (2011) combined both of these methods based on test results (see **Error! Reference ource not found.**). Two detailed phases in corrosion propagation mechanisms were recognized as kinetic and nonlinear diffusion. Rust production in the kinetic phase is regarded as linear whereas in the latter phase the rate of rust accumulation decreased when the amount of corrosion is too large to ignore. By comparing these two functions of corrosion rate the consumed mass is initially kept constant following Faraday's law and is then evaluated by Liu-Weyers function, see Equation 3-7:

$$M_s = \min(M_{s,FL}, M_{s,LW}) \quad (3\text{-}7)$$

$$Note: M_{s,FL} = 18.254 \cdot \pi \cdot R_i \cdot i_{corr} \cdot t(kg/m), M_{s,LW} = \sqrt{8.392 \cdot \pi \cdot R_i \cdot i_{corr} \cdot t}(kg/m)$$

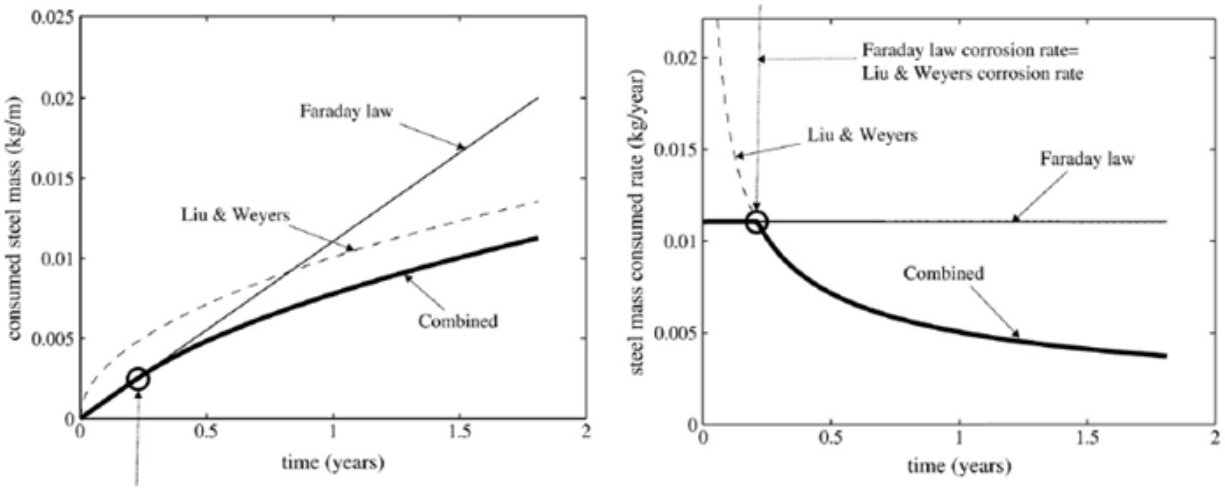

Figure 12 Steel consumed and rate of consumed mass versus time different rules

Pressure on Concrete Cover (p)

It is reasonable to assume that at an early corrosion stage a linear expansion of concrete occurs due to the pressure generated from the rebar corrosion products. Test results by Malumbela et al. (2011) estimated that a 1% mass loss of steel corresponds to a maximum corrosion-induced crack width of 0.0016 in. (0.04 mm.) As the volume of rust increases, the critical time for first-crack occurrence is when the tangential stress exceeds f_t. The pressure acting on the concrete can be found by considering equilibrium of the volume change (Balafas and Burgoyne 2010) as indicated by Equation 3-8.

$$\Delta V_s + \Delta V_c = \Delta V_{rc} \tag{3-8}$$

Note: ΔV_s, ΔV_c and ΔV_{rc} are the changes in steel, concrete and rust volume, respectively.

Cracking Width (w)

From the review, the function from a 23 year chloride exposure test was selected as the linear function to define the post cracking process, as given by Equation 3-9.

$$w_s = 0.1916 \cdot \Delta A_s + 0.164 \tag{3-9}$$

Note: ws = the surface crack width; and ΔAs = the average loss of rebar cross-section.

3.3 Prediction Results

The prediction results presented here were obtained for a single cubic block selected from the whole deck domain. Since transverse bars are more important than longitudinal bars for strength of the deck, the side with a transverse bar inside of the cubic block was chosen for investigation. Therefore, the 3D problem was simplified to a 1D problem by selecting a critical cross-section, which is a thick wall cylinder model with a concentric bar. According to MDOT's standard bridge slab design guides the minimum clear cover for transverse bars is 3 in. (76.2 mm). A #6 bar was chosen for the transverse bar. Table 5 lists the other key parameters with typical values for this deterministic analysis. The results are shown in Figure 13 to Figure 18.

Table 5. Model inputs for cover cracking evaluation

Variable	Value	Notes
$C_{0,}$ surface chloride concentration	3.5 (kg/m3)	Typical mean value
D, diffusion coefficient (m^2/s)	$D=Dw/c(t_R/t)^{0.2}$	Time-dependent
c, concrete cover	75.6 (mm)	3 in.
w/c, water to cement ratio	27/(fc/1000+13.5)	Vu and Stewart (2000)
$C_{th,}$ Threshold value	1.2 (kg/m3)	Typical value for black bar
fc, compressive strength of concrete	31.5 (Mpa)	4.5 ksi
Ec, elastic modulus of concrete	32.4 (Mpa)	
νc, Poisson's ratio of concrete	0.2	
ft', tensile strength of concrete	3.4 (Mpa)	
ρs, weight density of steel	7850 (kg/m3)	
d, diameter of reinforcement	19.05 mm (0.75 in)	Bar Size 06#
νs, Poisson's ratio of rebar	0.3	
Annual atmospheric relative humidity	40-85%	(min, max)
Annual atmospheric relative temperature	-5~35°C	(min, max)

Figure 13 shows that corrosion at the bar surface initiates at 21 years (T1) when the chloride content reaches the threshold level of black steel bar (1.2 kg/m^3). Since rust takes time to penetrate into the concrete pores, cracking at the cover-bar interface did not immediately initiate. Figure 14 shows that corrosion rate varies with changes in annual temperature and humidity. Figure 15 shows that crack initiation is predicted at 24 years (T2). It also can be seen in Figure 16 that the crack initiates at the bar radius (9.525 mm) and then propagates with increasing rust product pressure buildup. Figure 17 shows how the crack is predicted to propagate in a step-wise form toward the surface of the concrete cover as the energy release rate Gr reaches the concrete fracture energy limit (0.12 Mpa). The progression of the crack width at concrete/rebar interface is shown in Figure 18. The model also predicts that the time for the crack to reach the surface (T3) is equal to 49 years (1795 days).

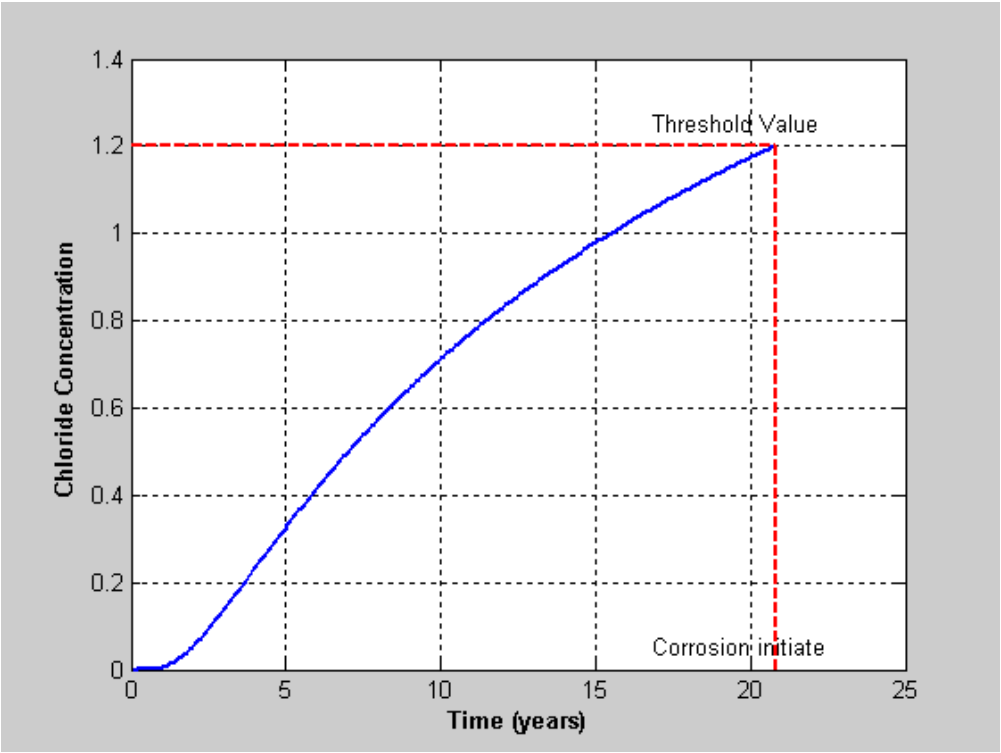

Figure 13 Chloride profile at the surface of rebar versus time

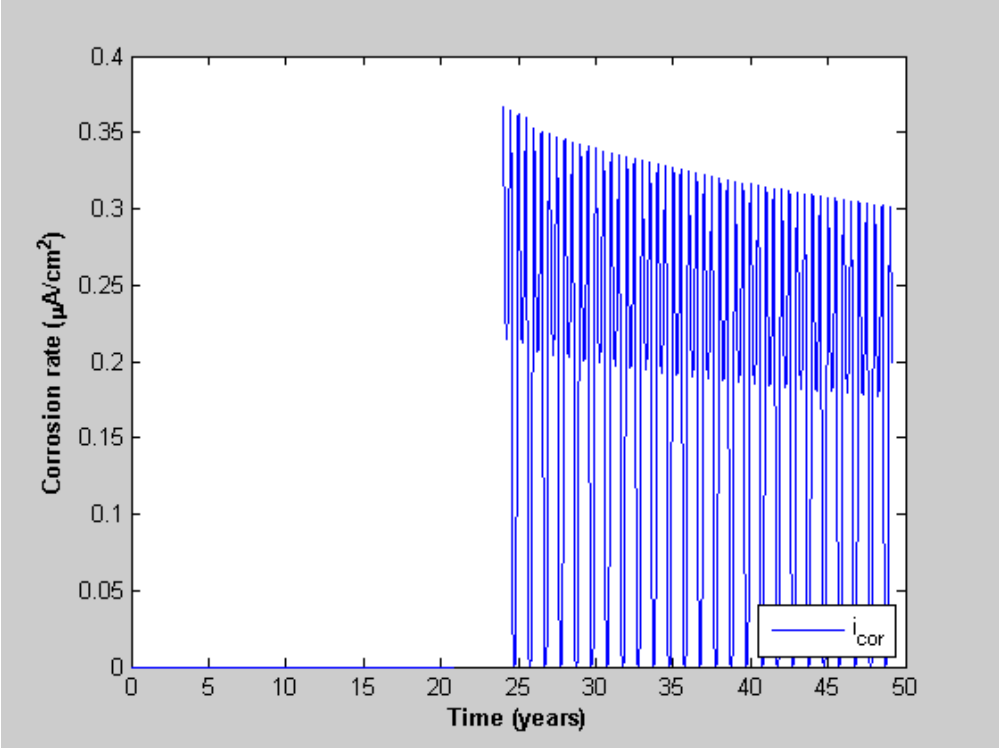

Figure 14 The time-dependent corrosion rate

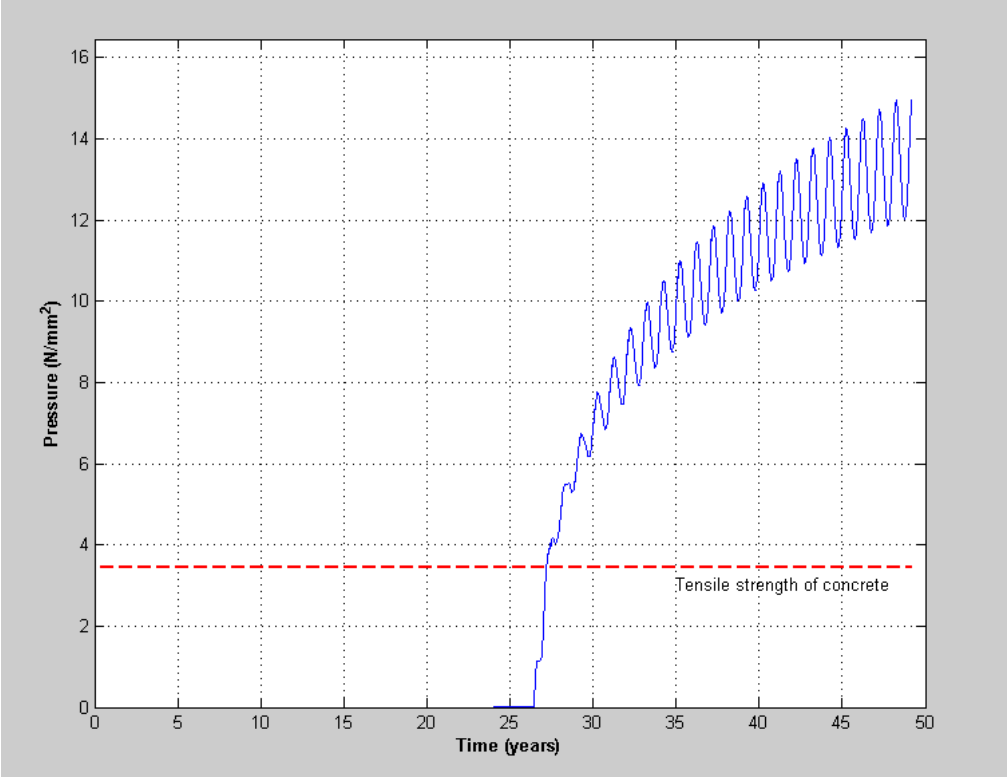

Figure 15 Pressure at interface between concrete and rebar

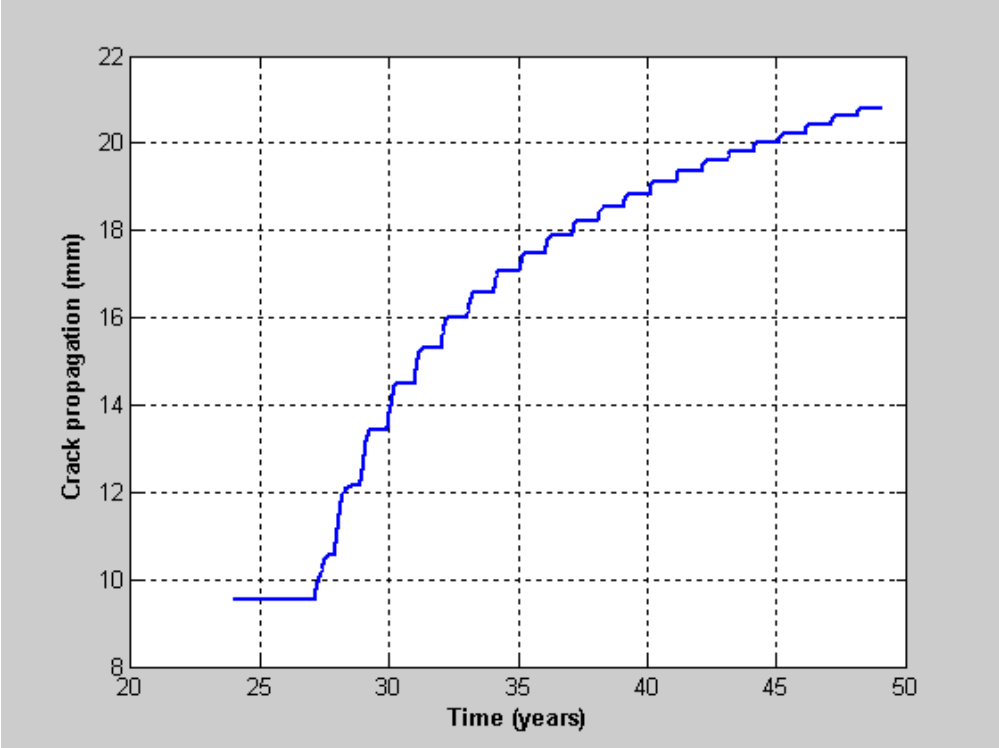

Figure 16 Crack propagation from the rebar surface to the crack front

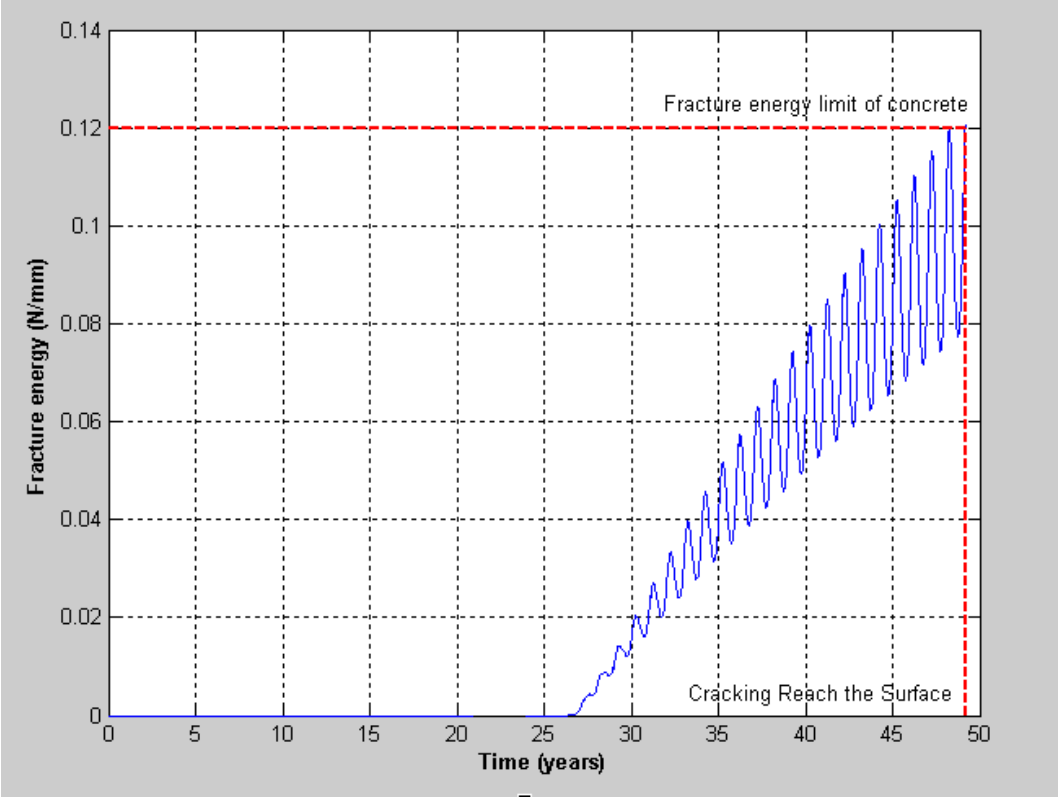

Figure 17 Total energy in the concrete ring

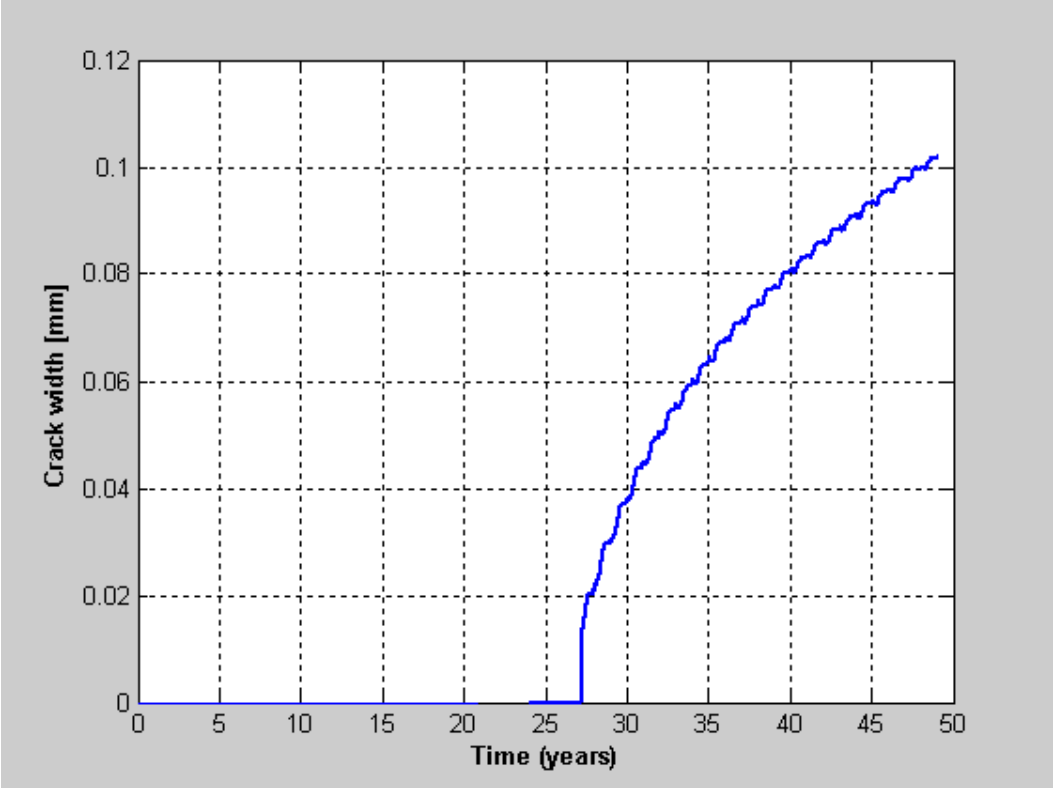

Figure 18 Crack width at the interface of concrete cover and rebar

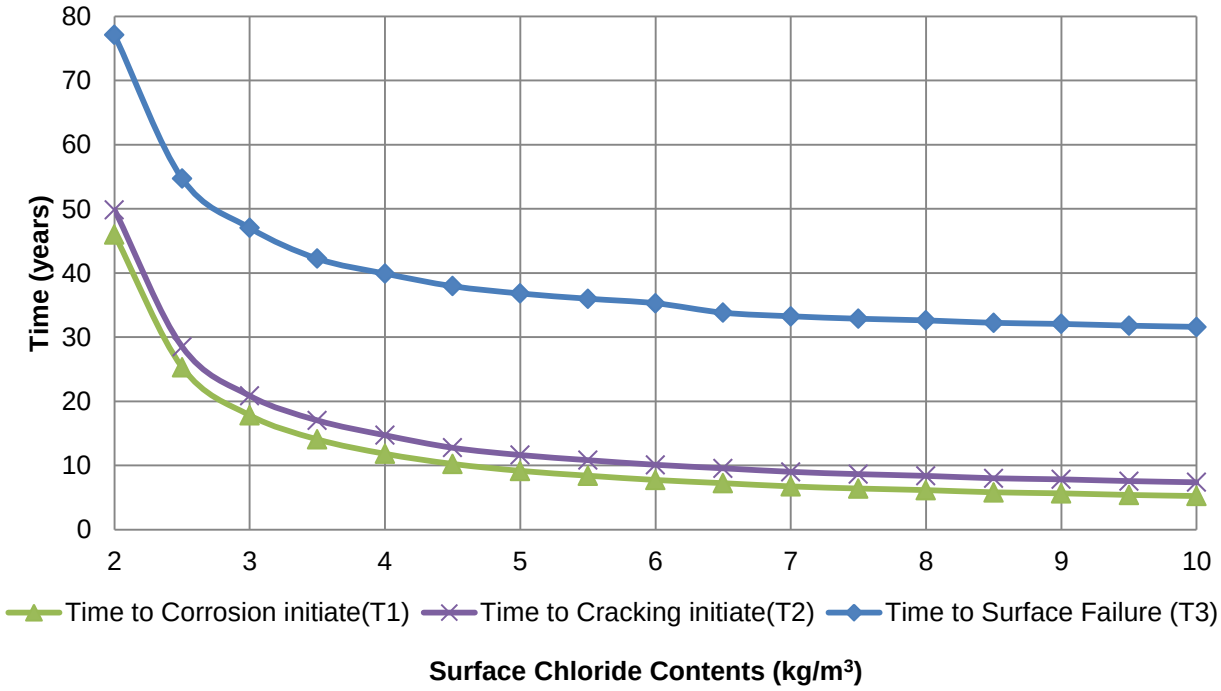

Figure 19 Influence of C_0 on the service life of a bridge deck

This example shows that the selected analytical models can provide useful information for degradation modeling, especially the time for cracking to reach the concrete cover surface. It can be agreed upon that the material and environmental properties of the whole deck domain are not the same. For example, the surface chloride content is clearly different due to the distribution of deicing chemicals. Therefore, the input data uncertainty motivates the need for a probability-based analysis and a reliability index to better assess the condition of a bridge deck. In this example of prediction at the local/cell level, C_0 was assumed to be a constant, but obviously it is a time-dependent variable that also varies throughout the deck. Figure 19 presents the result of T1, T2 and T3 for different C_0 values (from 2.0 to 10 kg/m^3, with 0.5 kg/m^3 increments). Obviously, T1 is a function of C_0, because the time to corrosion initiation is calculated from Fick's second law. There is no significant change between other time spans (T1 and T2, T2 and T3), which depend on environmental data (and other material properties) and design features like concrete cover and bar size. A similar trend can be observed in Figure 20, where the depth of concrete cover is a variable. It is worth noting that concrete cover does have a significant effect on the entire period of service life. Therefore, the service life in certain parts of bridge deck will drop very fast when concrete cover is reduced due to surface cracking, scaling or spalling.

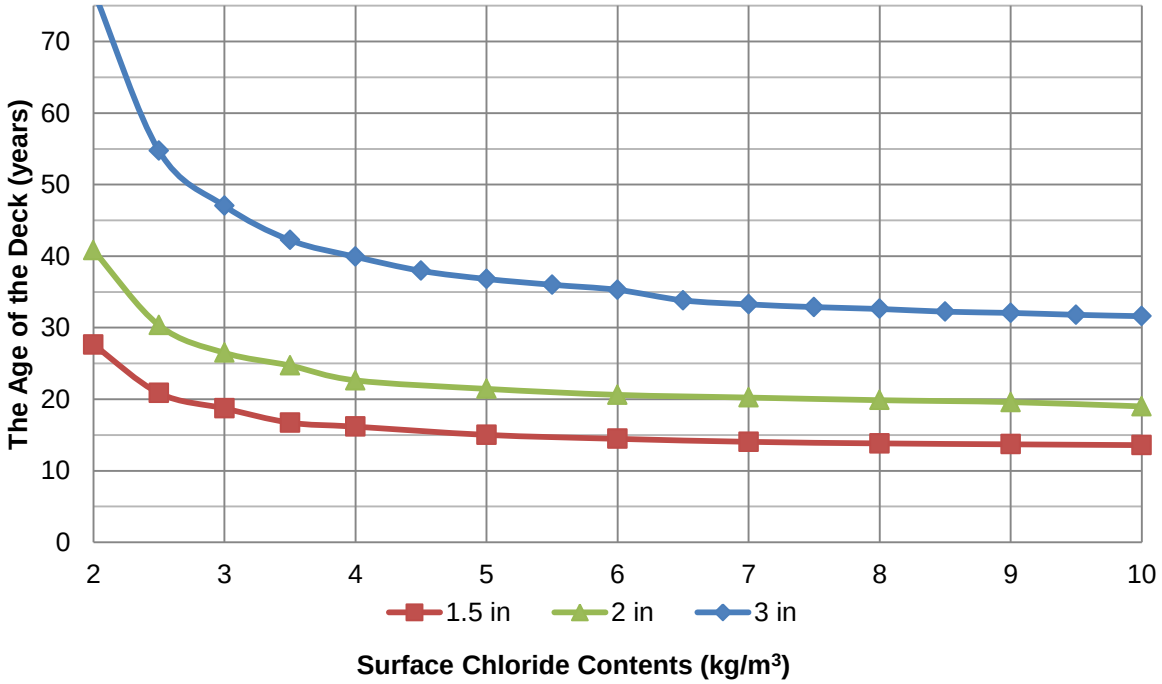

Figure 20 The influence of cover depth on time to surface cracking (T3)

Figure 19 and Figure 20 shows the need for a probability-based analysis with random input. Based on the selected deterministic model, the entire modeling process needs to be repeated for a large number of samples (e.g., 1000 times) so that the probability failure can be estimated. The only random input was C_0 with a mean of 5 kg/m^3 and a standard deviation of 1.5 kg/m^3. At the single cell level, there is no need to evaluate the structural dimension for bridge deck, since the deck was simplified to just one cell/block. An interesting comparison of the results for black steel (BS) rebar and epoxy-coated rebar (ECR) is shown in Figure 21 to Figure 23.

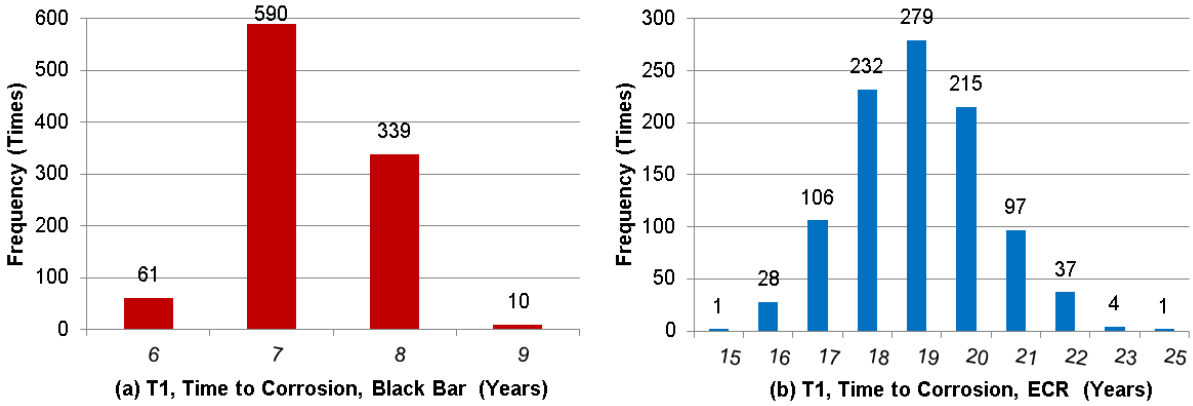

Figure 21 The distribution of corrosion time (T1) for BS amd ECR

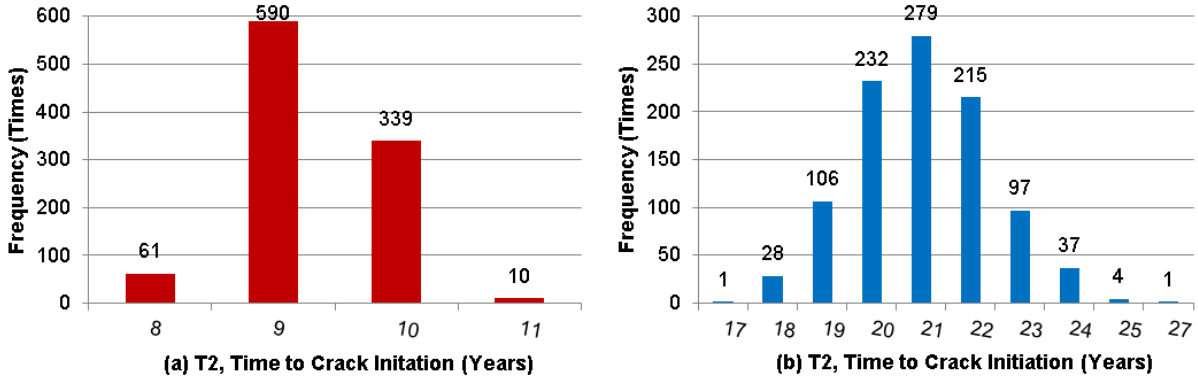

Figure 22 The distribution of crack initiation time (T2) for BS amd ECR

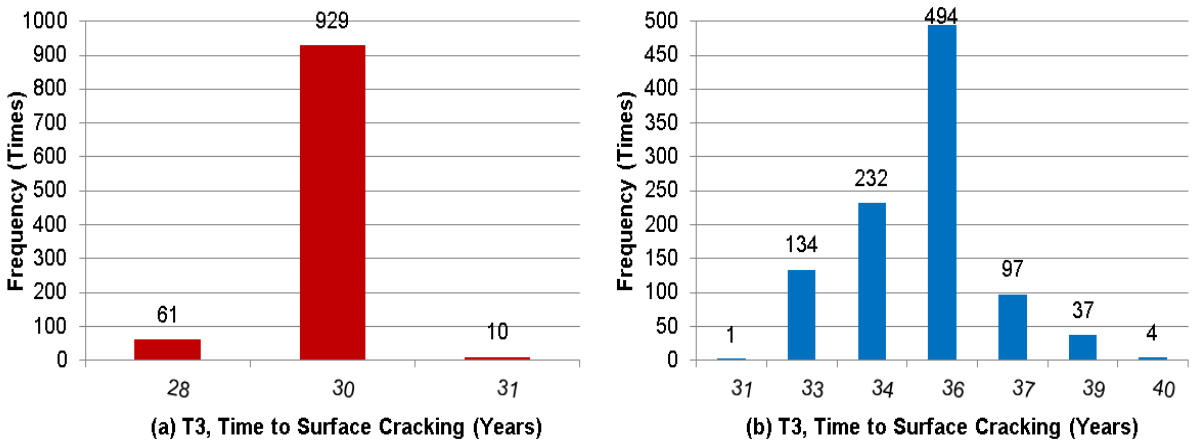

Figure 23 The distribution of different surface cracking time (T3)

The threshold value for corrosion was set at 1.2 kg/m^3 for BS and 2.2 kg/m^3 for ECR. Figure 21(a) shows that most of the corrosion in black rebar is predicted to start around 7 years. Use ECR slows down the corrosion process for almost 10 years at the bar surface. It is interesting to find that T2 had a very similar frequency as T1, see Figure 22. The reason for this result is that the gap between T1 and T2 is relatively short and the influence of random input on T2 is small. As for T3 in Figure 23, the distribution has a wider range for ECR than black steel, but the time to surface cracking in both cases still exhibits a normal distribution. The most frequent value of T3 for black steel is 30 years while for ECR it is about 36 years. Actually, it seems that ECR just delays the initiation of corrosion, but higher chloride content at the bar surface will also accelerate the corrosion rate later in the process, as shown in Figure 24. The results seem reasonable upon comparing to the statistical analyses by Winn (2011) and Winn and Burgueño 2012) which also indicate that time T3 for damage (or cracking) for BS was around 30 years and that ECR could extend service life by about 5 to 10 years.

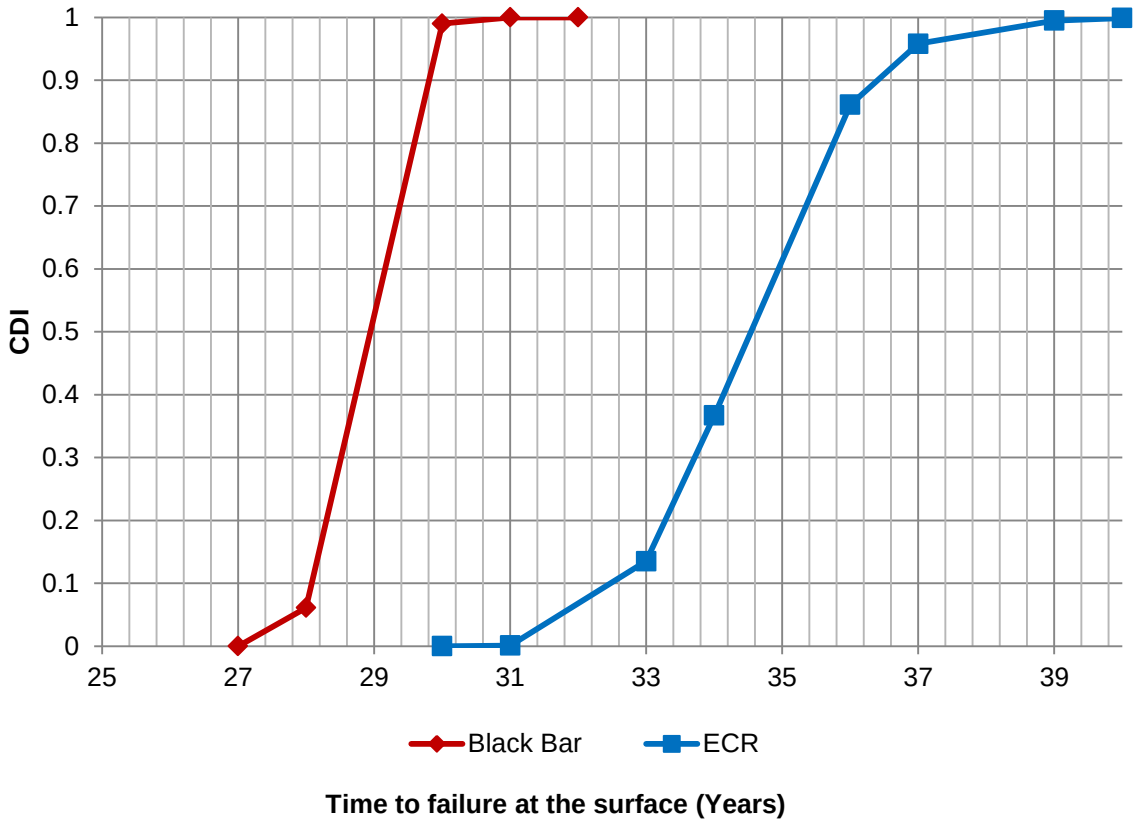

Figure 24 Cumulative Damage Index (CDI) at T3

3.4 Discussion

Mechanics-based models from the literature were identified and a three-phrase corrosion process was chosen for adoption in this research project. The model describes chloride corrosion including diffusion, rust permeation and crack propagation. Based on the summary of key parameters in the noted phases, a flow chart for the numerically implementation of the model was presented (see Figure 11). A computer program built on the Matlab environment was developed to predict the service life of RC decks due to chloride ingress. The selected deterministic models improves on the noted (see Section 2.1.2) shortcomings of existing commercial software for service life prediction

Available chloride-induced corrosion models are able to provide time-dependent information on important parameters and features of this important degradation process, including chloride

concentration at the bar surface, change of mass in the corroded bar (consumed in bar and accumulated in rust,) change in volume (in concrete, bar and rust), pressure at the interface of the concrete and bar, strain energy in the surrounding concrete ring, and crack width. Thus, the models can provide three meaningful time estimates relevant to the degradation and condition of a reinforced concrete element: the time to corrosion initiation (T1), the time to crack initiation (T2), and the time to crack propagation to the surface (T3).

However, it should be emphasized that there is no "perfect" solution since all models are based on diverse assumptions and all models have limitations by virtue of the assumptions on which they were developed. For example, the diffusion process is a very complicated mechanical-chemical-thermal coupling process. Fick's second law was chosen for this process because in spite its simplicity it provides reasonable results and it is most suitable for this project. Clearly, the service life prediction modeling could be improved by using more accurate deterministic models at the cell level. The example of statistical variance of some key parameters shows that deterministic models need to be further investigated by considering uncertainty in their parameters. Thus, a probabilistic analysis was conducted by using the presented deterministic model with consideration of random input, and it is the subject of the next chapter.

4 GLOBAL-LEVEL PROBABILISTIC DEGRADATION MODELING

The proposed framework for deck degradation modeling consists of a probability-based analysis through Monte Carlo simulations (MCS). The MCS is a general method where a desired response is determined by repeatedly solving a mathematical model using random samples from a probability distribution of inputs (Kirkpatrick et al. 2002). A similar work by Firouzi and Rahai (2011) investigated the likelihood of degradation due to chloride ingress by random sampling on a hypothetical deck. In order to mitigate the uncertain effects of material, structure and environment inputs on time to failure, probabilistic modeling provides a more reliable prediction than a deterministic model.

4.1 Monte Carlo Simulation

Reliability analysis has been discussed for life-cycle cost design of deteriorating bridge deck (Frangopol et al. 1997, Steward 2001). The general methodology for maintenance proposed by Estes and Frangopol (2001) can be summarized in three steps as shown in Table 6. It contains deterioration, cost, and decision modes (Frangopol et al. 2004).

Table 6. Optimization the lifetime maintenance of a deteriorating structure

Step 1 Deterioration	Step 2 Cost	Step 3 Decision
Input data; Mechanical model of corrosion; Criteria of structural failure;	Inspection methods and costs; Repair options; Probability of occurrence; Event tree for all of repair and no repair decision	Optimization criterion and imposed constraints The timing of inspections Updated field information

The methodology incorporates the time-dependent reliability analysis for the whole RC bridge deck domain by utilizing an appropriate number of random deterministic analyses. Ideally, the entire bridge domain should be divided into i equal elements with concrete cover and one rebar, according to the number of bars in the transverse (m) and longitudinal (n) directions of the bridge deck. The minimum number of elements i should be equal to m multiplied by n. Stewart and Mullard (2007) proposed a similar idea for service life prediction before the first time repair, which considered the bridge deck as a 2D domain and discretized it into k identical elements.

Once the domain has been defined, Monte Carlo simulations can generate stochastic random input sampled from probability distributions for each cell, using a parametric or simple bootstrap method. A large number of samples need to be repeated to solve the given model for the input variables (Kirkpatrick et al. 2002). In reality, the analysis contains many random variables, so that the precision of the simulation is based on the number of iterations.

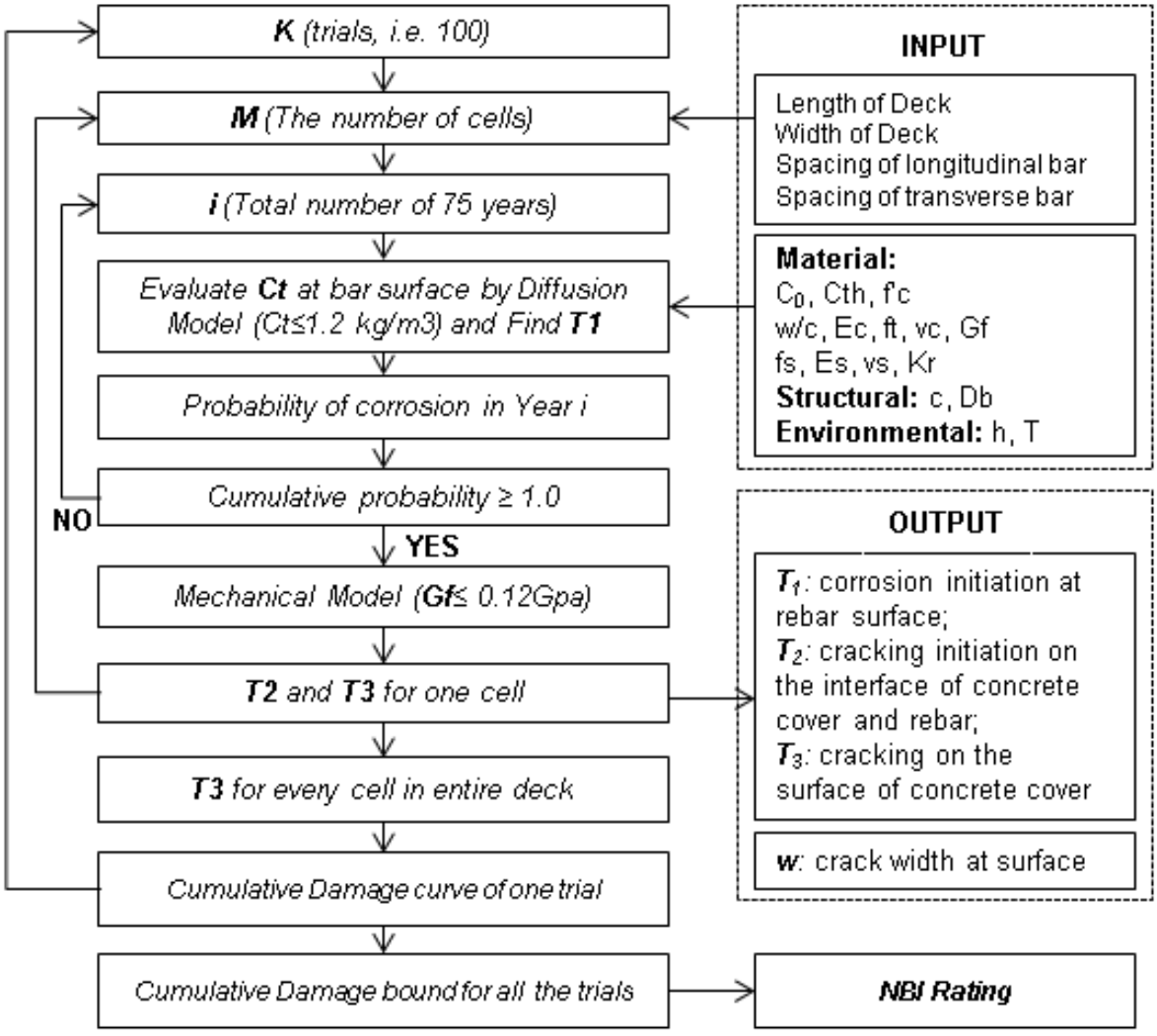

Figure 25 Flow-chart for Monte Carlo Simulation

The complete probabilistic modeling process is summarized as a flow chart in Figure 25. The process starts by calculating the total number of cells on the deck domain. The entire RC deck is divided into a large number of cells based on the deck reinforcement spacing in two directions so

that the mechanical deterministic model can be used for each cell. Note that the four key random inputs (C_0, c, f_c, D_b) are considered to be normally distributed, while the other inputs are regarded as constants with a typical value found from the literature. The next step is to calculate the corrosion time (T1) for each cell based on a random distribution of C_0 for each year. The selected range of C_0 was from 2.0 to 8.0 kg/m^3 as mean value. The time T1 in for each year was calculated by Fick's 2nd Law. A cumulative damage index (CDI) curve of the deck is calculated based on the predicted time to surface cracking from all the cells.

4.2 Statistical Random Input

An accurate deterioration model may result in a wrong prediction due to errors associated with statistical inputs. The accuracy of the model is depended on well selected input, including structural, material and environmental data. The deterioration level of bridges in Michigan varies significantly, not only with geographical location but also depending on bridge traffic, de-icing application policy, etc.. The key random statistical parameters for the Monte Carlo simulation in this project were C_0, (Surface chloride concentration), c, (Concrete cover), D_b (rebar diameter), and f'c (concrete compressive strength).

Table 7. Statistical values for C_0 in published literature (kg/m3)

Literature	Mean	COV	Distribution	Notes
Stewart and Rosowsky (1998)	3.5	0.5	Lognormal	Varied from 1.2 to 8.2
Lounis (2003)	4.56	0.4	Lognormal	
Stewart et al. (2004)	3.78	0.067	Normal	1.08% weight
Stewart and Mullard (2007)	3.05	0.74	Lognormal	
Lu et al. (2011)	2.85	0.5	Lognormal	

A debate still exists on whether some statistical values should be regarded as constant or time-dependent variable, particularly on C_0 and Cth. C_0 was considered as time-dependent and cumulative with time, because concrete deck are cyclically exposed to deicing salts. An accepted knowledge is that chloride content increases rapidly and reaches a maximum value at a certain depth of concrete cover, i.e., 12.7mm (0.5 in.) from the surface (Fanous and Wu 2005). This

means that the deck surface is subjected to changing volume of applied salts, but that the value reaches a quasi-constant in about 5 years at a certain depth (Lounis 2006). A typical range for the US reported in the literature is 1.2 to 8.2 kg/m^3, with a mean value of 3.5 kg/m^3, see **Error! eference source not found.**.

Key Parameter: Cth (threshold chloride level)

Road surfaces before 1975 were built without corrosion protection and bridges built before 1985 have little or no corrosion prevention. A typical range for a threshold value in US is from 0.6 to 1.2 kg/m3. Some literature (Kirkpatrick et al. 2002, Fanous and Wu 2005) has considered the use of epoxy-coated reinforcing (ECR) bars and typical values of Cth for ECR between 0.7 to 2.2 kg/m^3 have been suggested. Typical values for Cth are presented in Table 8.

Table 8. The statistical value for Cth in literatures (kg/m^3)

Literature	Mean or Range	COV	Distribution	Notes
Stewart and Rosowsky (1998)	0.9	0.19	Uniform	0.6-1.2
Kirkpatrick et al. (2002)	0.6~5.5	-	-	
Lounis (2003)	1.35	0.1	Lognormal	
Stewart et al. (2004)	1.4	0.125	Normal	0.4% weight
Fanous and Wu (2005)	0.73~2.19	-	-	
Stewart and Mullard (2007)	2.4	0.2	Normal	
Lounis and Daigle (2008)	0.7	0.2	Normal	0.6~0.9
Lu et al. (2011)	0.4-1.0	0.247	Uniform	

From the data presented in the tables above it can be seen that there is much debate on the correctness of data, since the data has been obtained from different laboratories and field testing. The best way to find the information for the current project would be is to look into the MDOT database, for example, all the chloride concentration measurements from concrete cores. If the data is not available, at least an appropriate range must be selected under certain assumptions. A

list of all inputs along with their typical values or ranges for the Monte Carlo simulation is given in Table 9.

Table 9. A proposed material data selection for model inputs

Item	Variable	Variable Type	Typical Value or Range
Concrete	$C_{0,}$ Surface chloride concentration	Random	2 to 8 (kg/m3)
	$C_{th,}$ Threshold value	Constant	1.2 for black rebar, 2.2 kg/m3 for ECR
	c, Concrete cover	Random	76.2 mm (3 in.) ± 11mm, 15%due to construction
	fc, compressive strength of concrete	Random	28 Mpa (4.0 ksi) to 35 Mpa (5.0 ksi)
	νc, the Poisson's ratio of concrete	Constant	0.2
	w/c, water to cement ratio	Dependent	27/(fc/1000+13.5), Vu and Stewart (2000)
	D, Diffusion coefficient	Dependent	$D=D_{w/c}(t_R/t)^{0.2}$ (cm^2/s)
	Ec, elastic modulus of concrete	Dependent	$4.73 (fc)^{1/2}$ in GPa where fc is in MPa
	ft', tensile strength of concrete	Dependent	$0.64 (fc)^{1/2}$, where fc is in MPa
Rebar	d, diameter of reinforcement	Random	#05 bar 15.62 mm ± 1.5mm, 10% due to construction
	Es, elastic modulus	Constant	210 Mpa
	νs, the Poisson's ratio of bar	Constant	0.3
	ρs, the density of steel	Constant	7850 kg/m3
Rust	Er, elastic modulus	Constant	60 Mpa
	νr, the Poisson's ratio of bar	Constant	0.485
	Kr, bulk modulus	Constant	0.667 Gpa

In Table 9: random variable refers to data with a probabilistic distribution; Cth is considered as constant that depends on rebar type; fc is considered as a time-dependent value that depends on the deck age; and d depends on different deck dimensions. Constant variables include factors that can be altered or chosen as a single value in practice, while dependent variables vary with the changes in random variables.

Highway bridges are obviously built with different structural properties. Structural data can be categorized by age, route, bridge type, length, width, etc. The proposed method for whole deck domain is based on the Monte Carlo simulation, which utilizes a deterministic mechanical model at local/cell units with random input from probability distributions. The number of iterations can be based on structural dimensions as shown in Table 10. A typical reinforcement arrangement in Michigan bridges consists of No. 6 bars spaced at 254mm (10 in.) for the top longitudinal reinforcement and No. 5 bars spaced at 229mm (9 in.) for the top transverse reinforcement. According to the number of bars in the transverse (m) and longitudinal (n) directions, the whole bridge domain is divided into i equal elements with concrete cover and at least one rebar inside. Table 10 shows two examples, the blue one for a short span bridge with 2 lanes while the red one is for a longer span with a wider deck. It is reasonable that more iterations need to be run for the latter case. Therefore, each cell in the deck domain (global level) provides a series of time-dependent information through the given local-level mechanical degradation model.

Table 10. Estimated number of MCS iterations for a given bridge deck

Length / Width	10m			20m			30m			40m		
	n	m	i	n	m	i	n	m	i	n	m	i
10m (2-lanes)	35	43	1505	35	87	3045	35	131	4585	35	174	6090
18m (4-lanes)	70	43	3010	70	87	6090	70	131	9170	70	174	12180
27m (6-lanes)	105	43	4515	105	87	9135	105	131	13755	105	174	18270

Note: n is the number of longitudinal bar; m is the number of transverse bar; i is n×m.

Environmental condition may vary significantly depending on their geographical location, which can have a significant effect on the amount and frequency of deicing substances and thus the level of surface chloride content (Frangopol and Akgul 2005). In the selected mechanical model by Liu and Weyers (1998a), corrosion rate is depended on chloride content, temperature and resistance of the concrete cover, where concrete resistance is also a function of humidity. Therefore, the corrosion rate is lowest in mid-summer and highest at end of autumn and the beginning of spring (Balafas and Burgoyne 2010). Environmental data can be found from many public online resources.

4.3 Prediction Results

Based on previous prediction results at the cell level (Figure 23 and Figure 24), it can be seen that the time to surface cracking is different for a single cell due to the variance of surface chloride concentration. However, the deterministic analysis was performed at the cell level on a single cubic cell/block that was selected randomly from the deck domain. In this section, the probabilistic analyses are carried out on an example RC deck has a length of 8 m (26 ft) and a width 3 m (9 ft). Typical bar spacing for the top transverse bars is 229 mm (9 in.). Thus, the length of deck was divided into 35 segments along the length and 12 segments along the width according to a typical spacing of 254 mm (10 in.) for the top longitudinal bars. As a result, the RC deck had a total of 420 cells with one bar inside each cell element.

The four key random inputs were C_0, c, f'_c and D_b. All these inputs were considered as normally distributed. The mean and standard deviations were [5, 1.5] (kg/m^3) for C_0, [76.2, 11] mm for the cover, [31.5, 1.75] MPa for f'_c, and [15.875, 1.58] mm for D_b, respectively. All the cells had the same C_{th}, temperature, humidity, rust properties, etc. The distribution of inputs for the entire deck is plotted in Figure 26.

The time to surface cracking for a cell can be found by executing the mechanistic model 420 times. Each deck can have a contour of T3 as shown in Figure 27. The time T3 for every cell is given by the contour levels, where the darker areas indicate earlier cracks on the surface. The distribution of T3 was calculated similar to the cell level. A cumulative damage index (CDI) curve for one cell was then estimated. The entire deck simulation was run 10 times so that 10 similar CDI curves were obtained and its mean value curve was found as shown in Figure 28. Due to the influence of random inputs, Figure 28 shows upper and lower bounds on the predicted

CDI. This is an important feature for assessment purposes because the percentage of cracking area can be mapped to the National Bridge Inventory (NBI) rating system (MDOT 2006). According to the NBI rating scale for bridge decks a deterioration area of 2% or less is rated as 6, while 2% to 10% of deterioration area is rated as 5, etc. In this case, the deck rating is predicted to decrease from sound to fair condition in 17 years, and then drop to grade 4 in 22 years. For ratings of 3 or less the deterioration of a RC deck becomes so serious so that evaluation and analysis are necessary to determine whether the deck can remain in service.

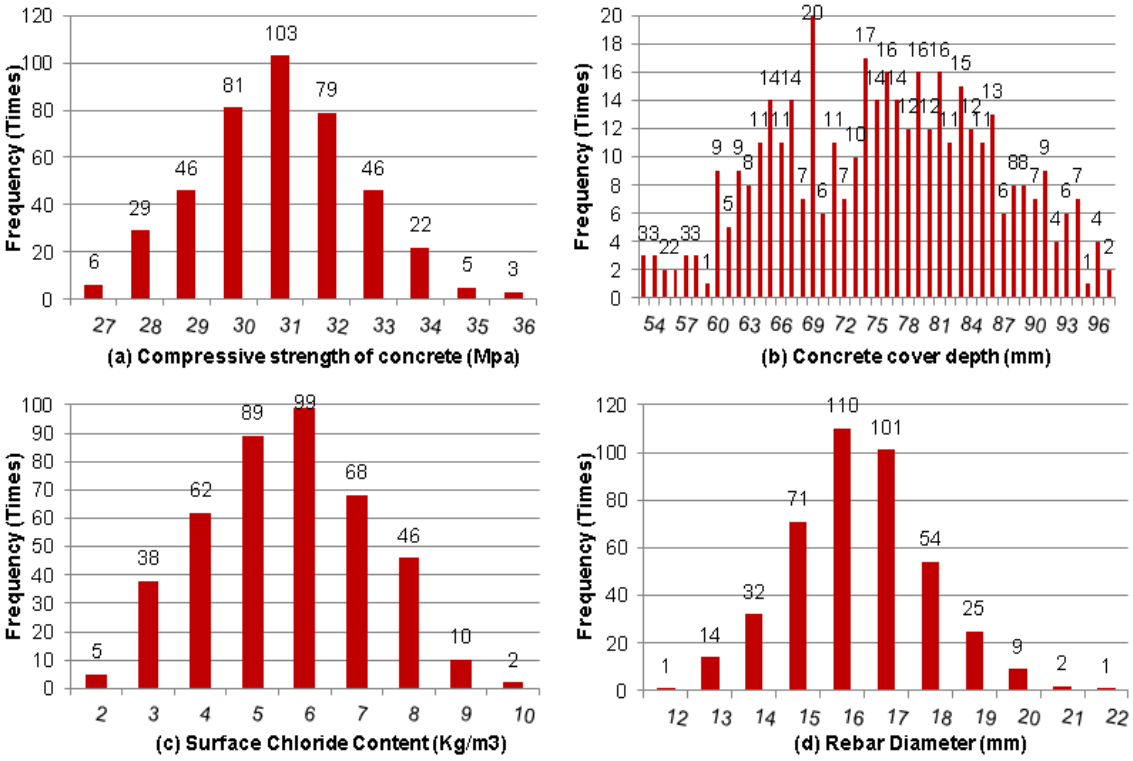

Figure 26 Distribution of random inputs

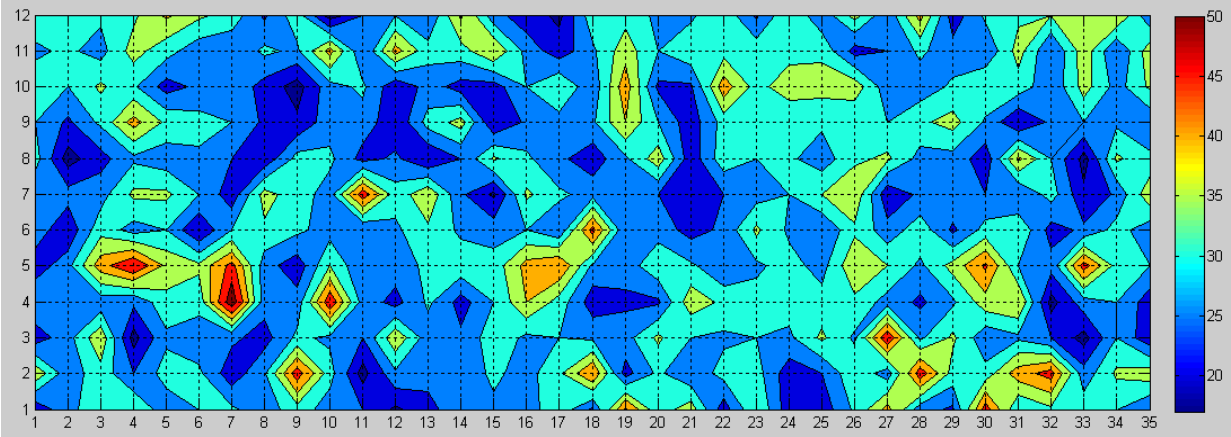

Figure 27 Contour plot of time T3 for the whole RC deck

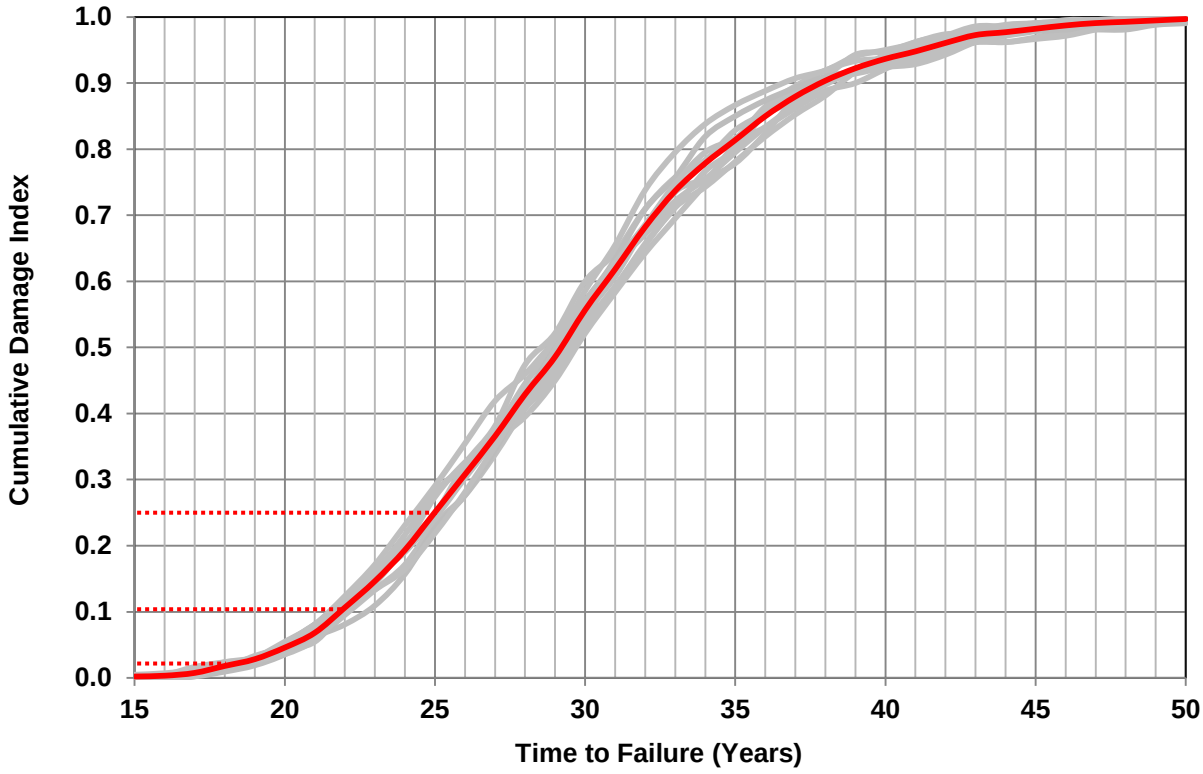

Figure 28 CDI curve and its mean value for 10 iterations through MCS

4.3.1 Single Deck in Different Time of Interest

From the contour of time to cracking (Figure 27), it can be seen that the random inputs have a significantly influence. In Chapter 3 a post-cracking function was selected (Equation 3-9) and

the time of interest (TOI) is required as an input at the beginning of the MCS. For each cell, if T3 is smaller than TOI, the MCS can proceed with the post cracking process until reaching TOI. If the T3 is larger than TOI, the cell has not cracked yet. Thus, a contour plot of crack width can be also be obtained. The post cracking process of the example deck can be plotted for different TOI. Figure 29 to Figure 31 show the crack width at years 20, 30 and 40. It can be seen that the spatial distribution of crack widths at different TOI varies significantly. Figure 29 shows that most of deck is still uncracked at year 20, while large crack widths are predicted throughout the deck surface at year 40 (Figure 31).

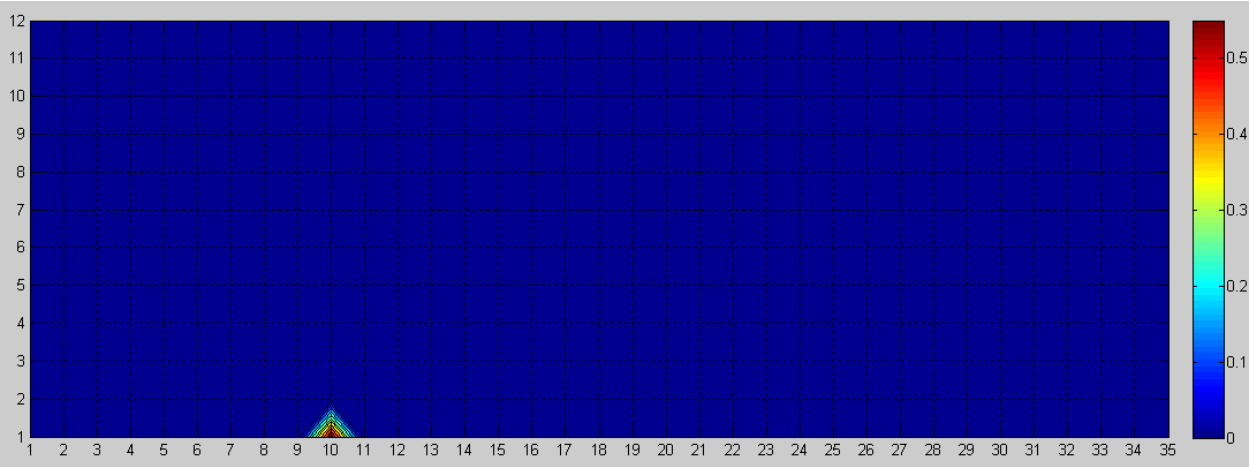

Figure 29: Contour plot of surface crack width at Year 20

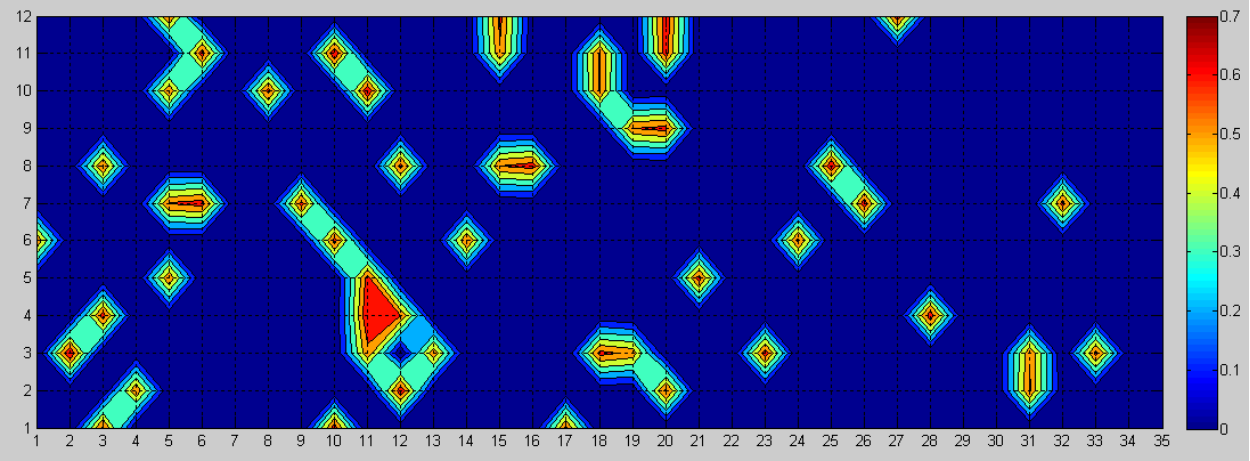

Figure 30: Contour plot of surface crack width at Year 30

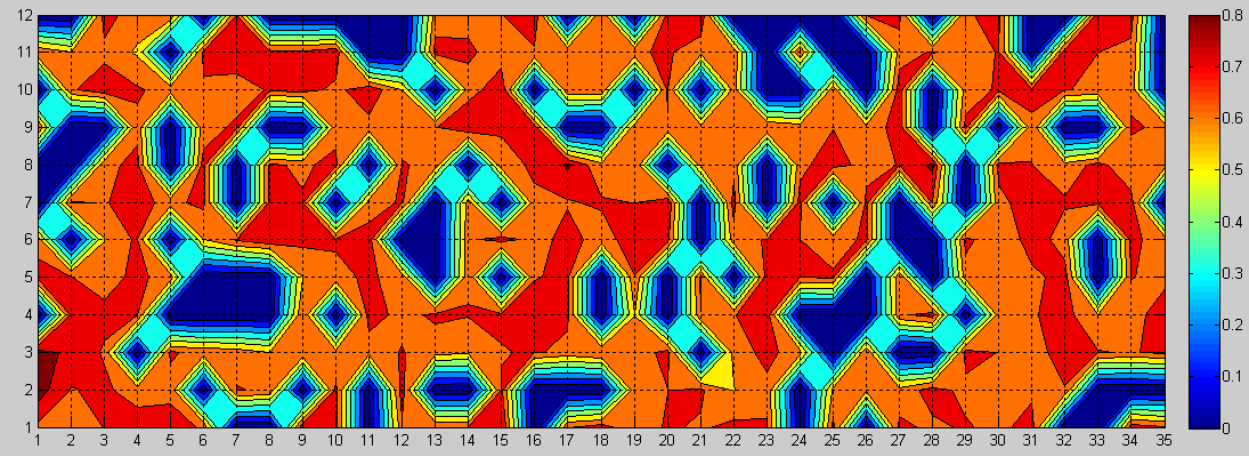

Figure 31: Contour plot of surface crack width at Year 40

4.3.2 One Deck in Different Regions

In the following example, the same RC deck is assumed to be at three different locations in Michigan. The environmental data is listed in Table 11. All decks are assumed built in 1975. For a year of interest (YOI) of 2012, the predicted crack width contour for the different locations is shown in Figure 32 to Figure 34. It is noted that the same deck in the rural area of Sault Ste. Marie in the Upper Peninsula is predicted to be in a very good condition, while a deck in a large city center or industrial zone is predicted to degrade much faster. Thus, the environmental data has a significant effect on the deck deterioration process.

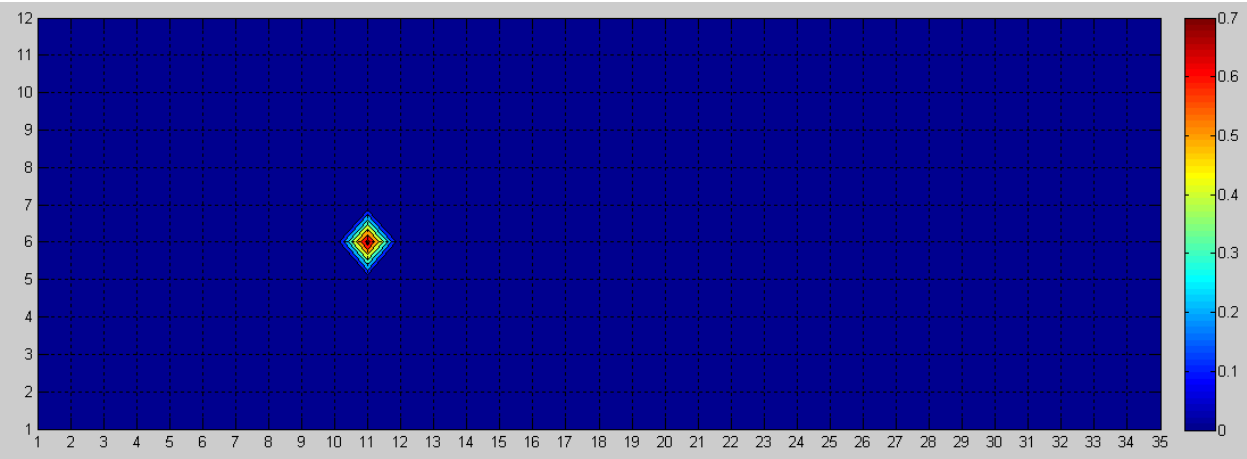

Figure 32: Contour plot of crack width in Sault Ste. Marie, MI (Year 2012)

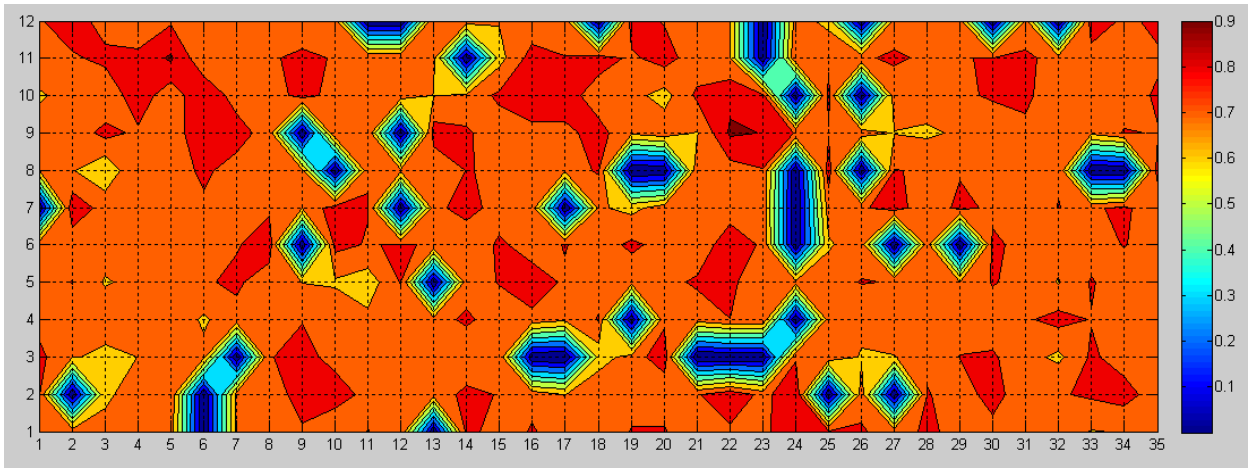

Figure 33: Contour plot of crack width in Lansing, MI (Year 2012)

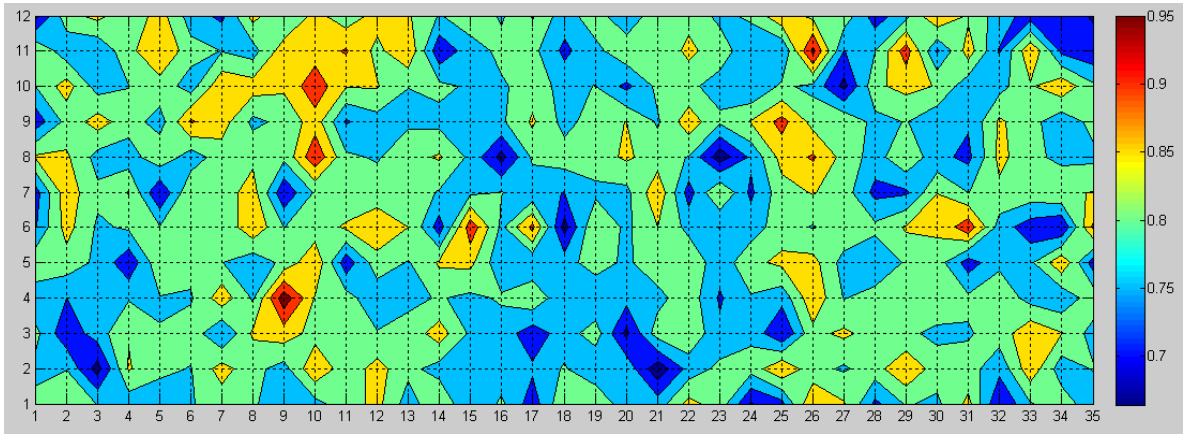

Figure 34: Contour of crack width in Detroit, MI (Year 2012)

Table 11. Environmental data for three different locations in Michigan

	Case 1	Case 2	Case 3
Location Type	Open Country	City Center	Industrial Zone
City Name	Sault Ste Marie	Lansing	Detroit
Humidity Range (%)	0.69~0.80	0.58~0.78	0.60~0.73
Temperature Range (°C)	-15~24	-10~28	-9~29
Chloride Content (kg/m3)	(1.8, 0.2)	(3.6, 0.4)	(5.4, 0.6)

4.4 Summary

A probabilistic-based model through Monte Carlo simulations (MCS) was developed to take into account the special distribution of input parameters according to statistical distributions. The MCS provide a more reliable prediction than deterministic models by considering the uncertainty in material, structural and environmental parameters. Appropriate statistical values for key parameters were selected for the MCS approach whereby material and environmental properties at the local/cell level were varied based on probability distributions. A cumulative damage index (CDI) curve for the deck was calculated based on the predicted time to surface cracking from all the cells. The damage severity of the decks was also presented as contour plots of the the time to failure/cracking and crack width. The prediction results show that the developed framework can capture the random nature of the degradation process.

5 MODEL VALIDATION

5.1 Mapping Predictions to Empirical Ratings

As mentioned in Chapter 4, the prediction results of cumulative damage and crack width from the MCS may assist in linking the results from the mechanistic model to the commonly used NBI rating system (MDOT 2006). The NBI rating system used by highway agencies is an empirical scale to describe the condition of the bridge elements measured on an integer scale of 0 to 9. The descriptors defining the different condition ratings are given in Table 12. Two major criteria used in the NBI rating are: (a) the percentage of damaged area, or damage extent, and (b) the amount of cracks (crack density), their width and their spacing, or damage severity.

The first criterion for the NBI rating is the damage extent, or percentage of damaged area. Maintenance decisions based on damaged area differs among agencies. Krauss et al. (2009) presents an interesting survey from 46 agencies on the evaluation of deck condition, including 41 US states, 4 Canadian provinces and Puerto Rico. The timing to replace the whole deck varies among states according to the damaged area, such as 20% in California, 25% in Virginia, 35% in Illinois, 50% in Massachusetts and Kansas. According to the NBI rating system used in Michigan, decks are graded to be in serious condition when the combined damaged area is more than 25%.

Table 12. NBI Condition rating system for bridge deck inspection

Code	Description
N	NOT APPLICABLE. Code N for culverts and other structures without decks, e.g., filled arch bridge.
9	NEW CONDITION. No noticeable or noteworthy deficiencies which affect the condition of the deck.
8	GOOD CONDITION. Minor cracking less than 1/32" wide (0.8mm) with no spalling, scaling or delamination on the deck surface or underneath.
7	GOOD CONDITION. Open cracks less than 1/16" wide (1.6mm) at a spacing of 10 ft or more, light shallow scaling allowed on the deck surface or underneath. Deck will function as designed.
6	FAIR CONDITION. Deterioration of the combined area of the top and bottom surface of the deck is 2% or less of the total area. There may be a considerable number of open cracks greater than 1/16" wide (1.6mm) at a spacing of 5 ft or less on the deck surface or underneath. Medium scaling on the surface is 1/4" to 1/2" (6.4 mm to 13 mm) in depth. Deck will function as designed.
5	FAIR CONDITION. Deterioration of the combined area of the top and bottom surface of the deck is between 2% and 10% of the total area. There can be excessive cracking in the surface. Heavy scaling 1/2" to 1" in depth (13 mm to 26 mm) can be present. Deck will function as designed.
4	POOR CONDITION. Deterioration of the combined area of the top and bottom surface of the deck is between 10 - 25% of the total area. Deck will function as designed.
3	SERIOUS CONDITION. The deck is showing advanced deterioration that has seriously affected the primary structural components. Deterioration of the combined area of the top and bottom surface of the deck is more than 25% of the total area. Structural evaluation and/or load analysis may be necessary to determine if the structure can continue to function without restricted loading or structurally engineered temporary supports. There may be a need to increase the frequency of inspections.
2	CRITICAL CONDITION. Deterioration has progressed to the point where the deck will not support design loads and is therefore posted for reduced loads. Emergency deck repairs or shoring with structurally engineered temporary supports may be required by the crews. There may be a need to increase the frequency of inspections.
1	IMMINENT FAILURE CONDITION. Bridge is closed to traffic due to the potential for deck failure, but corrective action may put the bridge back in service.
0	FAILED CONDITION. Bridge closed. Coordinate with SI&A item 41.

The second criterion for the NBI rating is damage severity, dictated by crack width and crack distribution. Cracking maps have practical significance because the decision maker can determine the repair time and corresponding repair options for extend the longevity of deck. Many published works discuss the acceptable crack width for controlling chloride corrosion and other factors. In TRB Research Circular E-C107 (2006) it is noted that cracks larger than 1 mm

will increase corrosion rate. As shown in Figure 35, a crack width of 0.3 mm (0.013 in) is frequently recommended as the maximum limit. Rahim et al. (2006) reported that some European countries set 0.2 mm as the limit crack width for service life. Other researchers have also noted that crack widths as small as 0.05 mm could be significantly detrimental to the durability of a concrete deck in a harsh environment, e.g., when subjected to applied salt or sea splash. However, it can be seen from Figure 35 that the smallest measurement level in a crack width estimator is 0.2 mm. Thus, it may be impractical for bridge inspectors to check crack widths smaller than this value.

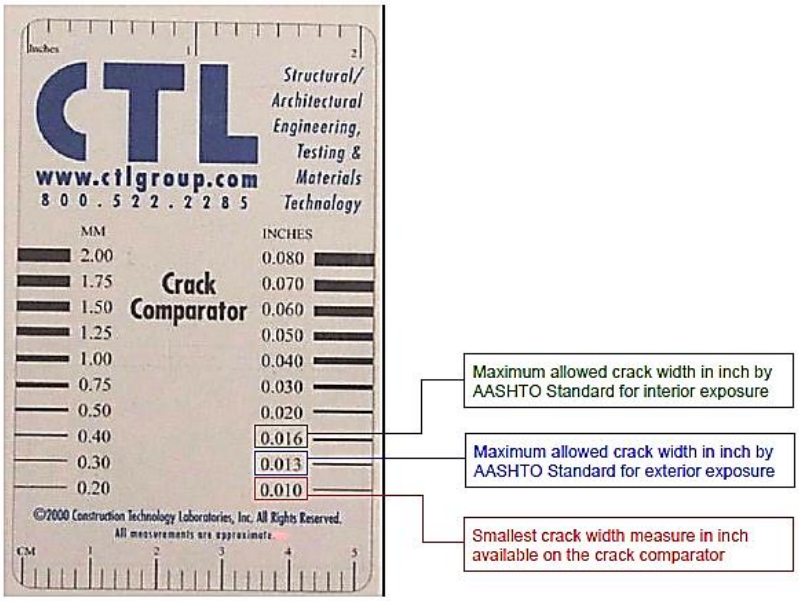

Figure 35: A typical crack comparator on field inspection (Choo and Harik 2006)

Finally, different crack widths should be cataloged as the percentage of total cracking based on the acceptable service limits. For instance, a bridge deck with an NBI rating of 5 must have damaged area between 2% to 10% according to the NBI rating guide (MDOT 2006). However, the description of cracked condition in the NBI rating guide is too vague. For example, it defines the fair condition 6 as "a considerable number of open cracks greater than 1.6 mm." Similar descriptions can be found in condition 5, namely "there can be excessive cracking in the surface." These descriptions are difficult to meet precisely and could thus lead to errors in

assigning a rating level. Therefore, the predicted NBI rating by the MCS is only estimated through the damaged area and the corresponding CDI curve.

Krauss's survey (2009) reported that all agencies evaluate the decks by visual inspection while only 13 out of 43 agencies check the crack map and width, as shown in Table 13. 21 out of 46 agencies carried out frequent chloride measurements while 30 out of 39 never conduct testing for freeze-thaw or air content. An interesting aspect in the survey is the expectation on different repair options. Two major repair techniques are the use of overlays and sealers. 90% of the 43 reported agencies expected that the longevity of a bridge deck can be extended by at least 10 years. Some agencies note that it is unnecessary to use sealer or overlays to protect the deck. Table 14 provides a general summary of information provided by the DOT officials.

Table 13. The use of the evaluation technique in the survey

Evaluation Technique/Frequency of Use	Typically	Occasionally	Never
Visual Inspection	45	0	0
Hammer or chain sounding	34	10	0
Crack mapping/width measurement	13	24	6
Core sampling and strength testing	13	25	5
Core sampling and petrographic evaluation	5	22	15
Chloride measurement	21	21	4
Half-cell potential measurement	8	20	14
Corrosion rate	2	13	24
Infrared Thermography	0	8	30
Freeze/thaw testing or air content	2	7	30
Pulse velocity-ultrasonic	0	3	35
Ground penetrating radar (GPR)	1	18	19
Impact/echo	1	11	27

As shown in Chapter 4, Monte Carlo simulations (MCS) can be implemented with random inputs. The most important output of the MCS process is the time to surface cracking at the cell level. The probability of damage on the whole deck domain is then calculated by accumulating time to failure for each cell. Due to the influence of random model input, the CDI curves can be estimated through a number of iterations. Thus, a CDI bound is found with upper and lower bands as shown in Figure 36.

Table 14. Summary of rehabilitation methods from survey (Krauss 2009)

Rehabilitation Method	Expected Service Life Range (years) [Mean]	Cost Range ($/sq. ft.) [Mean]	Overlay Thickness (in.) [Mean]	Estimated Installation Time	Current Use
Rigid Overlays					
High Performance Concrete Overlays	10 - 40 [16 - 29]	5 - 45 [17 - 25]	1 - 5 [1.6 - 3.5]	>3 days	Mixed
Low Slump Concrete Overlays	10 - 45 [16 - 32]	4 - 45 [13 - 19]	1.5 - 4 [2.0 - 3.1]	>3 days	Static
Latex Modified Concrete Overlays	10 - 50 [14 - 29]	1 - 150 [18 - 39]	1 - 5 [1.5 - 2.7]	<24 hrs (UHELMC)*, 1-3 days (LMC)**	Mixed
Asphalt-Based Overlays					
Asphalt Overlays with a Membrane	3 - 40 [12 - 19]	1.5 - 23.5 [3.1 - 7.6]	1.5 - 4 [2.4 - 3.1]	>3 days	Static
Miscellaneous Asphalt Overlays	5 - 20 [8 - 15]	1 - 3 [1 response]	0.38 - 2.5 [0.8 - 1.5]	1 - 3 days	Static
Other Rehabilitation Systems					
Polymer Overlays	1 - 35 [9 - 18]	3 - 60 [10 - 17]	0.13 - 6 [0.5 - 1.4]	<24 hrs	Increasing
Crack Repair	2 - 75 [19 - 33]	***	N/A	<24 hrs	Static
Sealers	1 - 20 [4 - 10]	0.33 - 15 [3 - 5]	N/A	<24 hrs	Increasing
Deck replacement	15 - 50 [27 - 32]	15 - 100 [43 - 53]	N/A	>3 days	Static

* Ultra high early cement with latex
**High early (Type III) cement with latex
*** Survey respondents did not provide cost estimates

Under the same random inputs, 100 iterations for the previous example deck (8m × 3m) were calculated and 100 CDI curves were obtained through the MCS method. Figure 37 presents 100 cumulative damage curves. A close up of the bounds defined by the multiple simulations is shown in Figure 38. Figure 39 exhibits part of the CDI bound because only the low CDI (≤ 25%) is needed for mapping the CDI result to the NBI rating. It can be seen that the CDI curves have upper and lower bounds because of the uncertainty of the input data. Thus, for any given NBI rating a time span can be provided by the CDI bounds. For example, the deck is predicted to drop to an NBI rating of 4 when the combined damaged area is 10%, i.e., 22 and 24 years in this case.

According to the damage area in the NBI rating, the corresponding predicted NBI bound was calculated and the mean value was found after getting all the NBI bounds, as shown in Figure 38.

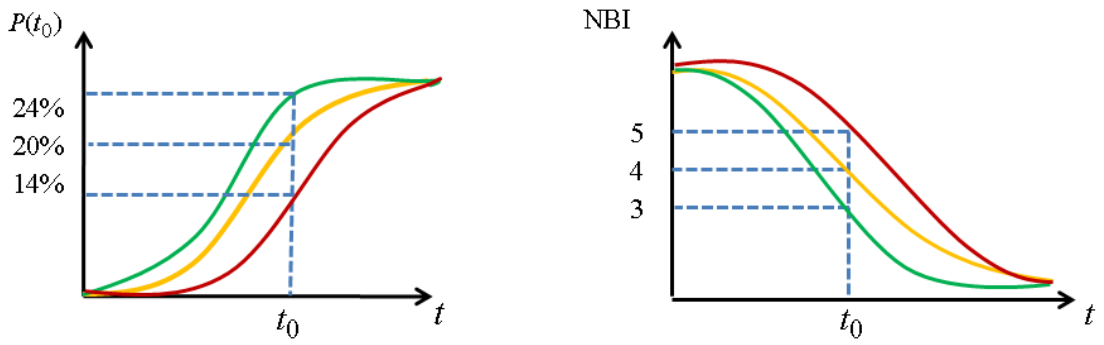

Figure 36 Schematic of the CDI curve and the corresponding predicted NBI rating

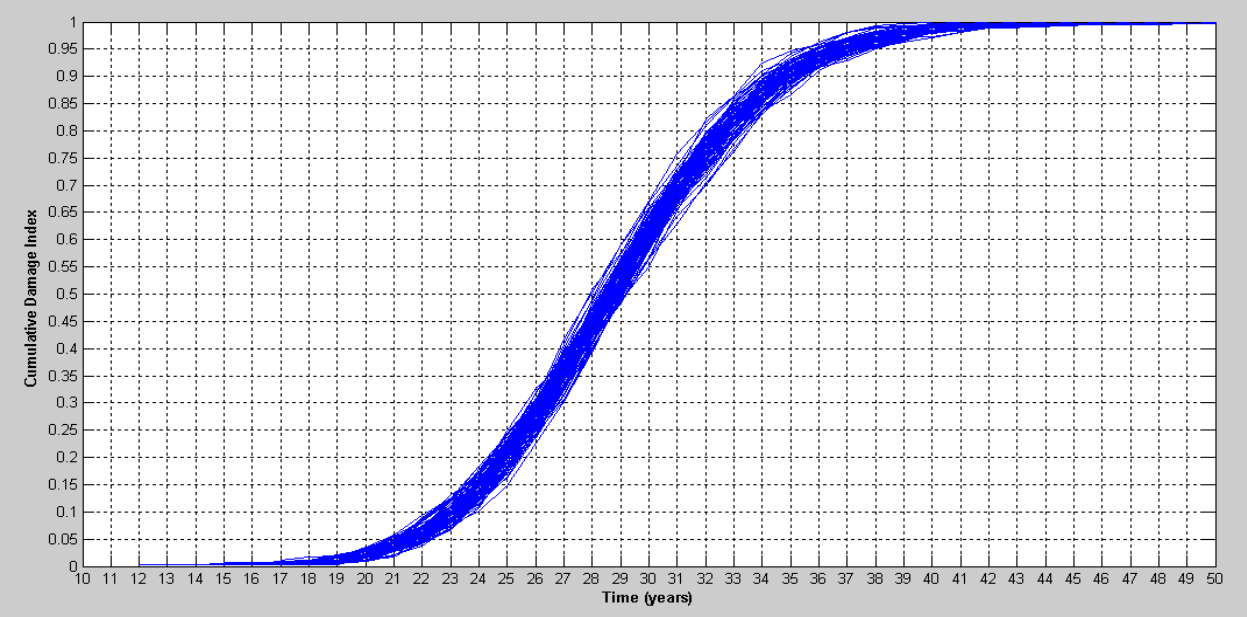

Figure 37 Cumulative damage bound

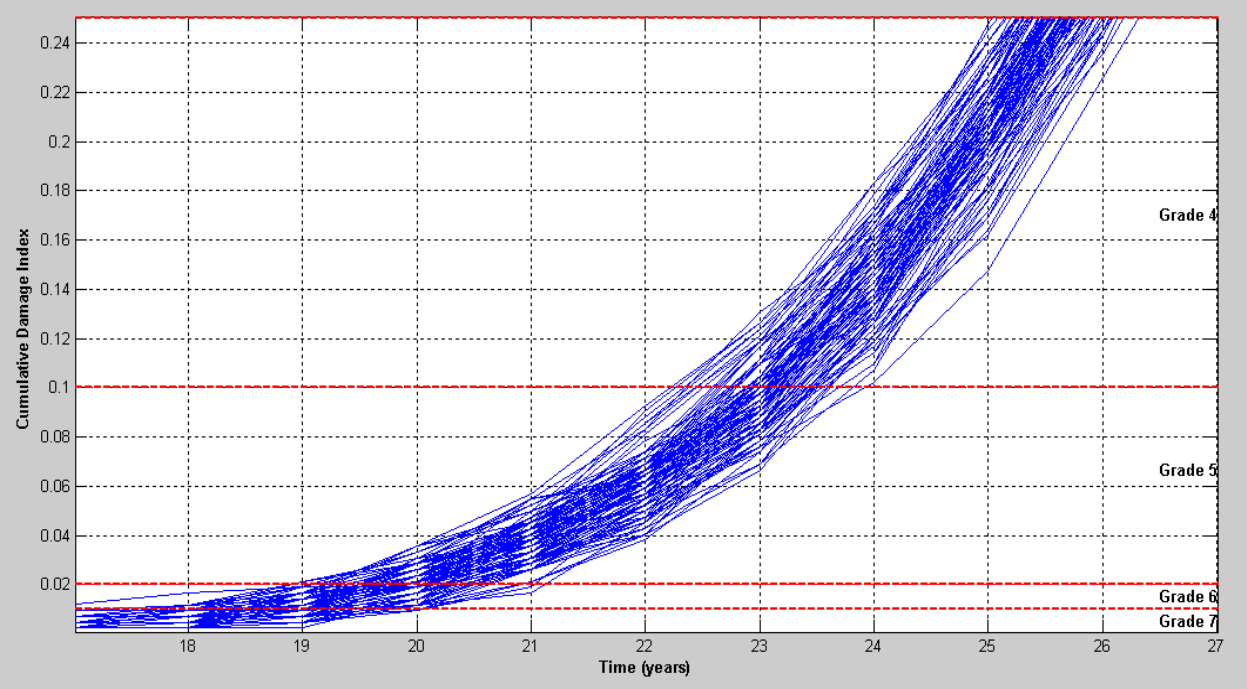

Figure 38: Details view on CDI bound and NBI rating

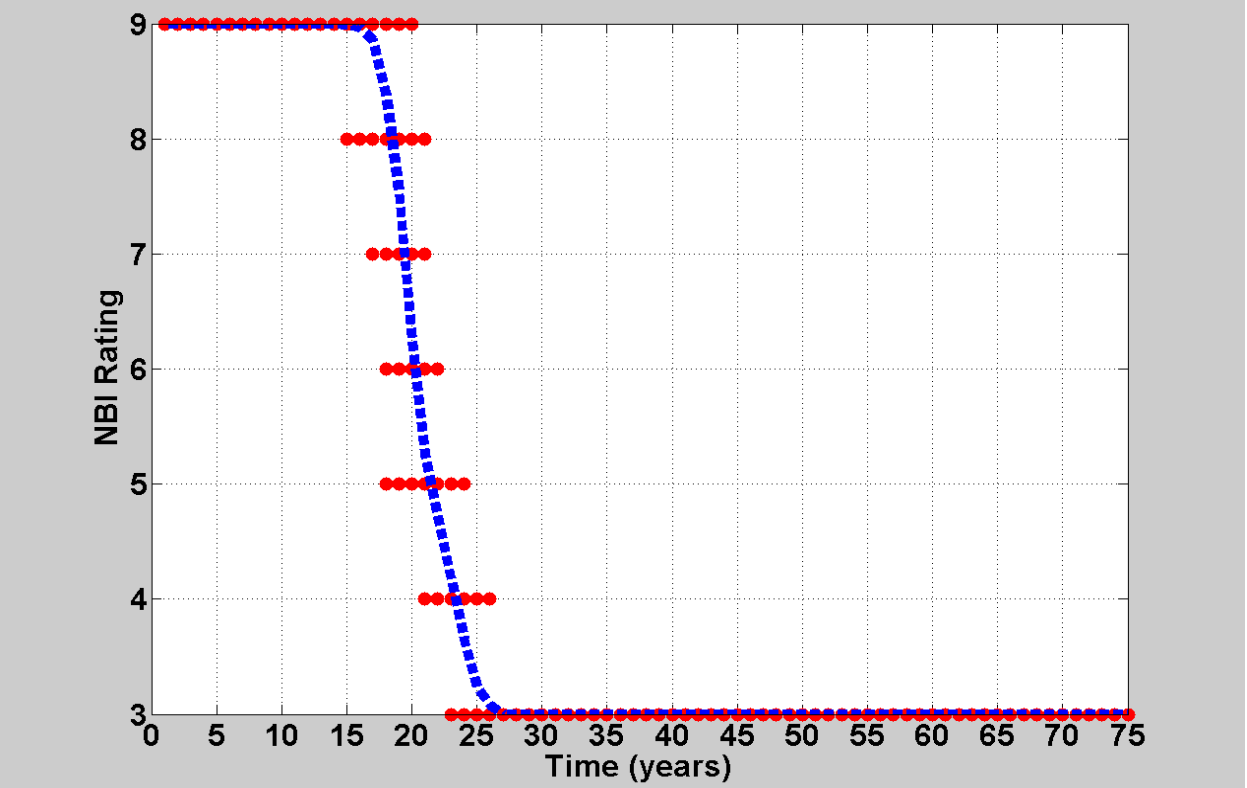

Figure 39 The Predicted NBI rating bound and Mean Value Curve

5.2 Representative Cells

A deterministic analysis at the cell level can provide the time to surface cracking and crack width due to chloride-ingress. However, at the deck level, the statistical-based prediction needs to take the spatial variation of the localized prediction into account. For a real bridge, there could be a very large number of cells in the deck domain. Thus, determining the appropriate sample size is a necessary step in the modeling process. Choosing random samples to spatially represent the whole population of cells on the deck is necessary to achieve an acceptable prediction. Three constraints for estimating the appropriate sample size of the cells were:

(a) The requirement of one bar per cell in the deterministic model;

(b) Equal probability of damage on the entire deck;

(c) The resolution according to the NBI rating (for example, 2% damaged area for a 7 rating);

The first constraint is a prerequisite for the cell-level deterministic model. The mechanics-based local degradation model has only one bar per cell. The dimension of the cell was chosen to be equal to the spacing of the transverse bars. Cracks occurring above one bar cannot represent the condition of all the bars. More bars in one cylinder could underestimate other failure modes like the spalling or delamination (Zhou 2005). Thus, it is necessary to keep one bar per cell.

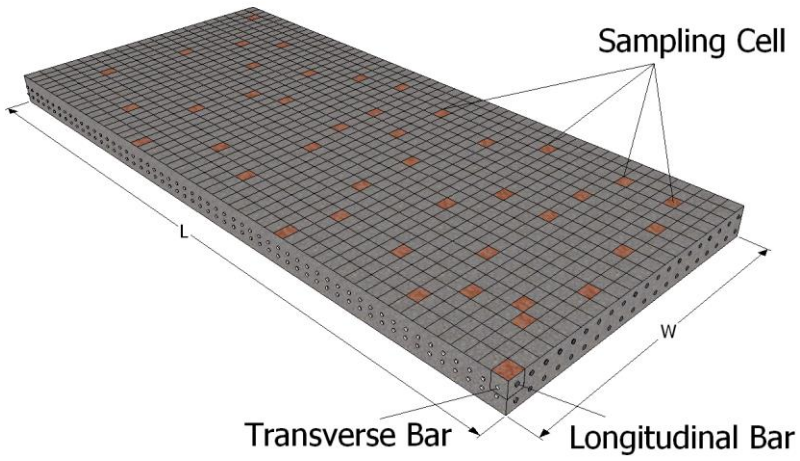

Figure 40: The sampling cells for the MCS

The second constraint represents an equal probability of damage. Given that the deterioration of the RC deck is assumed to be only associated with environmental conditions, the probability of damage in each cell should be similar. As shown in Figure 40, a number of cells are selected as the samples to represent the condition for the entire deck. However, there is no set percentage that this is accurate for every RC deck. At the same time, it would be inefficient, if too many cells are chosen with no significant improvement in the accuracy of prediction. Thus, Equation 5-1 was used to determine the sample size (Watson, 2001):

$$n = \frac{P \cdot (1-P)}{A^2/Z^2 + P \cdot (1-P)/N} \tag{5-1}$$

where n = sample size required; P = estimated variance in population, as a decimal: (0.5 for 50-50, 0.3 for 70-30); A = precision desired, expressed as a decimal (i.e., 0.03, 0.05, 0.1 for 3%, 5%, 10%); Z = based on confidence level: 1.96 for 95% confidence, 1.6449 for 90% and 2.5758 for 99%; N = number of samples in the population. In this case, the prediction assumes Z as 95%, P as 50% and A as 5%. N is the total number of cells on the entire deck, obtained based on the bar spacing. It is estimated that 394 cells are required for a total number of 25,000.

The third constraint is about the resolution of the deterioration on the deck. After estimating T3 in each cell the number of damaged cells along any time in service life can be determined. The number of cells must be enough to capture the damaged area required by the NBI rating criteria. For example, consider a deck with a total number of 100 sample cells. In the NBI rating, 2% damaged area is rated as a 7. If the model needs to predict a rating 7, at least 2 damaged cells should be captured. Decks with a rating lower than 3 were not considered in this study.

5.3 Deck Selection for the Validation

Beside the uncertainty in the random inputs, another impediment for the validation of degradation models is the lack of sufficient realistic data. The 2010 NBI database currently used in this study is a rich source of realistic and historic condition assessments of bridges across the state of Michigan. The use of these records can provide a unique set to validate the prediction models. Winn (2011) and Winn and Burgueño (2012) noted that inspection records are only available after 1992 and that inspections do not always occur on the ideal biannual basis. In

addition, some inspection records are missing or miscoded and there are many inspections that occur after reconstructive work. Refinement of the data carried was out by Winn (2011) to minimize the potentially negative effects when using this data for prediction model development and/or validation for simulating the degradation process.

It is known that corrosion due to environmental conditions becomes a dominant factor in the later period of a deck's service life. It should be noted that decks with ECR were built since the 1980s, which means that most of these decks are less than 30 years old. Thus, degradation modeling for these bridges with relatively young ages is not the focus of this study. Decks that have chloride corrosion related deterioration are the suitable candidates for the MCS framework presented here. Thus, it is more reasonable to compare observed data of decks that are between 20 and 40 years of age with the predicted NBI rating.

Ten decks were chosen randomly to show the importance of appropriate selection of the decks. These ten decks (Network 1) are located across the University Region as shown in Figure 41. Decks with black steel (BS) are marked in red (1-5) and those with epoxy coated reinforcement (ECR) in blue (6-10). The technical parameters of the network are summarized in Table 15. The bridges were selected with consideration of the diversity in the sample population by five influential parameters: year built, average daily truck traffic (ADTT), average daily traffic (ADT), span length, and the number of spans.

Figure 41: Numbering of bridges from the University Region (Network 1)

The manual inspection data for Network 1 is listed in Table 16. For all the decks in this simulation the number of sampling size was estimated between 350 and 400. For both deck groups with BS and ECR, the assumed environmental scenario was exposure to a moderate chloride level. Since those decks are exposed to similar environmental condition and have similar sampling size, the prediction of deck deterioration by the MCS was run only one time for BS and one time for ECR. However, the actual chloride content on the deck surface is still random. Thus, two mean values based on the literature were assumed: low chloride (1.8 kg/m^3) and (3.6 kg/m^3). Two hundred (200) trials of the MCS were run for both mean values.

Table 15. Technical parameters of bridges in Network 1

#	Bridge ID	Year Built	Lanes	ADT	Skew	Material	Spans	Max Span (ft)	Length (ft)	Width (ft)	Rebar
1	58158033000S020	1961	2	2250	31	3	4	82	242.8	32.8	0
2	58158033000B052	1948	2	17569	0	3	3	49.9	119.8	47.6	0
3	33133035000S070	1966	2	16286	8	3	3	67.9	138.8	42.3	0
4	81181105000S090	1966	2	13648	10	5	3	42	114.8	42.6	0
5	23123061000S030	1972	2	3875	13	3	7	91.9	476	50.2	0
6	30130071000B050	1991	2	5142	0	5	1	30.8	30.8	51.2	1
7	19119042000S140	1989	2	17652	40	5	3	66.9	146	46.9	1
8	47147082000R020	2006	2	18396	0	5	3	55.4	123.7	63	1
9	76176024000S060	1988	2	15505	0	5	3	81	169.9	46.9	1
10	58158152000B041	2009	3	26929	12	4	3	90	200	61.3	1

Note: ADT means the average daily traffic volume; Material (3 Steel, simple or Cantilever, 4 Steel continuous, 5 Prestressed Concrete); Rebar (1, Epoxy Coated Reinforcing, 0, none).

Table 16. Inspection data for bridges in Network 1

#	Bridge ID	94	95	96	97	98	99	00	01	02	03	04	05	06	07	08	09	10
1	58158033000S020								3		3							
2	58158033000B052						6		6		6	5						
3	33133035000S070										6	5						
4	81181105000S090	7																
5	23123061000S030		6		4		4											
6	30130071000B050	8		8		8		7										
7	19119042000S140	9			7	6		6		7		6		6		6		5
8	47147082000R020																8	
9	76176024000S060		8		8		7		8		8		7		7		6	
10	58158152000B041																7	

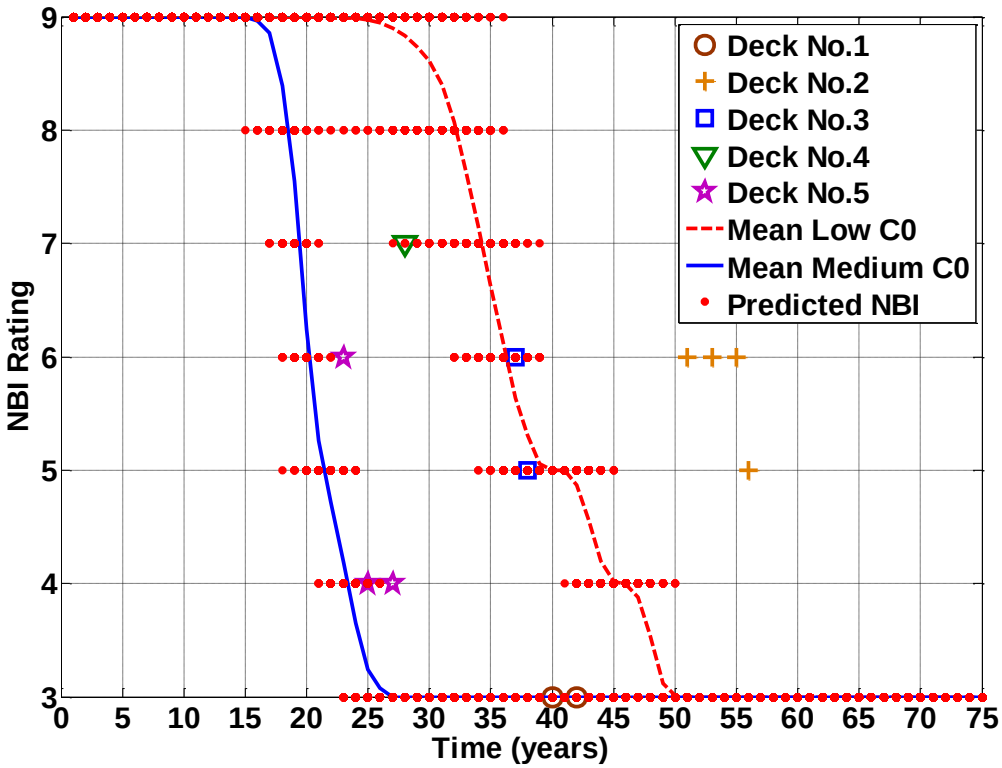

Figure 42: Predicted degradation and actual NBI ratings for Network 1 decks (BS)

The predicted degradation curve in terms of NBI ratings for decks with black steel (BS) rebar is given in Figure 42. The mean value of the predicted NBI is presented as a solid line for low C_0 and a dashed line for medium C_0. The corresponding NBI bound is plotted in small dots. Regardless the deterioration due to other mechanisms, the manual data fits the predicted data reasonably well. It can be seen that the severity of these decks is different. Deck No. 2 has an old age but a high rating. Since this deck exhibits the evidence of repair or replacement, it is not considered appropriate for validation of the model. Decks Nos. 1 and 5 matched the predicted NBI rating with low mean C_0, while Decks Nos. 3 and 4 fit the predicted NBI with medium mean C_0. However, it is hard to draw a conclusion at this point because all of these decks were also exposed to other effects. Therefore, more decks need to be investigated for further validation.

Similarly, the predicted NBI degradation curves for decks with ECR are shown in Figure 43. However, the inspection data of all these decks is offset from the prediction of both low and medium C_0. It is worth to note that ECR decks have been built starting around the early 1980s.

Thus, most of the decks have an age less than 30 years. The degradation at early age can also be due to other reasons. For example, Decks Nos. 7 and 9 have a similar age, ADT, span length, and the number of spans, but the deterioration of Deck No. 7 is faster than that of No. 9. A possible explanation is that Deck No. 7 has a skew angle of 40 degrees while Deck No. 9 is a straight bridge.

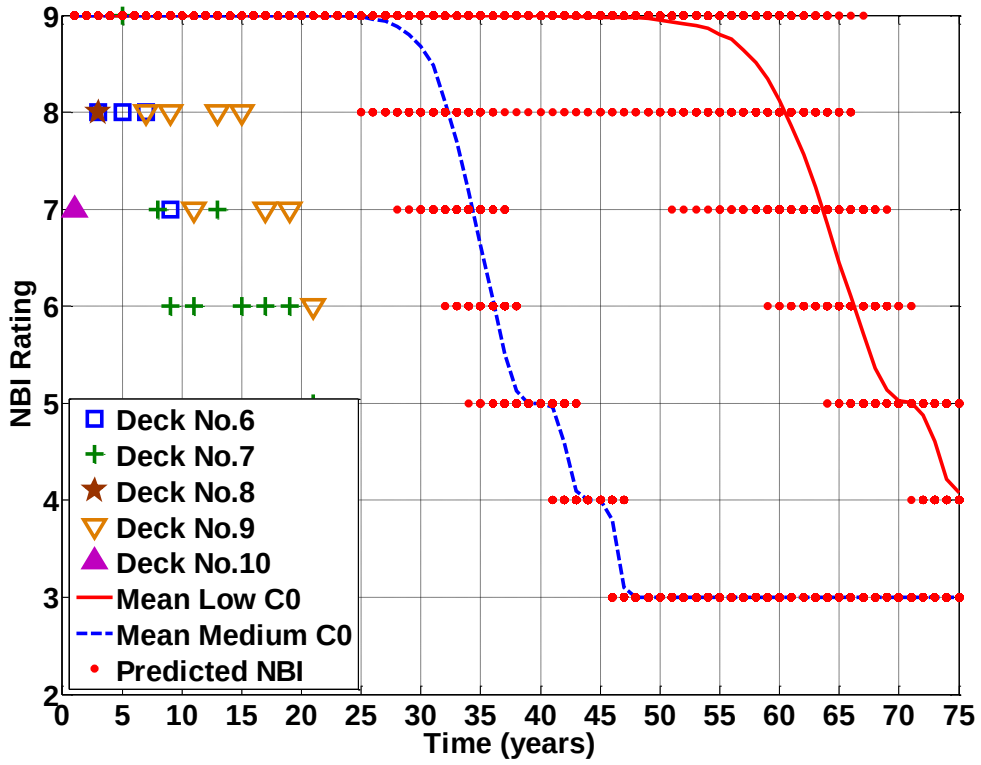

Figure 43: Predicted degradation and actual NBI rating for Network 1 decks (ECR)

Thus, it can be seen that the prediction for young bridges with ECR is not easy to validate due to the lack of inspection data at later ages and the effect of multiple mechanism in early age degradation. Corrosion due to the environment becomes a dominating factor in the later period of the service life (i.e., 20 or 30 years). Thus, only decks with BS rebar are selected for model validation.

5.4 Prediction Result at the Project Level

Based on the results presented in Section 5.3, only one simulation is necessary to represent a group of decks in same region or with similar environmental conditions. Due to the lack of actual data, two levels of surface chloride content were considered so that two NBI bounds and a mean curve could be determined. In this prediction, Network 2 consisted of ten decks built between 1966 and 1972, all built with BS bars. The technical parameters of this network are summarized in Table 17. The manual inspection data of Network 2 is listed in Table 18. The locations of these decks are shown in Figure 44. Most of them intersect with highway US-127 in Lansing. It was assumed that all the decks are exposed to a moderate chloride level.

Figure 45 shows the two predicted NBI bounds and the corresponding mean value curves obtained with 200 trials. The results did not vary much from the result obtained with 100 iterations. Overall, most of the NBI inspection data plots within the two predicted bounds. Decks Nos. 7, 8 and 9 have similar ages, width, and number of spans, but Deck No. 8 has a relatively higher ADT, skew angle and span length. It can be seen that the deterioration of Deck No. 8 is faster than that No. 9. However, all the inspections for Deck No. 7 are away from the predicted bounds. The low rating of Deck No. 7 may be due to other unknown reasons. It is also interesting to see that Decks Nos. 1 to 5 (Group A) are close to the NBI bound with medium C_0, while Decks Nos. 6, 8, 9, and 10 (Group B) are close to the NBI bound with low C_0. It is worth noting that Group A has higher ADT than Group B. These results may imply the influence of ADT on the deicing salt policy. The more salt used on the deck, the higher surface chloride the deck should have. However, this hypothesis needs to be investigated further with more available inspection data. Nonetheless, it can be seen that predictions at the project level are feasible and that improved predictions are likely to be achieved with actual field data for the model's input.

Table 17. Technical parameters of bridges in Network 2

#	Bridge ID	Year Built	Lanes	ADT	Skew	Material	Spans	Max Span (ft)	Length (ft)	Width (ft)	Year Overlay
1	33133172000S010	1972	6	31200	16	3	2	118.8	236.9	100.4	
2	33133171000S080	1970	4	20897	1	3	2	63	126	66.3	1998
3	33133171000S050	1970	2	33069	0	5	3	53.8	112.9	43	1998
4	33133045000B010	1970	3	33453	45	3	5	139.8	445.9	50.2	2000
5	33133082000R020	1977	2	27408	41	3	3	86	198.8	41	
6	33133035000S090	1966	2	16286	8	3	3	67.9	133.9	42.3	2005
7	33133035000S030	1966	2	1000	23	3	4	77.8	220.8	34.1	2005
8	33133035000S100	1966	2	7702	47	3	4	123	399.9	35.1	2005
9	33133032000S030	1967	2	660	23	3	4	55.8	180.8	38.4	
10	33133031000S030	1966	2	3100	0	4	2	84	167	35.1	

Note: Material (3 Steel, simple or Cantilever, 4 Steel continuous, 5 Prestressed Concrete).

Table 18. Inspection data for bridges in Network 2

#	Bridge ID	94	95	96	97	98	99	00	01	02	03	04	05	06	07	08
1	33133172000S010	6		6	5	6		5	5			4		6		6
2	33133171000S080	6		5		5										
3	33133171000S050	6		7	5	5										
4	33133045000B010	6		5		5		5								
5	33133082000R020	6		7		7		7		7		7		7		
6	33133035000S090			5		5		5		5	5	4				
7	33133035000S030			4		3		3		3		3				
8	33133035000S100			5		5		5		5		5				
9	33133032000S030			6		6		6		7		6		6		6
10	33133031000S030									5		5		5		5

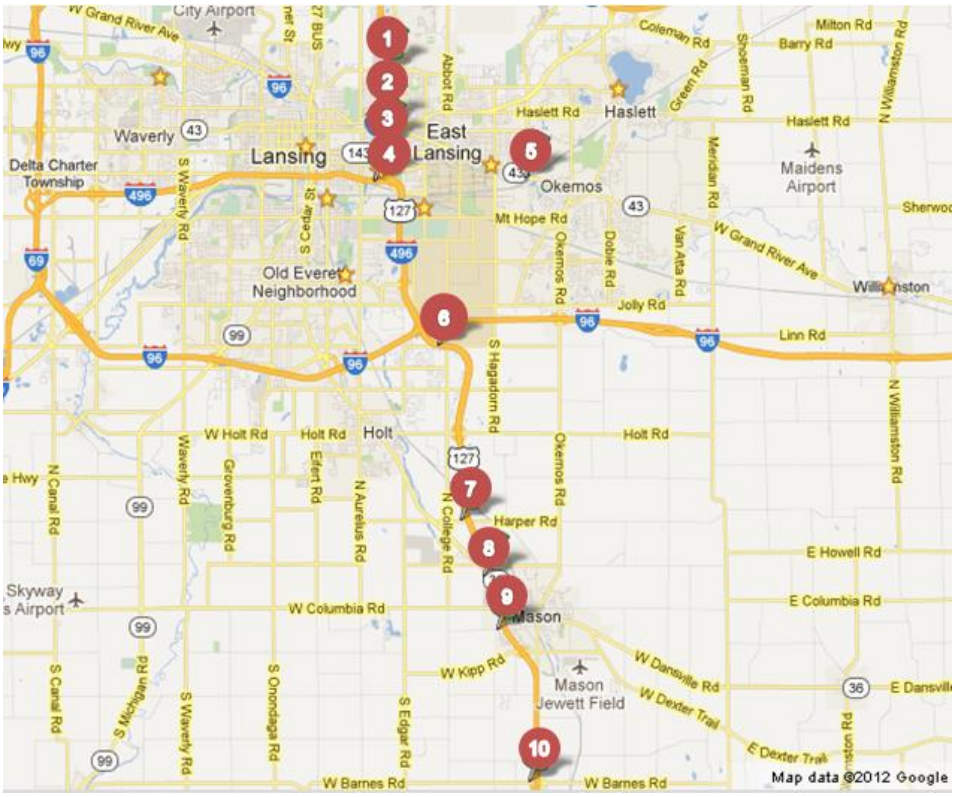

Figure 44: Numbering of bridges in Network 2

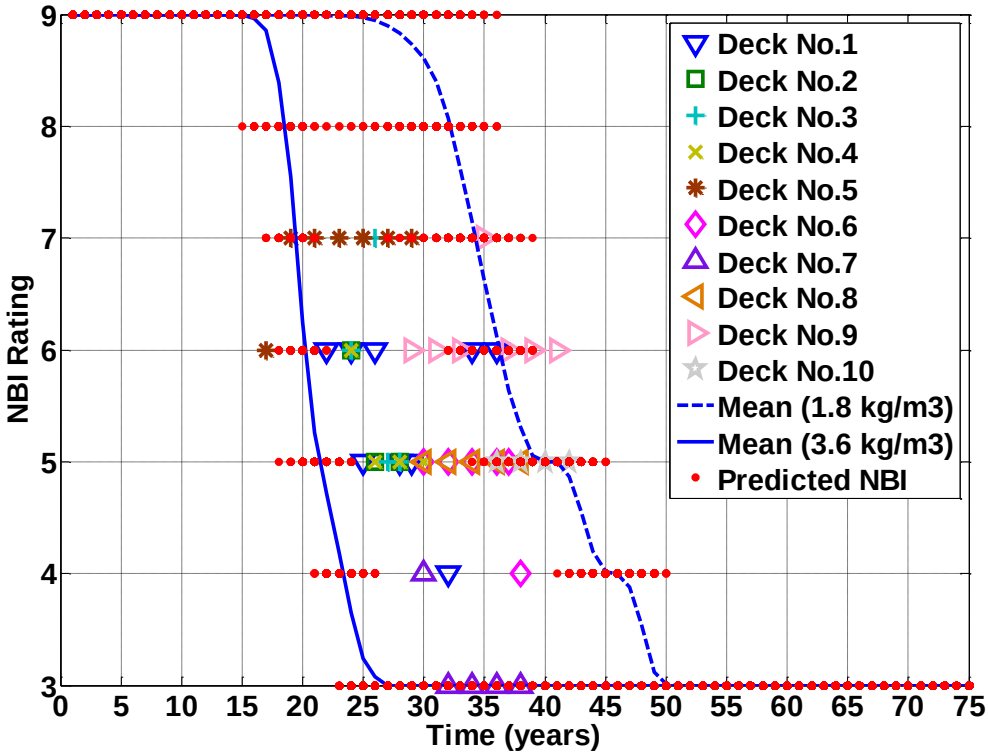

Figure 45: Predicted degradation curve and NBI rating for Network 2 decks

5.5 Prediction Result at the Network Level

Based on the of project-level results (Section 5.4), it was noted that more field data was needed for further validation. For the convenience of network modeling, temperature and humidity were categorized based on regions as defined by MDOT, that is, seven regions as shown in Figure 46. The MDOT region office and transportation service centers are listed in Table 19. Based on this information, the temperature and humidity of those cities in Michigan was collected from an online climate database, as shown in Table 20. It should be emphasized that all these values are the monthly mean and not the maximum or minimum ones. The seven regions can be further divided into three larger regions due to the similarity of temperature and humidity. In addition, the variability can be considered as normally distributed with a standard deviation.

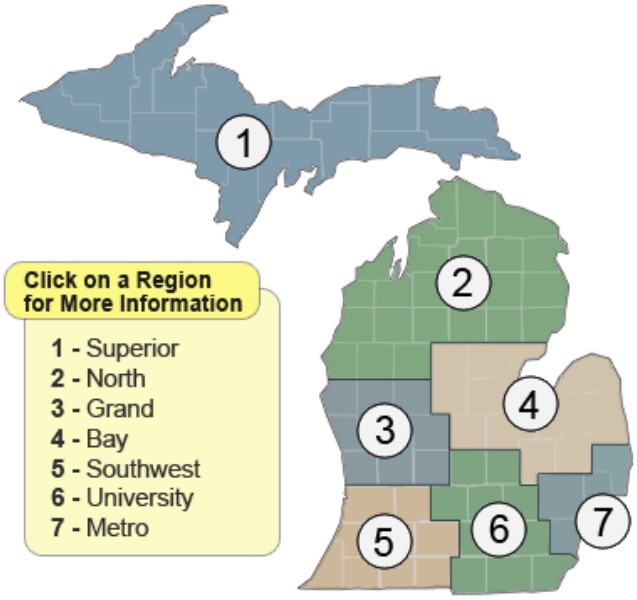

Figure 46: Seven regions defined by MDOT

A simple case study was carried out to verify the necessity of defining the three big regions. Decks with the same structural and material dimension were assumed to be exposed in the three proposed regions. Temperature and humidity values were selected from Table 20. The maximum temperature considers a standard deviation (SD) of 2 °C and the minimum temperature has a SD of 1 °C. Both maximum and minimum humidity had a SD of 1%. The mean and SD for the three regions are, for Region A: -9, 19; 0.69, 0.81; for Region B: -4, 22; 0.64, 0.77, and for Region C: -

5, 24; 0.67, 0.81). Fig. 18 shows that decks in regions A and B had a relatively slower deterioration than in region C. Thus, lower temperature and humidity conditions can delay the degradation of a deck. Therefore, the definition of three larger regions was considered reasonable.

Table 19. MDOT offices by region

Region	Region Office	Transportation Service Center
1-Superior	Escanaba	Crystal Falls, Ishpeming, Newberry
2-North	Gaylord	Alpena, Cadillac, Traverse City
3-Grand	Grand Rapid	Muskegon
4-Bay	Saginaw	Bay City, Davison, Mt. Pleasant
5-Southwest	Kalamazoo	Coloma, Marshall
6-University	Jackson	Brighton, Lansing
7-Metro	Southfield	Detroit, Oakland, Macomb/St. Clair, Taylor

Only 10 decks were selected for validation at the project-level prediction. However, it will be more reasonable to compare the predicted NBI degradation curve with more observed data. Inspection records in MDOT's NBI database are only available after 1992 and the inspections do not always occur on a two year basis. The NBI database used for this project, including Phase 1 reported by Winn and Burgueño (2012), includes inspection records up to March 2010, This means that if a bridge was built before 1992, the absolute longest period of time that one bridge can cover is 18 years. It can be seen from Figure 48 that most decks have between 1 and 9 inspection data points.

From a statistical point of view, a deck with at least 5 inspection data points can be considered as a candidate. Thus, a program was written to identify the number of observed data for each deck. The results are given in the Table 21. It can be seen that only 361 out of 1048 decks had at least five inspection records. Further, 27 out of 1048 decks have very high ratings while having and old age. A possible explanation is that these decks have been replaced and the new built age was not updated. After further filtering the data, 334 decks were chosen, including 13 in Region A, 173 in Region B and 148 in Region C.

Table 20. Mean temperature and humidity of major cities in Michigan

Region			Humidity Max (%)	Humidity Min (%)	Avg. Tmax °C	Avg. Tmin °C
A	1-Superior	Escanaba	76	68	18	-12
		Crystal Falls	83	73	18	-12
		Ishpeming	82	68	19	-10
		Newberry	84	67	18	-9
		Average	**81.3**	**69.0**	**18.3**	**-10.8**
	2-North	Gaylord	83	64	20	-8
		Alpena	79	67	15	-11
		Cadillac	84	67	20	-7
		Traverse City	78	66	21	-6
		Average	**81.0**	**66.0**	**19.0**	**-8.0**
B	3-Grand	Grand Rapids	79	65	23	-4
		Muskegon	78	65	22	-3
		Average	**78.5**	**65.0**	**22.5**	**-3.5**
C	4-Bay	Saginaw	79	65	22	-5
		Bay City	79	67	22	-5
		Davison	79	66	22	-6
		Mt. Pleasant	83	65	22	-6
		Average	**80.0**	**65.8**	**22.0**	**-5.5**
	5-Southwest	Kalamazoo	82	69	23	-3
		Coloma	80	71	23	-3
		Marshall	81	65	22	-6
		Average	**81.0**	**68.3**	**22.7**	**-4.0**
	6-University	Jackson	81	68	22	-4
		Brighton	81	64	22	-5
		Lansing	80	68	22	-4
		Average	**80.7**	**66.7**	**22.0**	**-4.3**
B	7-Metro	Southfield	75	56	22	-5
		Detroit	74	61	23	-3
		Oakland	80	68	22	-5
		Macomb/St. Clair	78	68	22	-4
		Taylor	76	64	23	-3
		Average	**76.6**	**63.4**	**22.4**	**-4.0**

Data from: www.weatherspark.com and http://www.weather.com

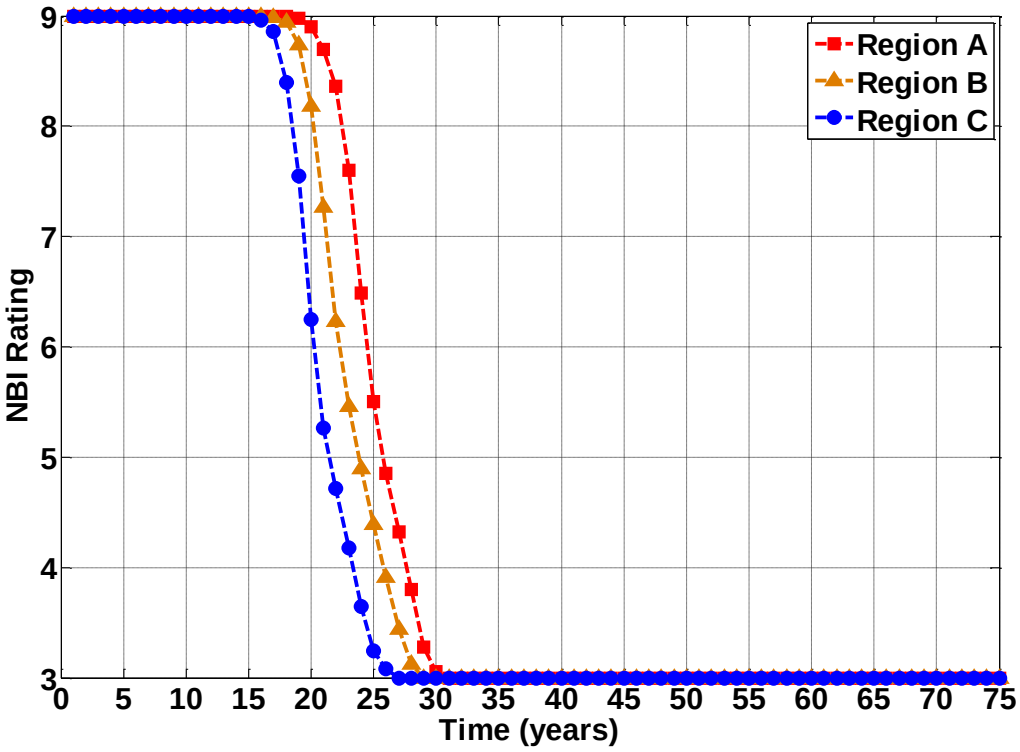

Figure 47: Influence of geographical location on deck deterioration

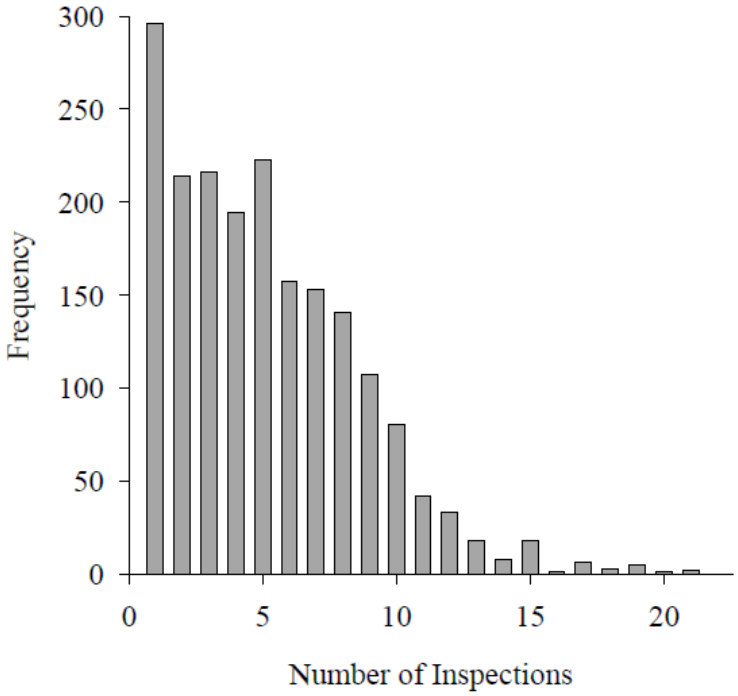

Figure 48: Distribution of the number of inspections (Winn 2011)

Table 21. RC decks with various manual data (⩾5)

Number of manual data	BS(1048)	ECR(541)
5	361	285
6	241	212
7	173	177
8	111	138
9	62	54
10	40	15
11	24	5

Figure 49 to Figure 51 show that the predicted NBI bounds with 200 trials from the MCS and the corresponding mean value curves for all three regions. For each region, the NBI ratings are predicted based on three different C_0 levels. The manual inspection data is plotted with the predicted rating. It can be seen that the predicted NBI ratings are in a reasonable range for the three regions. The proposed framework is thus able to predict the deck deterioration, but it should be noted that all these predictions are based on a number of assumptions, both in the model and in the input. In addition, only chloride-induced corrosion is considered. Thus, numerous improvements are possible and needed to obtain more accurate predictions.

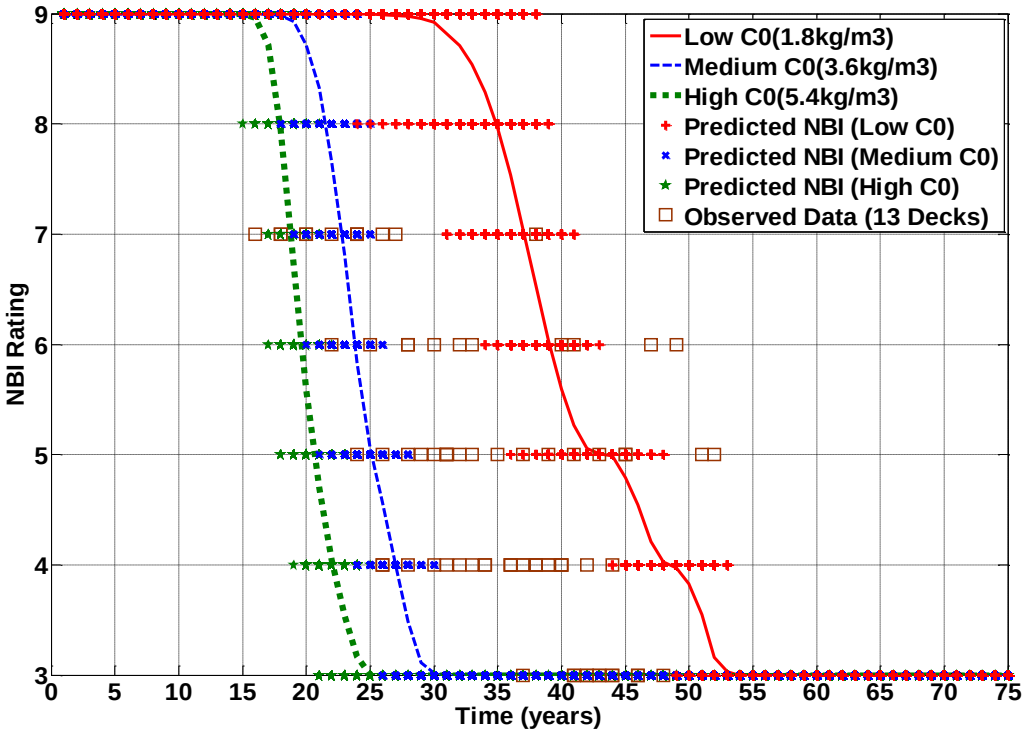

Figure 49: Observed and predicted NBI ratings for different C_0 (Region A)

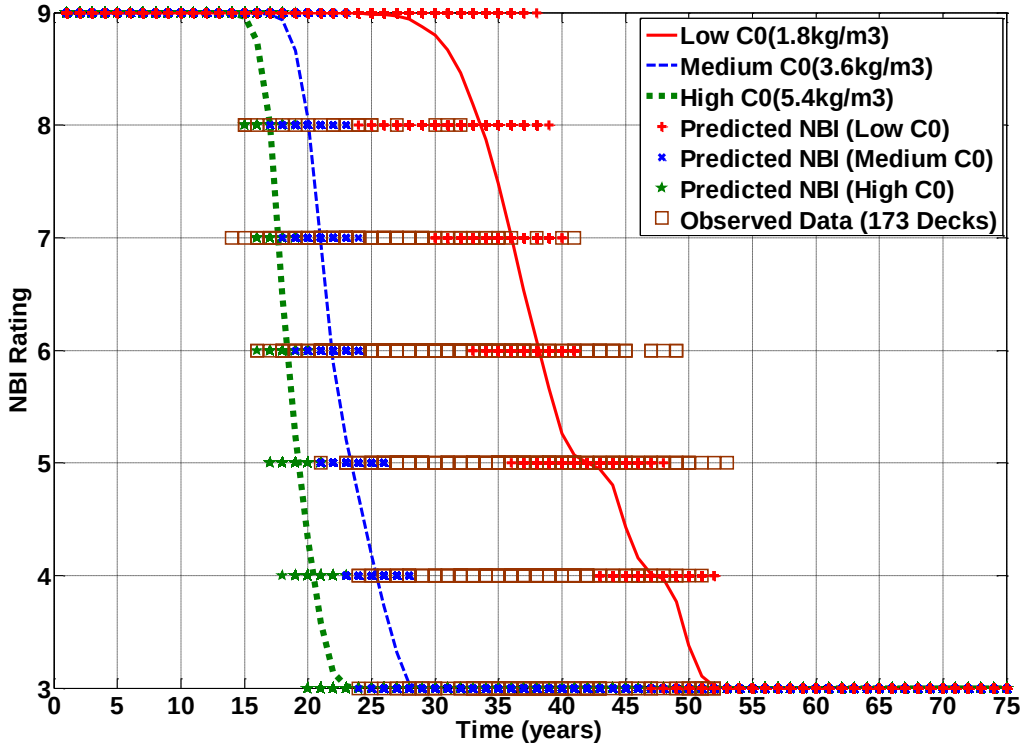

Figure 50: Observed and predicted NBI ratings for different C_0 (Region B)

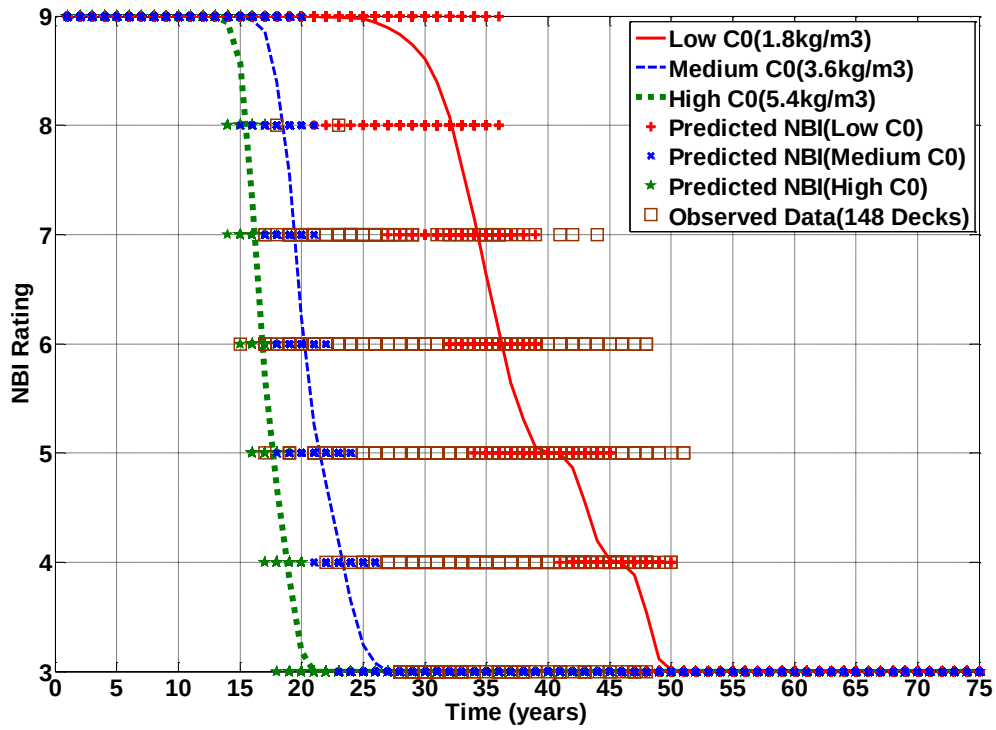

Figure 51: Observed and predicted NBI rating for different C_0 (Region C)

5.6 Parametric Study

This section presents results from a parametric study carried out to identify the influence of key parameters on the service life prediction. Table 22 shows the cases for the parametric study. Case No.1 is a reference deck, which has the typical parameters from the previous simulations. In cases No. 2 through 8, one key input is changed from the reference deck. The predicted NBI rating was again estimated based on 200 trials by the MCS.

The predicted NBI rating range and its mean value for all the cases are listed in Table 23. It can be seen that the deterioration of the reference deck drops to 4 (mean value) at 24 years of age. Decks with higher surface chloride concentration exhibit a somewhat faster degradation, dropping to a rating of 4 after 19 years. The predicted ratings in cases Nos. 3 and 4 indicate that higher compressive strength and larger concrete cover depth can significantly improve the durability of the deck: 33 and 32 years, respectively for these two decks to reach a rating of 4. The deck with larger rebar size shows no significantly difference with the reference deck, while the use of ECR delays the deck degradation, taking 45 years to reach a rating of 4. Two

important environmental parameters are temperature and humidity. It has been noted that lower temperature and humidity will also delay the deterioration of a deck. The mean value curve of the predicted NBI rating is shown in Figure 52.

Table 22. Data of parametric study

Case	C_0 (kg/m3)	f'c (Mpa)	Cover (mm)	Db (mm)	Bar Type	Temperature (ºC)	Humidity (%)
1	3.6	31.5	76	15.8	BS	-5,24	67-81
2	**5.4**	31.5	76	15.8	BS	-5,24	67-81
3	3.6	**42.0**	76	15.8	BS	-5,24	67-81
4	3.6	31.5	**89**	15.8	BS	-5,24	67-81
5	3.6	31.5	76	**19**	BS	-5,24	67-81
6	3.6	31.5	76	15.8	**ECR**	-5,24	67-81
7	3.6	31.5	76	15.8	BS	**-10,18**	67-81
8	3.6	31.5	76	15.8	BS	-5,24	**55-70**

Table 23. The prediction of NBI rating under different case of the parametric study

Case / NBI	**No.1 Base**	**No.2 C_0**	**No.3 f'c**	**No.4 Cover**	**No.5 Db**	**No.6 ECR**	**No.7 Temp.**	**No.8 Humidity**
8	15-21 (18)	14-17 (16)	19-29 (26)	21-29 (25)	15-20 (18)	25-36 (32)	18-24 (23)	17-22 (20)
7	17-21 (19)	14-18 (16)	23-29 (27)	22-29 (26)	16-21 (19)	28-37 (34)	21-25 (24)	19-22 (21)
6	18-22 (20)	15-18 (17)	25-30 (28)	24-30 (28)	17-22 (20)	32-38 (36)	23-25 (25)	21-22 (22)
5	18-24 (21)	16-19 (18)	26-33 (30)	26-32 (29)	17-24 (21)	34-43 (40)	24-27 (26)	22-24 (23)
4	21-26 (24)	17-20 (19)	30-36 (33)	28-34 (32)	21-26 (23)	41-47 (45)	26-2 (28)	25-26 (25)

Another concern in the parameter study is about time-dependent material propriety variables. In the current model, all the material parameters were kept constant without any consideration about variation with time. For example, compressive strength (f'_c) is the most important

parameter controlling the overall quality of concrete and it is well known that f'_c continues to increase with time. Figure 53 shows that deck deterioration is affected by this time-dependent feature. The dashed line shows that the gain in strength has a considerable improvement on deck condition, especially later in the life of the deck.

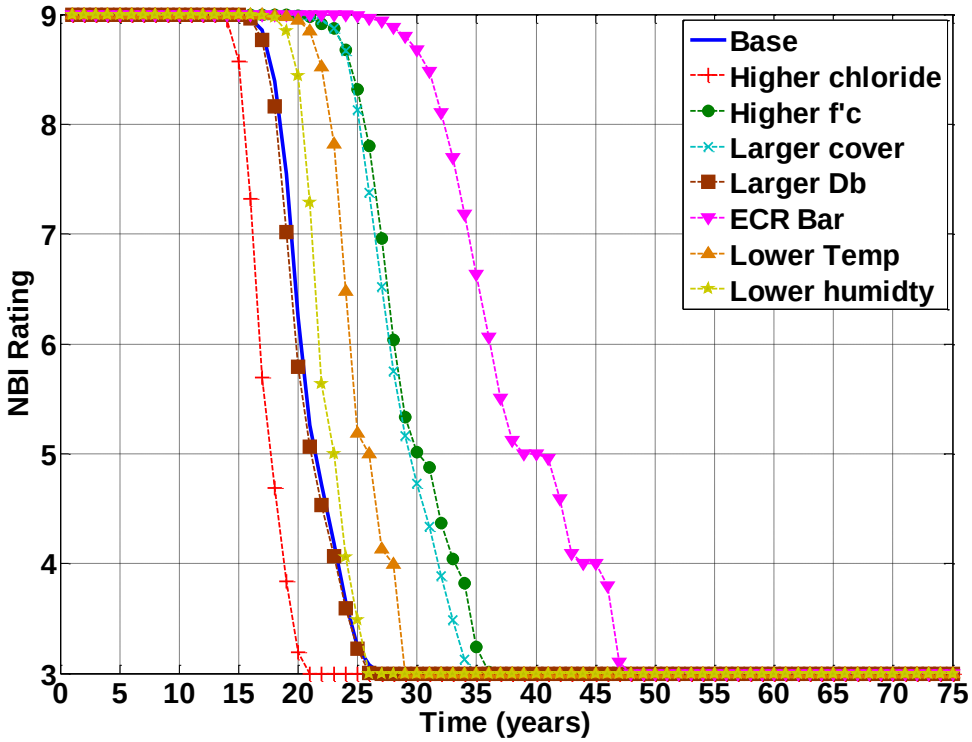

Figure 52: Influence of key parameters on the prediction of deterioration

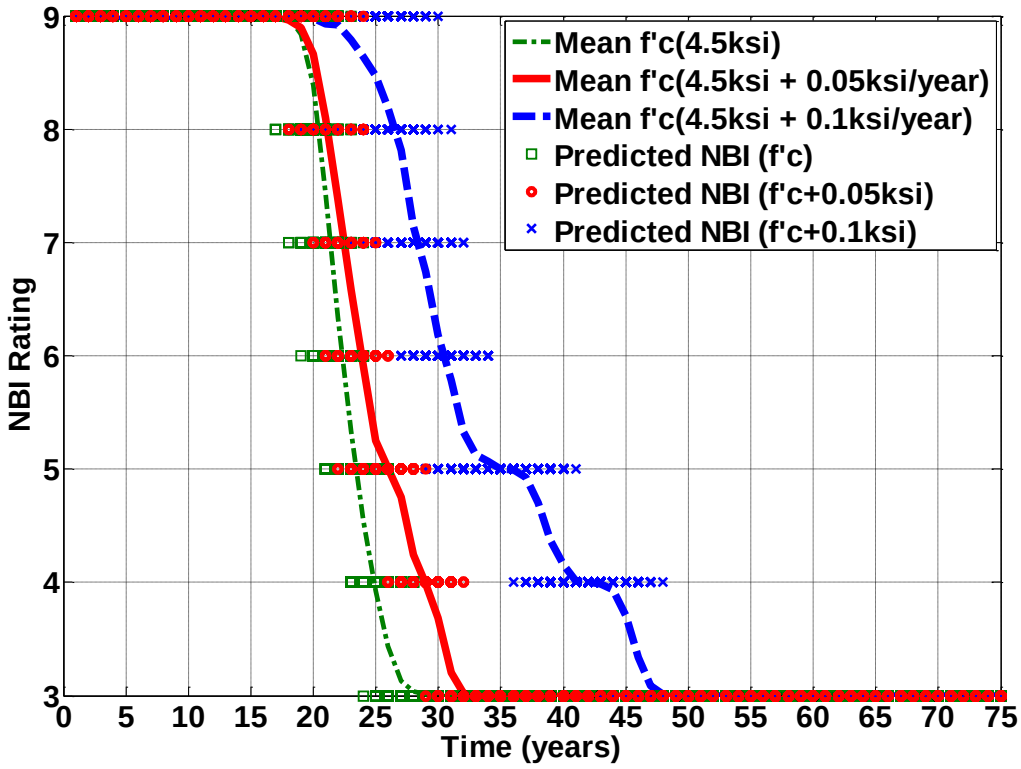

Figure 53: Influence of time-dependent f'c values on the prediction of deterioration

5.7 Reference Charts

Based on the parametric study of key material and environmental properties, a series of simple charts were developed to facilitate use of the developed model. Three environmental conditions were considered, with the surface chloride content having a typical value for each environment. The values of 1.8 kg/m3, 3.6 kg/m3 and 5.4 kg/m3 were chosen for low, medium and high chloride contents, respectively. Temperature and humidity was based on data from the three proposed agglomerated regions in the state (see Table 20).

Three material properties were also considered. First, the use of ECR should have a larger threshold level (Cth) to initiate the corrosion at the rebar surface. Based on the previous report, a value of 2.2 kg/m^3 was selected for ECR while the Cth for BS was 1.2 kg/m3, as used in the previously presented cases. Second, f'$_c$ was considered with different mean values according to the year the deck was built. In previous chapters, a value of 31.5 MPa at 28 days (4.5 ksi) was used. For these charts f'$_c$ was divided in three grades: 21 MPa (3 ksi) for decks built before 1950, 31.5 MPa (4.5 ksi) for decks built from 1950 to 1980, and 42 MPa (6 ksi) for decks built after

1980. Third, the requirement of minimum cover depth is another way to reduce the deterioration of decks. According to MDOT's standard bridge slab design guides, the minimum clear cover for transverse bars is 76 mm (3 in.). Thus, the concrete cover also had three mean values: 64 mm (2.5 in.), 76 mm (3 in.) and 89 mm (3.5 in.). All these mean value considered the same standard deviation of 4mm (0.16 in.) due to construction variability. Finally, the small effect of bar diameter (Db) needed further validation. Thus, three mean values were considered: 64 mm (0.5 in.), 16 mm (0.625 in.) and 89 mm (0.75 in.). The same 10% standard deviation (± 1.5 mm) was considered to account for construction variability. The values of f'_c, cover and Db were considered to be normally distributed.

Deterioration curves were developed based on the different material properties and environmental conditions and arranged as a series of tables. For the same region the decks are sub-divided into those with BS and ECR rebar. In addition, the decks were assumed to be exposed to three different regions. Thus, six reference charts were developed for simple assessment of the deterioration of bridge decks under different parameters, as shown in Table 24 to Table 29.

Table 24. Reference Chart (Region A, BS)

	f'c: 21, 31.5, 42 (MPa)	Cover: 64, 76, 89 (mm)
Low C_0 (1.8, 0.9) kg/m3	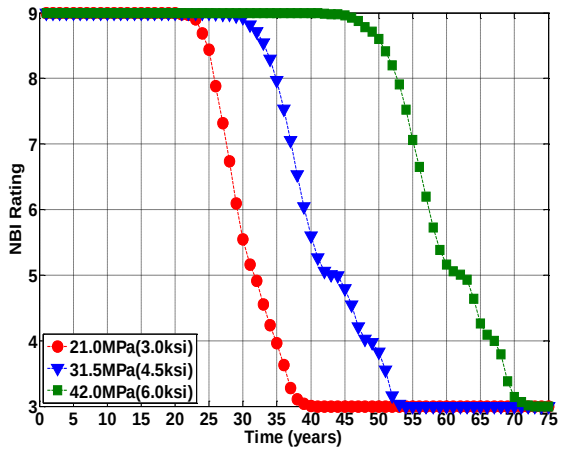	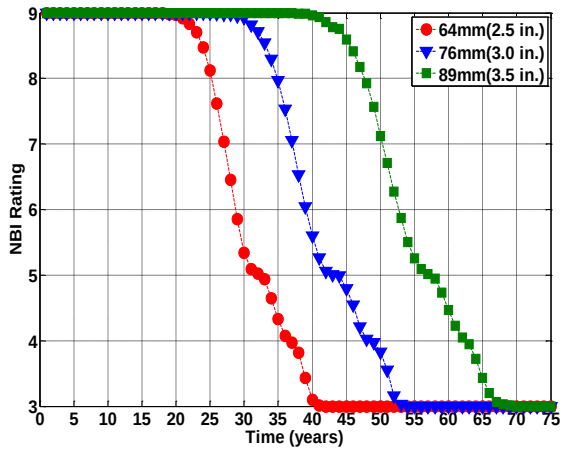
Medium C_0 (3.6, 0.9) kg/m3	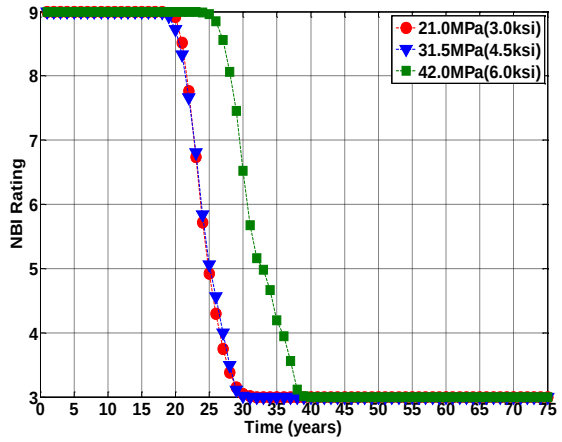	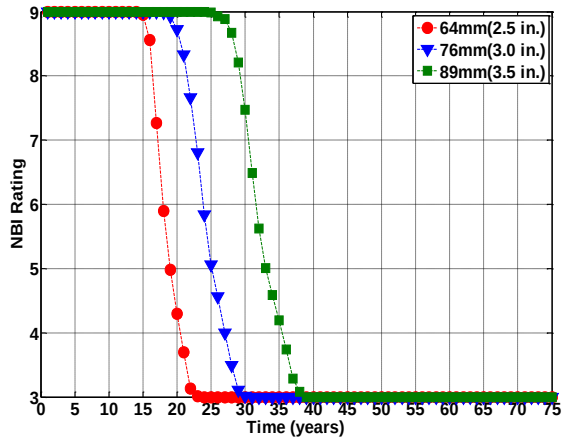
High C_0 (5.4, 0.9) kg/m3	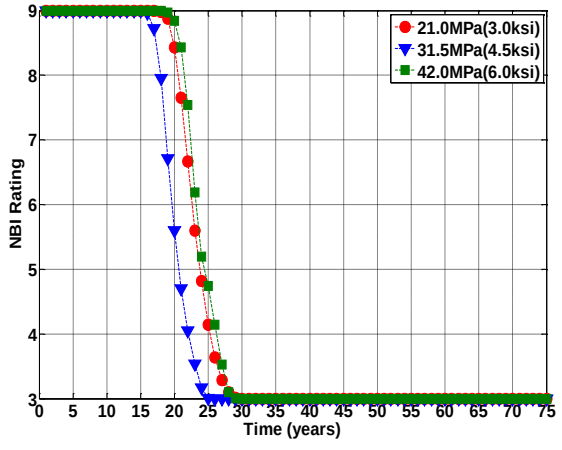	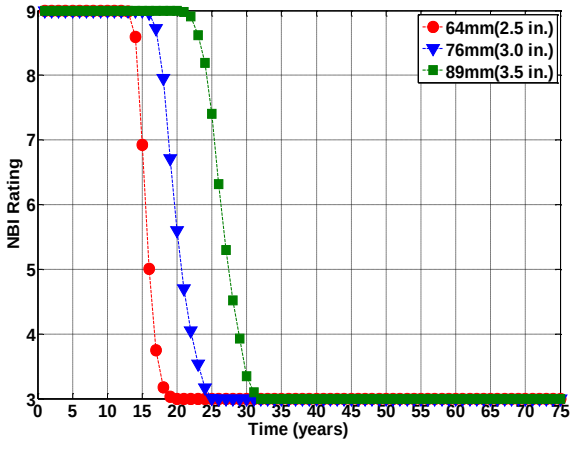

Table 25. Reference Chart (Region A, ECR)

	f'c: 21, 31.5, 42 (MPa)	Cover: 64, 76, 89 (mm)
Low C_0 (1.8, 0.9) kg/m3	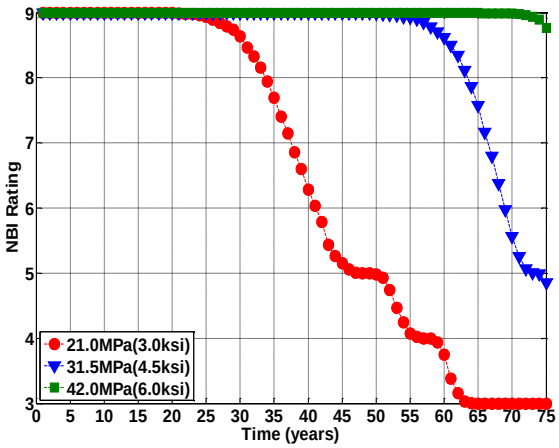	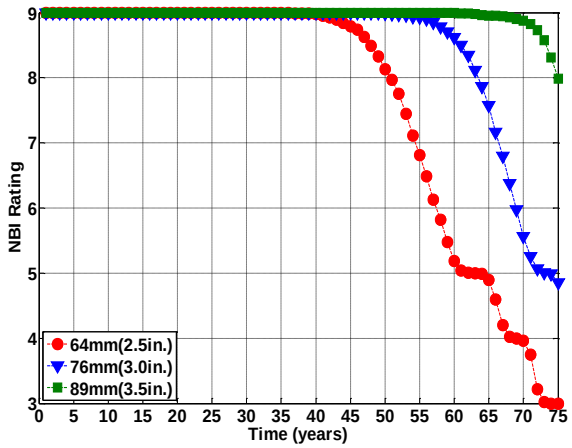
Medium C_0 (3.6, 0.9) kg/m3	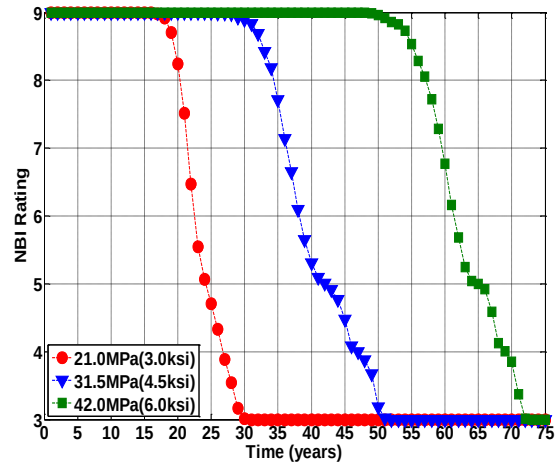	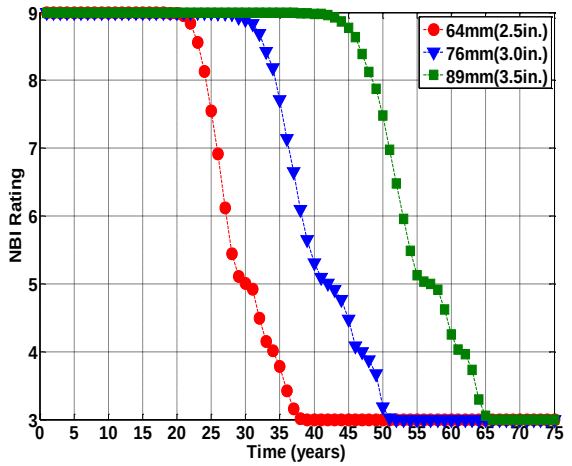
High C_0 (5.4, 0.9) kg/m3	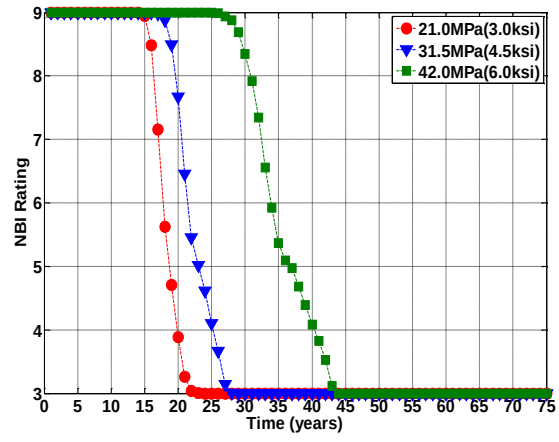	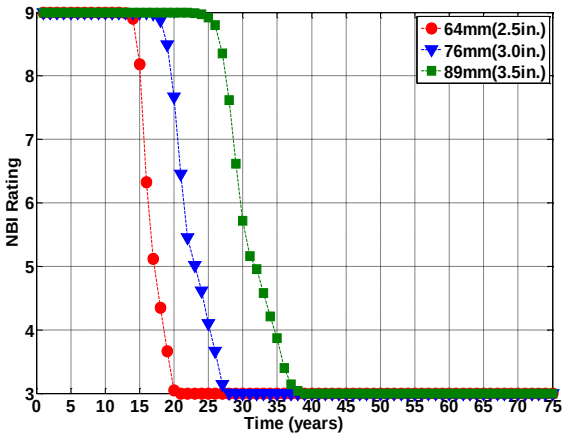

Table 26. Reference Chart (Region B, BS)

	f'c: 21, 31.5, 42 (MPa)	Cover: 64, 76, 89 (mm)
Low C_0 (1.8, 0.9) kg/m3	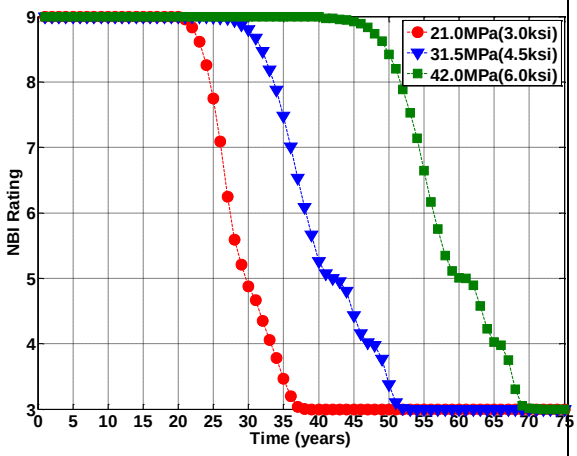	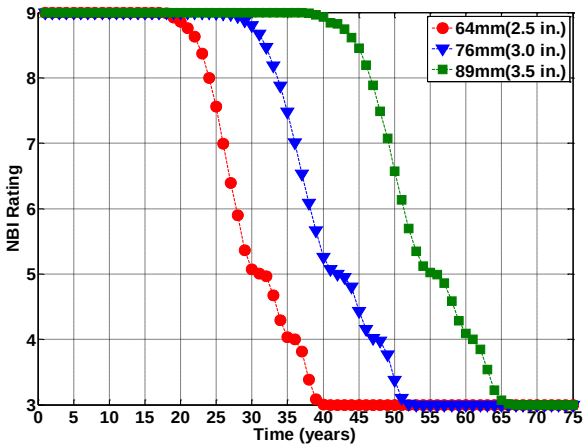
Medium C_0 (3.6, 0.9) kg/m3	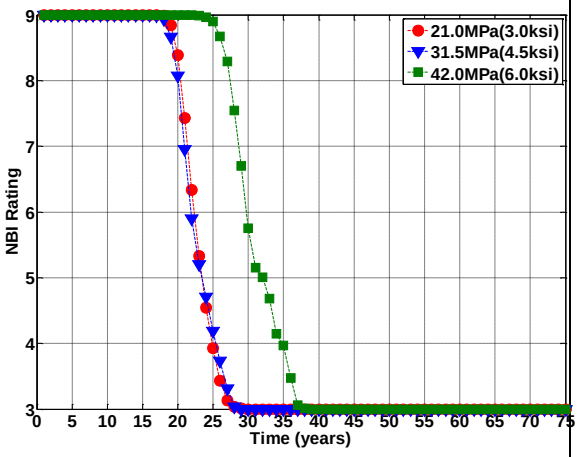	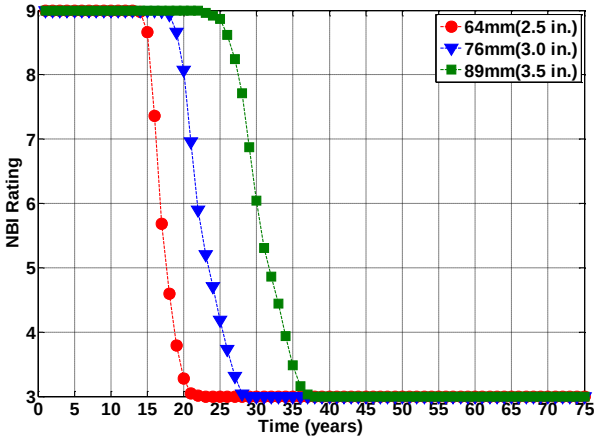
High C_0 (5.4, 0.9) kg/m3	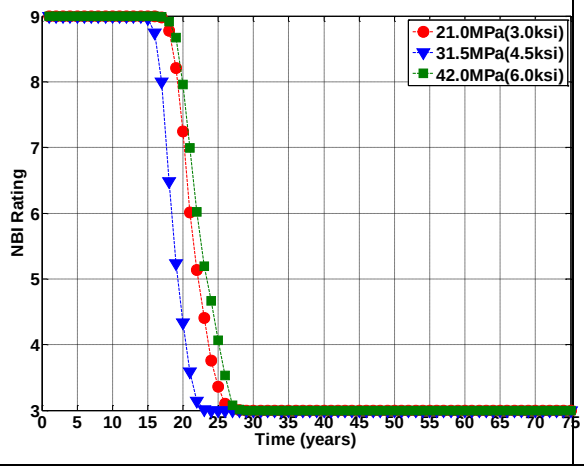	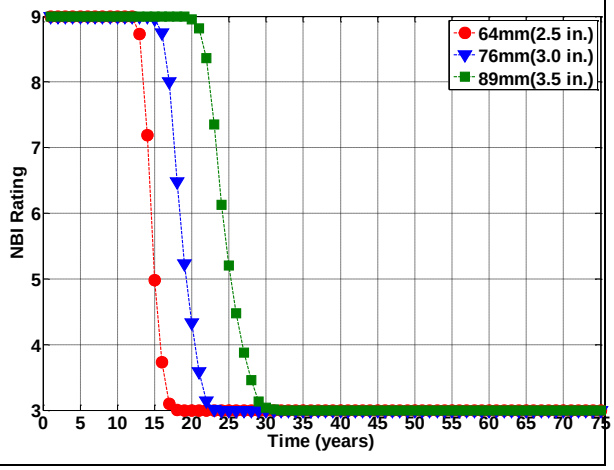

Table 27. Reference Chart (Region B, ECR)

	f'c: 21, 31.5, 42 (MPa)	Cover: 64, 76, 89 (mm)
Low C_0 (1.8, 0.9) kg/m3	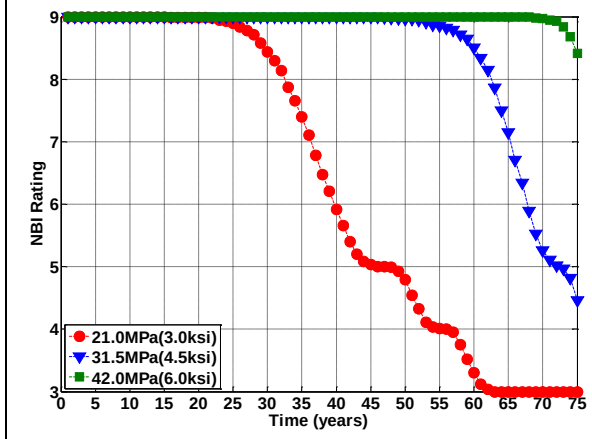	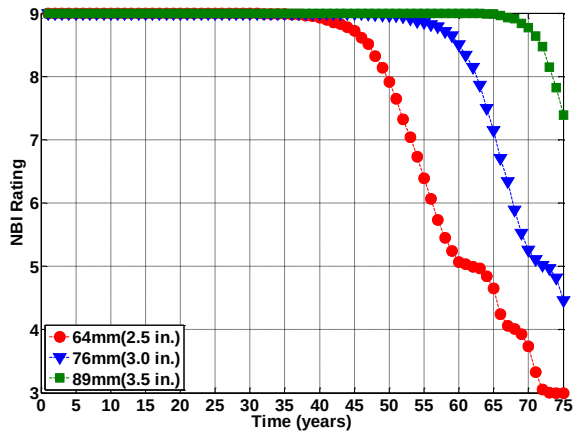
Medium C_0 (3.6, 0.9) kg/m3	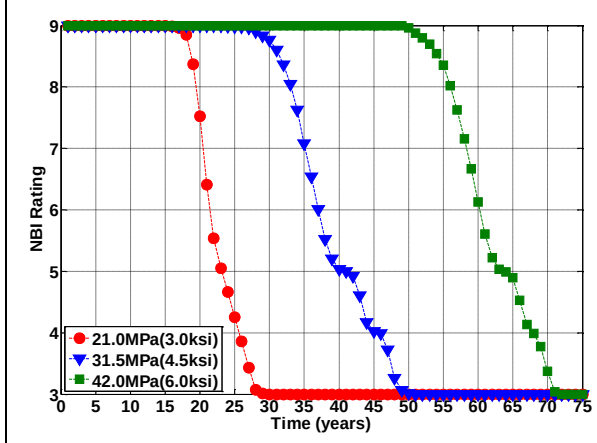	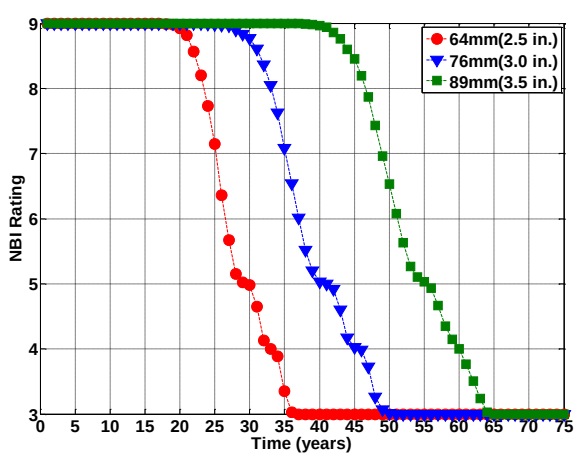
High C_0 (5.4, 0.9) kg/m3	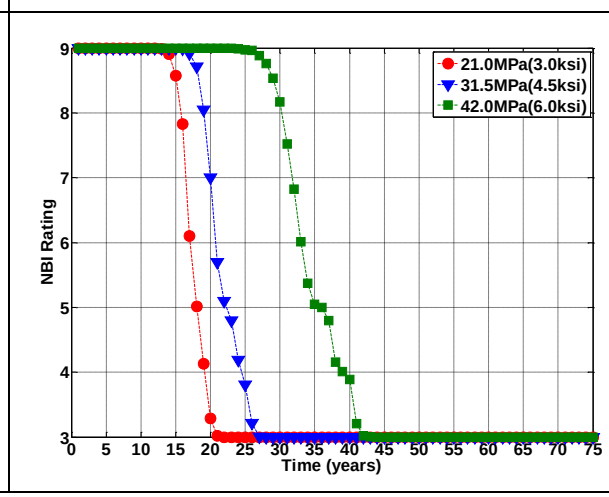	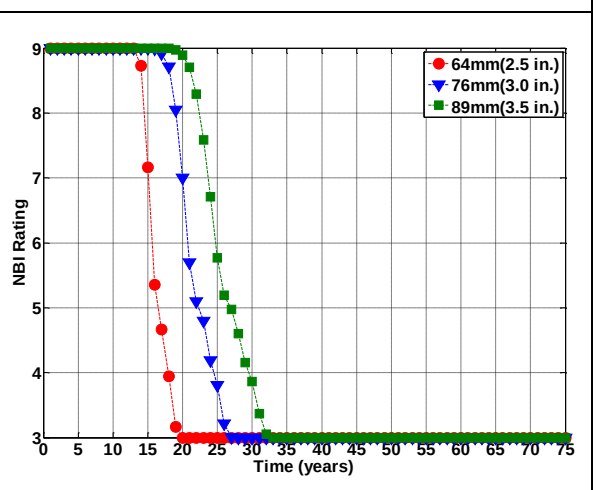

Table 28. Reference Chart (Region C, BS)

	f'c: 21, 31.5, 42 (MPa)	Cover: 64, 76, 89 (mm)
Low C_0 (1.8, 0.9) kg/m3	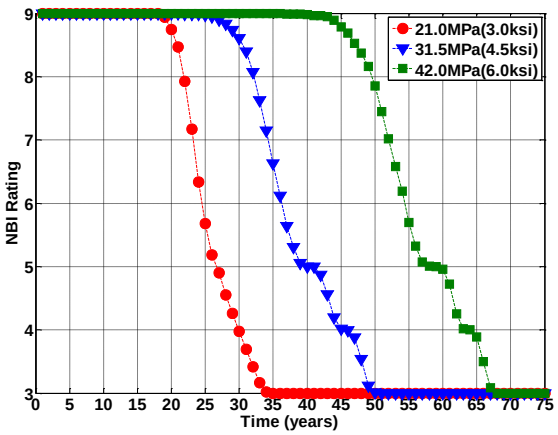	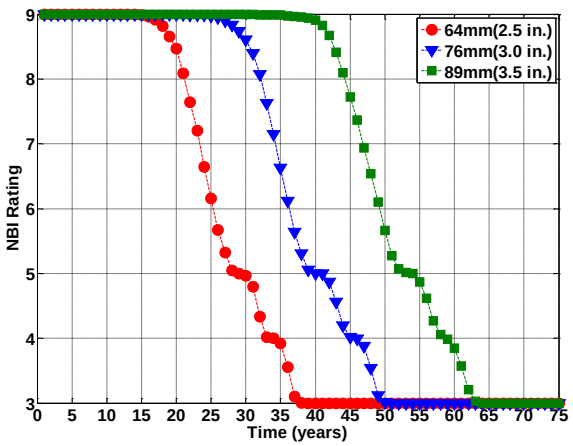
Medium C_0 (3.6, 0.9) kg/m3	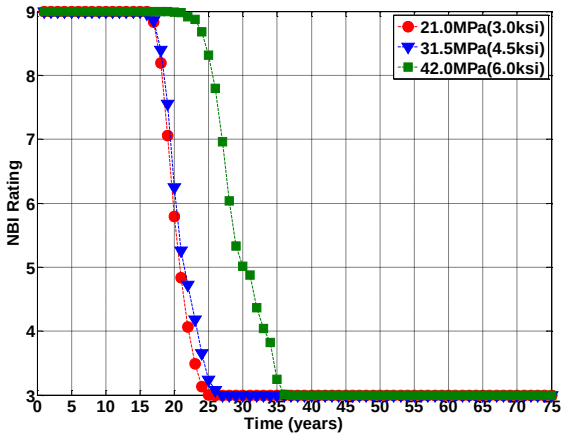	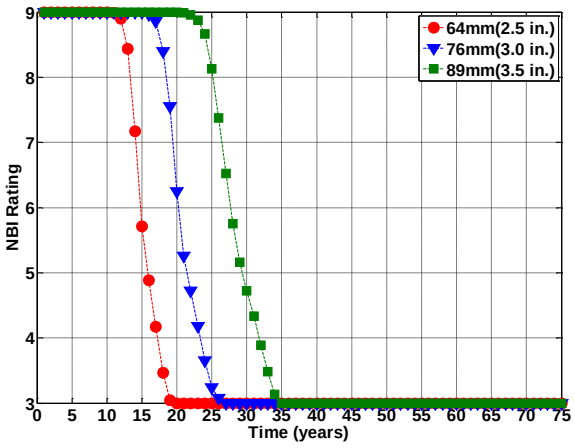
High C_0 (5.4, 0.9) kg/m3	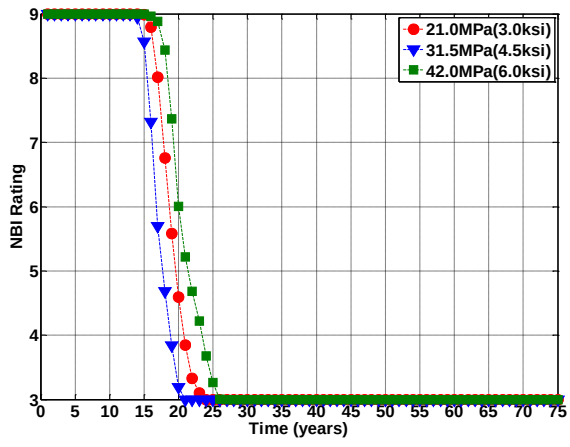	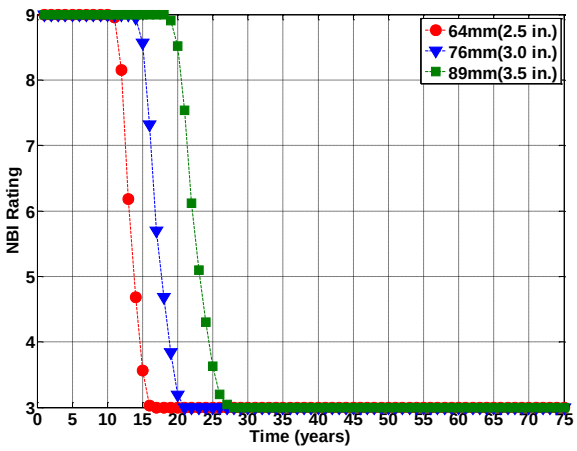

Table 29. Reference Chart (Region C, ECR)

	f'c: 21, 31.5, 42 (MPa)	Cover: 64, 76, 89 (mm)
Low C_0 (1.8, 0.9) kg/m3	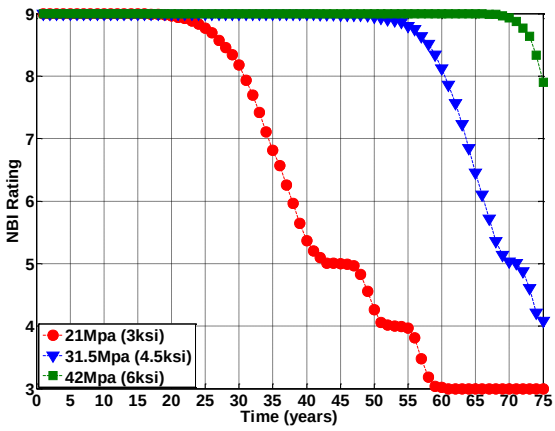	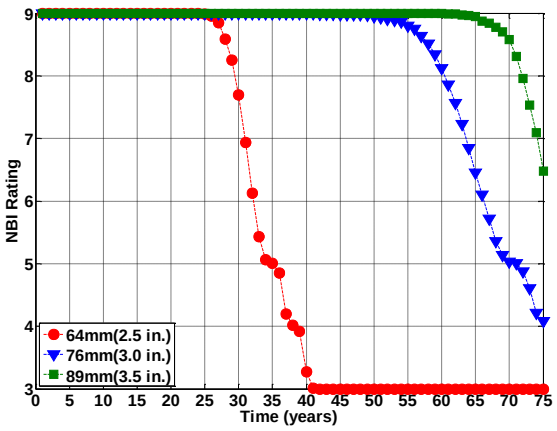
Medium C_0 (3.6, 0.9) kg/m3	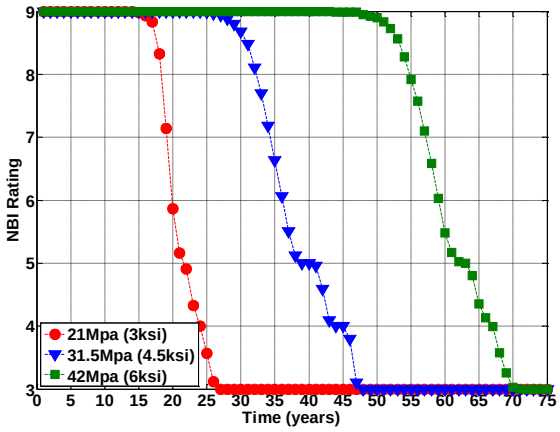	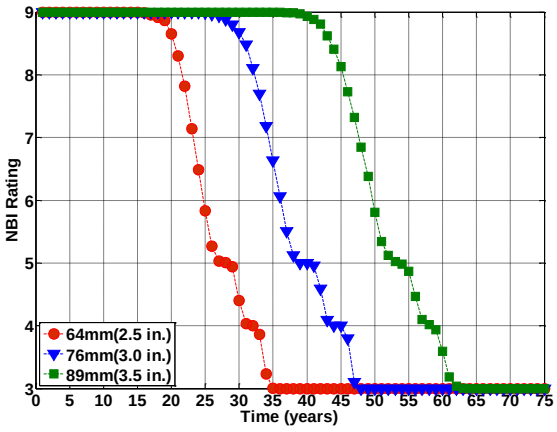
High C_0 (5.4, 0.9) kg/m3	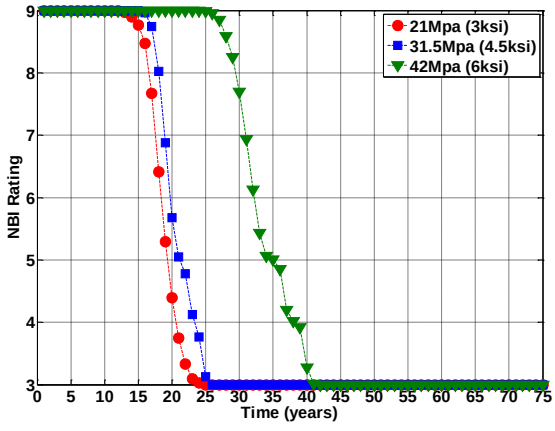	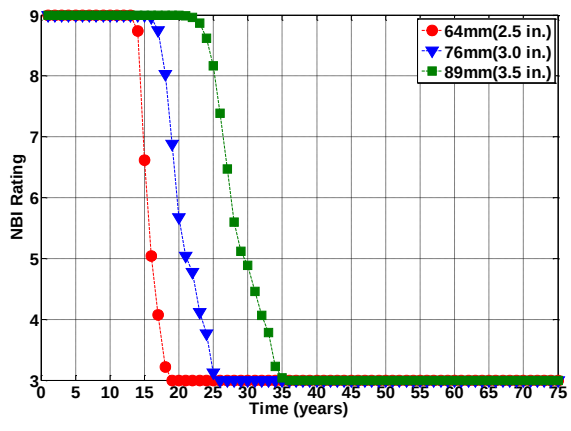

5.8 Summary

A discussion was presented on relating the prediction from the MCS probabilistic-based framework to the National Bridge Inventory (NBI) rating system. The percentage of damaged cells on the deck was used as a criterion to achieve the mapping between the cumulative damage index (CDI) and the NBI rating. At the deck level, the number of representative cells size was calculated for the improvement of computer efficiency. A series of investigations were carried out for the validation of the proposed mechanistic-based framework. At the project level the observed ratings of 10 decks properly bounded the predicted NBI ratings. At the network level, generalized deterioration curves were obtained by the MCS method and used to represent decks in in different regions of Michigan. Based on the environmental data, three larger regions were proposed to group decks in different locations. Decks with at least five inspection records were chosen to evaluate the model's prediction. It was found that the predicted rating bounds have reasonable ranges that bracket most of the observed ratings. Further, a parametric study was presented to investigate the influence of key parameters on the deck degradation. The results showed that the use of ECR, concrete compressive strength and concrete cover are the top three material factors influencing deck deterioration. Three environmental parameters (temperature, humidity and surface chloride concentration) also have an effect. Bar diameter did not significantly change the prediction of NBI ratings. Based on these parametric studies, six tables (36 reference charts) were created to facilitate use of the model's predictive capabilities, such as the effect of different parameters on bridge deck degradation.

6 DECK DEGRADATION MODELING DUE TO DUAL EFFECTS

The framework presented in the previous sections showed the potential to provide useful information on bridge deck degradation with the aim of assisting MDOT in their maintenance strategy. However, chloride-induced corrosion is only one of the major factors affecting the durability of RC decks. All the predictions from the MCS have neglected many real conditions, such as the presence of early age cracks, the effect of vehicle loading, etc. As discussed in the literature review, carbonation also has an effect on the diffusion process of the deck deterioration. Thus, degradation due to carbonation is a direct extension from the chloride induced degradation model already implemented. The aim of this chapter is to implement the degradation modeling of dual effects, namely chloride and carbonation induced corrosion.

6.1 Selected Model of Carbonation

Corrosion time (T1) at the cell level can be determined by the diffusion process of CO_2 and the threshold value of carbonated depth in the concrete cover. Modeling of the diffusion process from carbonation is summarized in Figure 54. Due to recent concerns about global warming and CO_2 increase, the strategy used in this project is to separate carbonation-induced corrosion into two different periods. Before the year 2000, the time T1 was estimated by the equations of Papadakis et al. (1992) and Morinaga. After the year 2000, the prediction models proposed by Stewart et al. (2011) were selected.

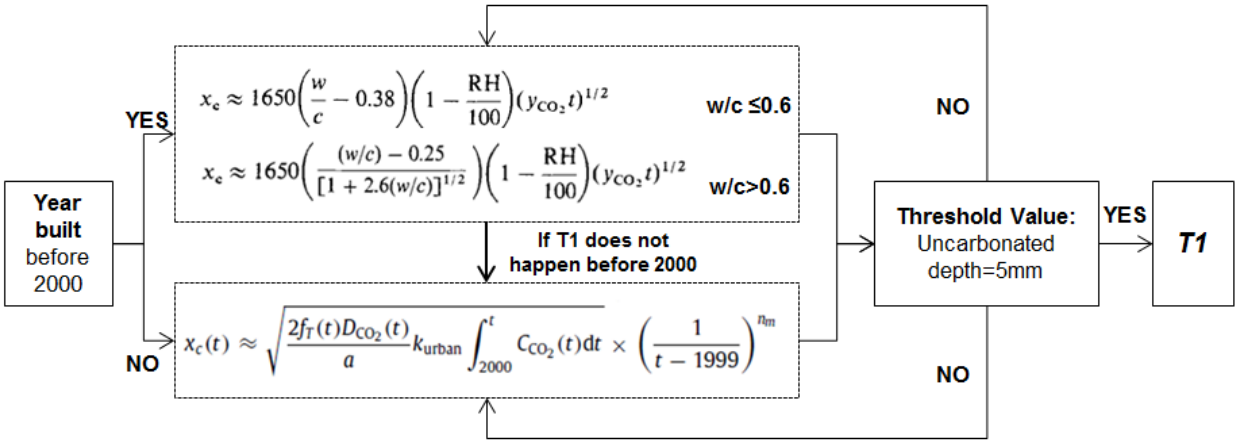

Figure 54 Flow chart to determine T1 from carbonation induced corrosion

Equation 6-1 shows a widely accepted diffusion model for carbonation established by Papadakis et al. (1992), which was used here to determine the carbonation depth:

$$D_{e,CO_2}(m^2\,s^{-1}) = (1.64 \times 10^{-6})\varepsilon_p^{1.8}[1 - (RH/100)]^{2.2} \quad (6\text{-}1)$$

where ε_p is the total porosity (%), which is a function of water/cement ratio (w/c), volumetric mass of the cement, and water; and RH is the relative humidity (%).

Papadakis et al. (1992) proposed a simplified expression (Equation 6-2) to estimate the carbonation depth. Papadakis et al. also reported an empirically function in which carbonation depth was estimated for different w/c ratios as given by Equation 6-3 and Equation 6-4. It has been shown that the carbonation depths obtained from these two equations are in good agreement with Equation 6-2 for w/c ratios between 0.5 and 0.65. For this reason, the carbonation depth and the critical time was calculated by these two empirical functions.

$$x_c \approx 350\left(\frac{\rho_c}{\rho_w}\right)\frac{(w/c) - 0.3}{1 + (\rho_c/\rho_w)(w/c)}\left(1 - \frac{RH}{100}\right) \times \left\{\left[1 + \left(\frac{\rho_c}{\rho_w}\right)\frac{w}{c} + \frac{\rho_c}{\rho_a}\left(\frac{a}{c}\right)\right] y_{CO_2} t\right\}^{1/2} \quad (6\text{-}2)$$

$$x_c \approx 1650\left(\frac{w}{c} - 0.38\right)\left(1 - \frac{RH}{100}\right)(y_{CO_2} t)^{1/2} \qquad (w/c \leq 0.6) \quad (6\text{-}3)$$

$$x_c \approx 1650\left(\frac{(w/c) - 0.25}{[1 + 2.6(w/c)]^{1/2}}\right)\left(1 - \frac{RH}{100}\right)(y_{CO_2} t)^{1/2} \qquad (w/c > 0.6) \quad (6\text{-}4)$$

where a/c is the mass aggregate/cement ratio, and ρc, ρw and ρa the volumetric mass of the cement, water and aggregate (g/cm^3), and y_{CO2} is the ambient CO2 content (%), normally 0.05% in urban areas.

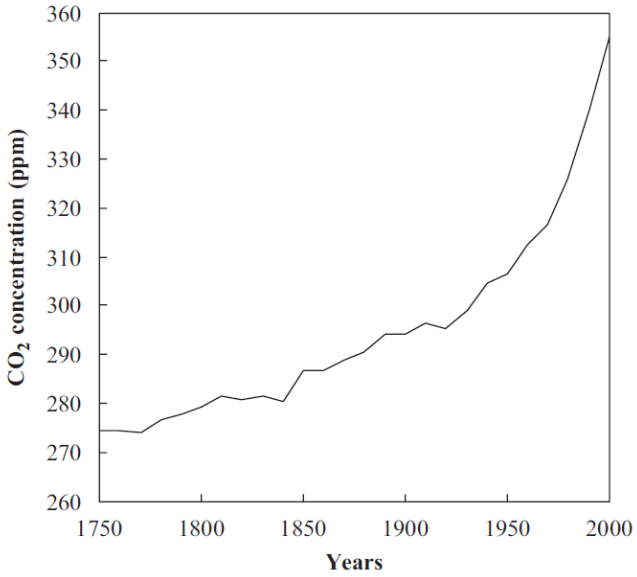

Figure 55 Change of atmospheric CO_2 concentration at a global scale (Yoon et al. 2007)

As previously mentioned, CO_2 concentration has been significantly increasing since the 1970s, especially after the year 2000. The influence of global climate change on carbonation in concrete has been recognized by many researchers (Yoon et al. 2007, Stewart et al. 2011, and Talukdar et al. 2012). Due to increasing concerns about the global warming and CO_2 emission, more research works have been carried out on the effect of carbonation on urban RC structures in the past decade. Saetta and Vitaliani (2004) argued that it oversimplifies the corrosion process, which assumes the failure take place when carbonation front reach the reinforcement surface, because the propagation period is disregarded. Results from their research showed that the concentration of CO_2 affects the rate of carbonation most among other environmental parameters. Helene and Castro-Borges (2009) reported that concrete structures in urban areas exposed to a humid environment can suffer severe degradation due to carbonation. Yoon et al. (2007) investigated the effect of climate change on the long-term prediction of carbonation in concrete structures. Figure 55 shows that CO_2 concentration has been significantly increasing since the 1970s. A regression equation (Equation 6-8) is given to predict the future CO_2 concentration throughout the 21st century. Another important parameter, the CO_2 diffusion coefficient is discussed on the basis of their experimental results. It is concluded that the CO_2 diffusion coefficient depends on the w/c ratio. The diffusion model revised by Stewart et al. (2011) is based on the model recommended by Yoon et al. (2007). Comparing to the model in Equation 6-2 to Equation 6-4, a wide range of parameters was considered as shown in Equation 6-5.

$$x_c(t) \approx \sqrt{\frac{2f_T(t)D_{CO_2}(t)}{a} k_{urban} \int_{2000}^{t} C_{CO_2}(t)dt} \times \left(\frac{1}{t-1999}\right)^{n_m} \quad t \geq 2000 \tag{6-5}$$

$$f_T(t) \approx e^{\frac{E}{R}\left(\frac{1}{293}-\frac{1}{273+T_{av}(t)}\right)} \quad \text{and} \quad T_{av}(t) = \frac{\sum_{i=2000}^{t} T(t)}{t-1999} \tag{6-6}$$

$$D_{CO_2}(t) = D_1 (t-1999)^{-n_d} \tag{6-7}$$

$$C_{CO_2} = 12.61 \ln(t) - 95.172, \quad 2000 < t < 2100. \tag{6-8}$$

$$a = 0.75 C_e C_a O \alpha_H \frac{M_{CO_2}}{M_{CaO}} \tag{6-9}$$

where x_c is the carbonation depth (in cm); $f_T(t)$ is the effect of temperature on diffusion coefficient, see Equation 6-6; $D_{CO2,}$ is the time dependent diffusion coefficient, see using Equation 6-7; k_{urban} is the factor to account for the increase in CO_2 level; C_{CO2} is the CO_2 concentration throughout the 21st century using Equation 6-8; and n_m is the C_{CO2} level associated with the frequency of wetting and drying cycles. E is the activation energy of the diffusion process (40 kJ/mol); R is the gas constant (8.314×10^{-3} kJ/mol); and T (t) is the average temperature over time. D_1 is the CO_2 diffusion coefficient after a year (cm^2s^{-1}); and nd is the age factor for D_{CO2} with typical values as shown in Table 30. C_{CO2} is the mass concentration of ambient CO_2 (10^{-3} kg/m^3); C_e is the cement content (kg/m^3); C_aO is the CaO content in cement (0.65); α_H is the degree of hydration, which estimates by as a function of water/cement ratio ($1-e^{-3.38w/c}$); M_{CO2} is the molar mass of CO_2 (56 g/mol); and M_{CaO} is the molar mass of CaO (44 g/mol).

Table 30. Values for D_1 and n_d

w/c	$D_1 \times 10^{-4}$ cm^2 s^{-1}	n_d
0.45	0.65	0.218
0.50	1.24	0.235
0.55	2.22	0.240

It is well known that corrosion of reinforcing bar begins when the carbonation front reaches the rebar surface and the pH at concrete cover drops to certain level (8.3 to 9.5). Yoon et al. (2007) reported that carbonation-induced corrosion starts slightly before the carbonation depth reaches the rebar surface, as shown in Figure 56, when the uncarbonated depth is about 8 mm without

consideration of chloride ions. The corrosion will be triggered earlier when the uncarbonated depth has a value of 20 mm, if chloride ions are taken into account. However, this effect is ignored by Fick's first law in Equation 2-1. Thus, T1 was estimated when the uncarbonated depth drops to 5 mm.

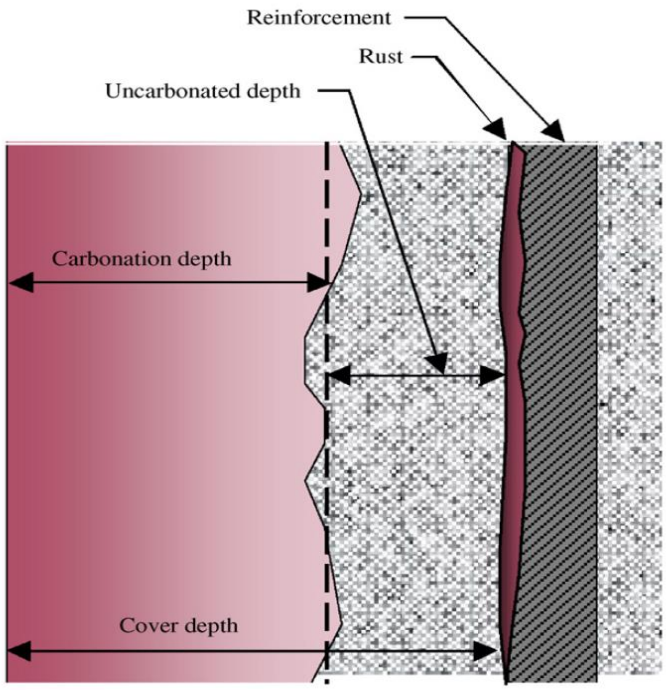

Figure 56: Schematic diagram of uncarbonation depth (Yoon et al. 2007)

After corrosion initiates at the surface of the reinforcing bar a similar phenomenon to that of chloride-induced corrosion will begin, that is, a reduction in bar diameter and the accumulation of rust products around the bar. There are few available functions on time-dependent corrosion rate for carbonated RC structures. Stewart et al. (2011) recommended Equation 6-10 for rust production

$$i_{corr}(t) = i_{corr\text{-}20}\,[1 + K(T(t) - 20)] \tag{6-10}$$

where $i_{corr\text{-}20}$ is the corrosion rate at 20 ºC given in Table 31; K = 0.025 if T (t) < 20 °C and K = 0.073 if T (t) > 20 °C; and T (t) is the average temperature over time.

Crack propagation was modeled in the same way as for chloride-induced corrosion. A detailed explanations with flow-charts can be found in Chapter 4.

Table 31. Corrosion rate icorr-20 for various exposures (Stewart et al. 2011)

Exposure class	Mean	Standard deviation	Distribution
Carbonation			
C1—Dry	0.0[a]	0.0	Lognormal
C2—Wet-rarely dry (unsheltered)	0.345 μA/cm^2	0.259 μA/cm^2	Lognormal
C3—Moderate humidity (sheltered)	0.172 μA/cm^2	0.086 μA/cm^2	Lognormal
C4—Cyclic wet-dry (unsheltered)	0.431 μA/cm^2	0.259 μA/cm^2	Lognormal

[a] Assume negligible = 0.1 μA/cm^2.

6.2 Prediction Results

In this example, the same bridge used for the project-level prediction of chloride corrosion was selected to simulate carbonation induced corrosion. The measurement in different conditions is shown in Table 32. The example deck was assumed to be located in three different CO_2 concentration levels, corresponding to the open country, a city center and an industrial zone. The effect of different CO_2 concentration levels on RC deck degradation are plotted as CDI curves in Figure 57. If the deck is assumed to be at a location of high chloride and high CO_2 levels, two CDI curves can be found, as shown in Figure 58. In this scenario, chloride corrosion is faster than carbonation. It can be seen that whichever corrosion process controls depends on the specific environmental condition. This case study proved that the severity of RC deck varied with the change in locations. The limitation is that the interaction between two corrosion processes is hard to take into account and the ever-changing microstructure of concrete cover cannot be modeled at this point.

Table 32. Concentration of CO2 measured in different types of environment

No.	Sample from	CO_2 [μV s]	CO_2 concentration [% vol.]
1	Open country	2293	0.015
2	City center	5469	0.036
3	Industrial zone	6814	0.045
4	Well-aired stable	6880	0.046
5	Stable	11,217	0.075
6	Motor car exhaust	2,513,424	16.690
7	Human breath	545,152	3.62

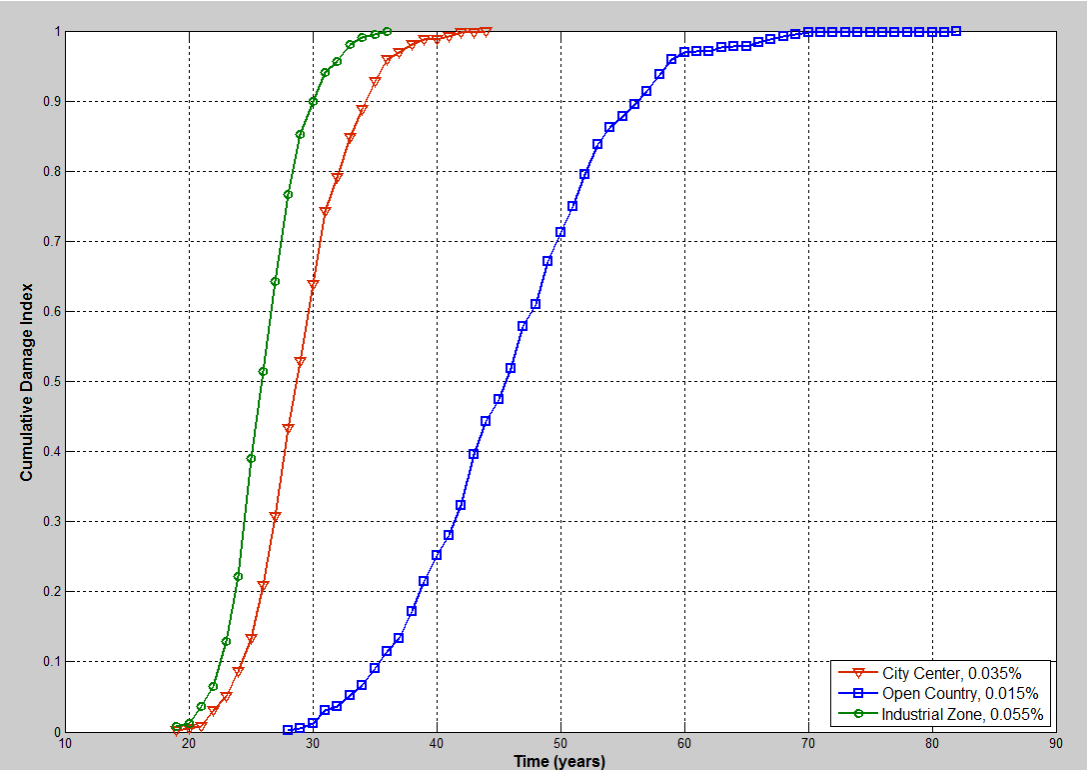

Figure 57 Comprasion of CDI curves under different CO_2 concentration

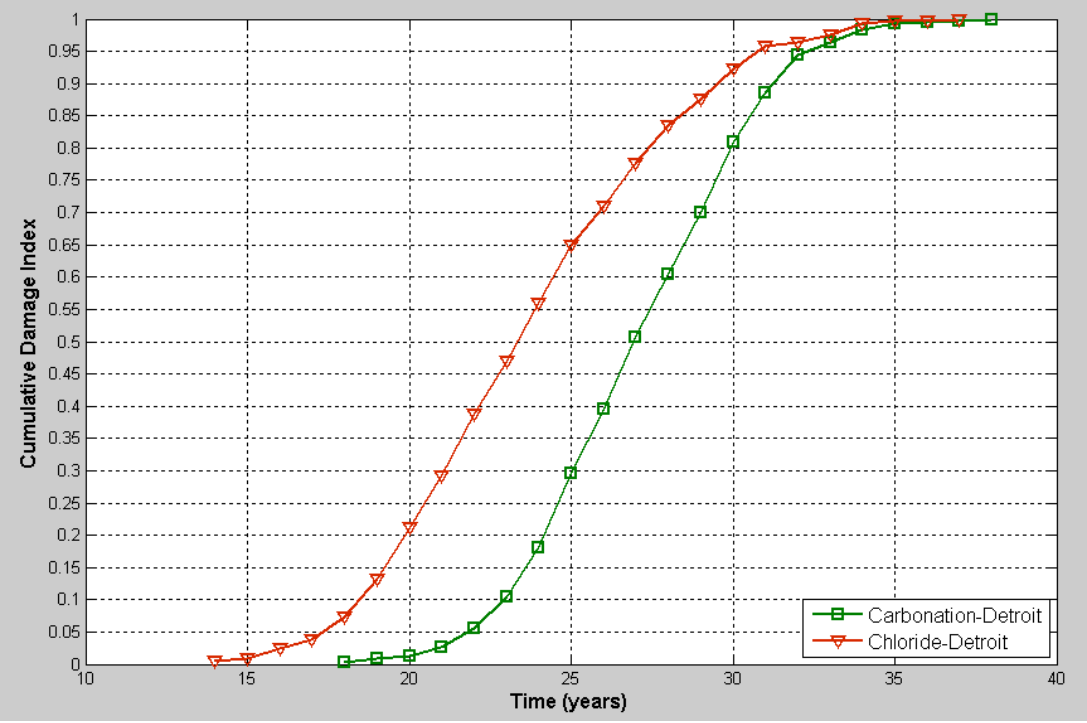

Figure 58 CDI curves due to two diffusion processes

Region B was selected to investigate the influence of different diffusion mechanisms on deck degradation, i.e. chloride- and carbonation-induced corrosion. A simplifying assumption is that the corrosion process due to carbonation is independent to that of chloride-induced corrosion. The dominating mechanism in each cell was determined after calculating the T1 for both processes. If T1 for chloride-induced corrosion was larger than T1 for carbonation, then carbonation-induced corrosion was considered critical for that cell, and vice versa. Previously, typical values for surface chloride content (C_0) and carbon dioxide content (CO_2) were reported. For this study, both C_0 and CO_2 had three levels, and C_0 was considered to have a normal distribution. The three mean values for C_0 were 1.8 kg/m^3, 3.6 kg/m^3, 5.4 kg/m^3. A 0.9 kg/m^3 standard deviation was used. The surface CO_2 was considered as a uniform distribution with the following ranges: 0.01 – 0.02%, 0.03 – 0.04%, 0.05 – 0.06% for open country, city center and industrial zone, respectively. The difference between Cl- and CO_2 concentration is that Cl- content was varied for each cell while $C0_2$ content was the same for the entire deck.

Concrete cover, concrete compressive strength and rebar diameter were again considered to be normally distributed. Three other statistical parameters were also included. CO_2 concentration (yco2) is the environmental input for carbonation corrosion, which is regarded to be uniformly distributed. The fracture energy of concrete (Gf) is an important material parameter that has a significant effect on T3. Gf was taken as a constant value (0.12 GPa), but it may vary slightly in different parts of the RC deck. As a result, it considered as a uniform distribution (0.12, 0.128). Uncarbonated depth was also considered as a uniform distribution (0.005, 0.010 m). Like Cth in chloride corrosion, uncarbonated depth is the threshold value for carbonation corrosion. Thus, there are a total number of 18 curves to represent the different environmental scenario in Region B, 9 for decks with BS and 9 for with ECR.

Table 33 and Table 34 show the prediction results for decks with BS and ECR, respectively. The predicted NBI rating was calculated from the cumulative damage of all the sampling cells on the deck. The damage in the cell may be caused by either chloride or carbonation. It can be seen in Table 33 that five out of the nine cases is a chloride-dominating deterioration process. In the first row of Table 33, carbonation dominates for conditions with low chloride content. In the second row, at about medium chloride content, carbonation corrosion is only critical for conditions with high CO_2 content. In the third row, chloride corrosion dominates for all the CO_2 contents. For the ECR cases carbonation corrosion dominates in eight out of nine cases as show in Table 34.

Table 33. Dominating corrosion mechanism in Region B (BS)

	Low CO_2 (0.01-0.02%)	Medium CO_2 (0.03-0.04%)	High CO_2 (0.05-0.06%)
Low C0 (1.8, 0.9) kg/m3	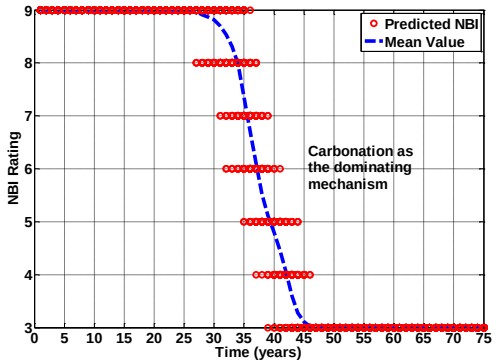	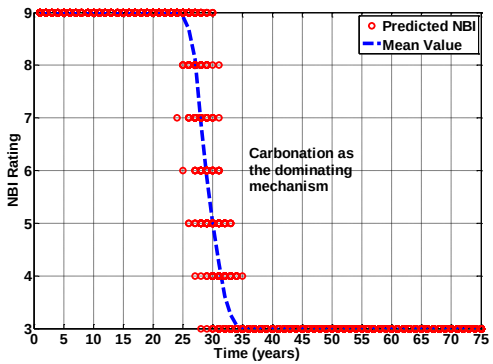	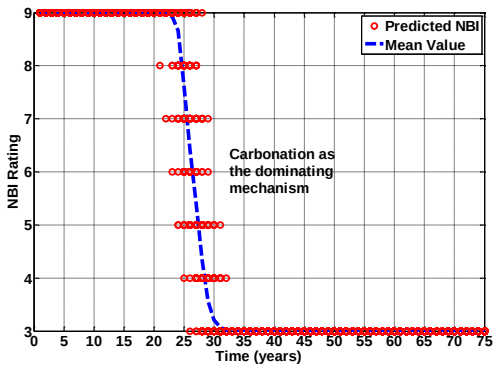
Medium C0 (3.6, 0.9) kg/m3	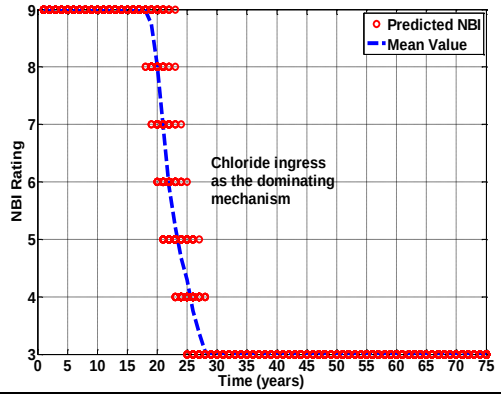	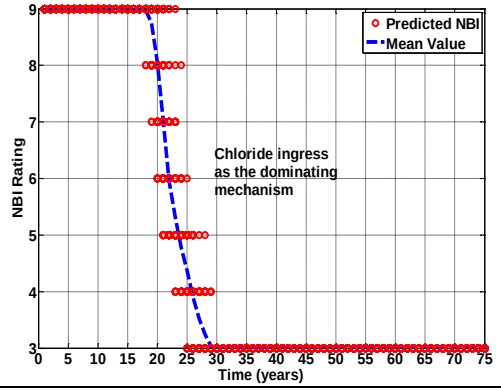	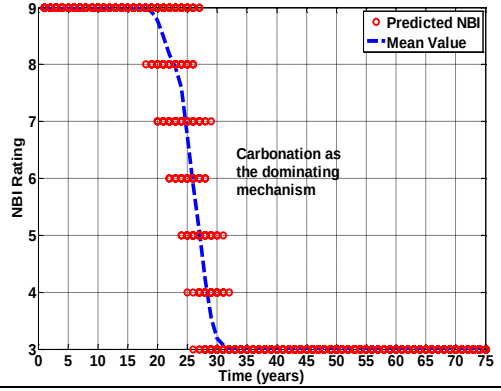
High C0 (5.4, 0.9) kg/m3	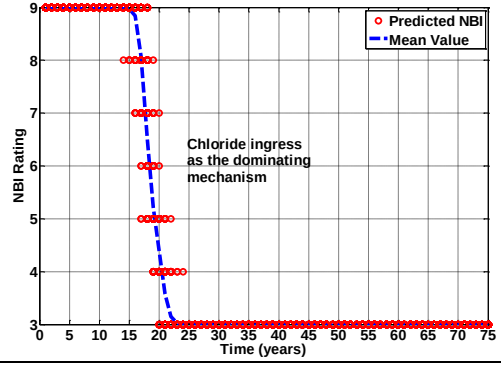	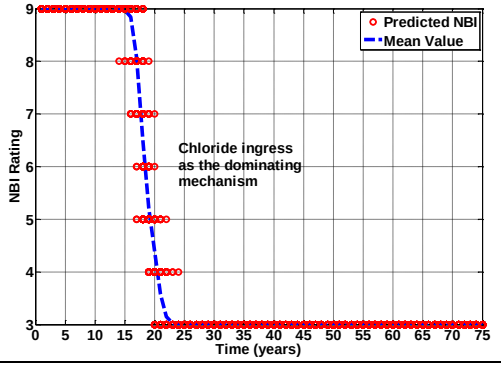	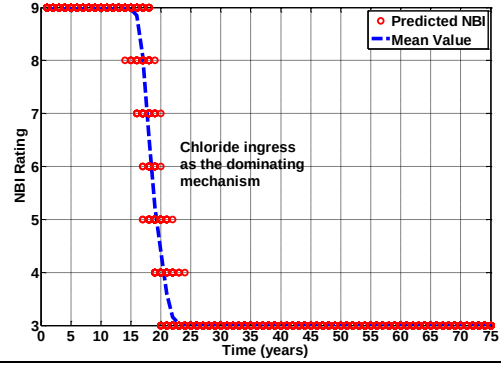

Table 34. Dominating corrosion mechanism in Region B (ECR)

	Low CO2 (0.01-0.02%)	Medium CO2 (0.03-0.04%)	High CO2 (0.05-0.06%)
Low C0 (1.8, 0.9) kg/m^3	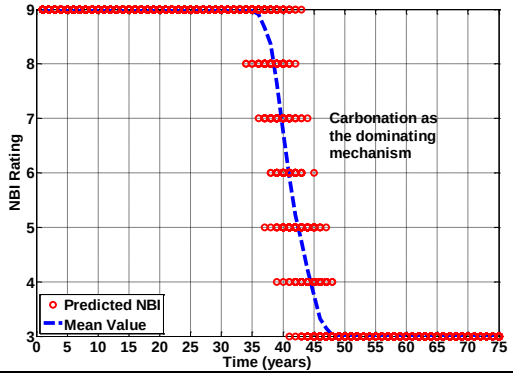	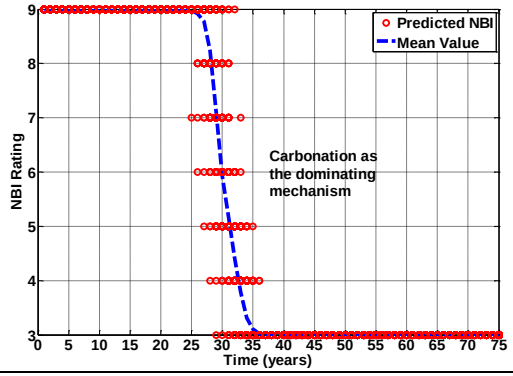	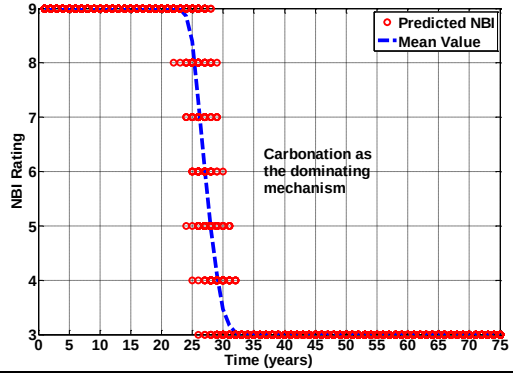
Medium C0 (3.6, 0.9) kg/m^3	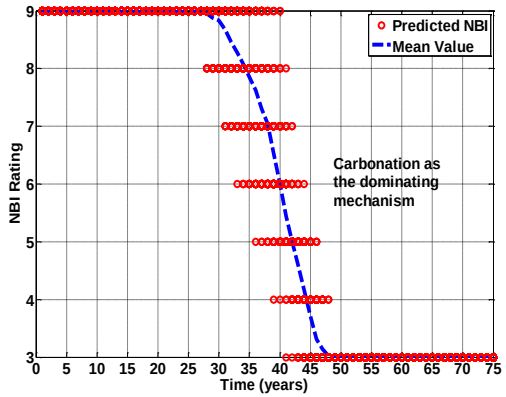	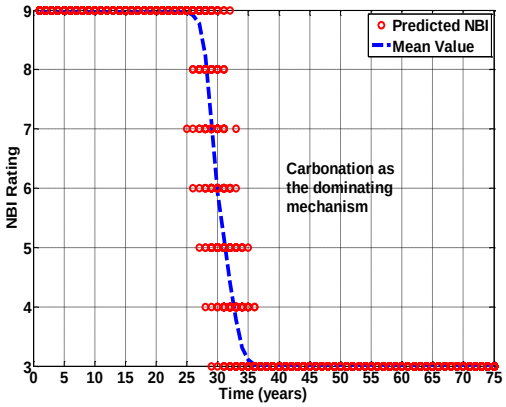	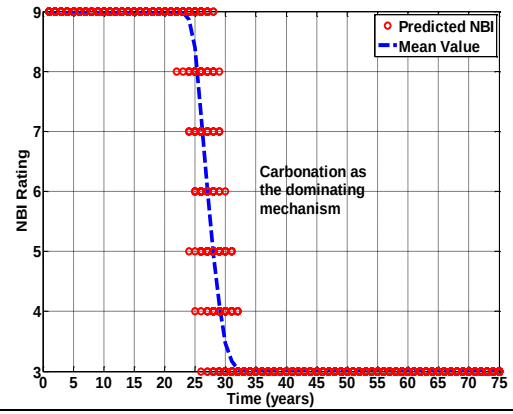
High C0 (5.4, 0.9) kg/m^3	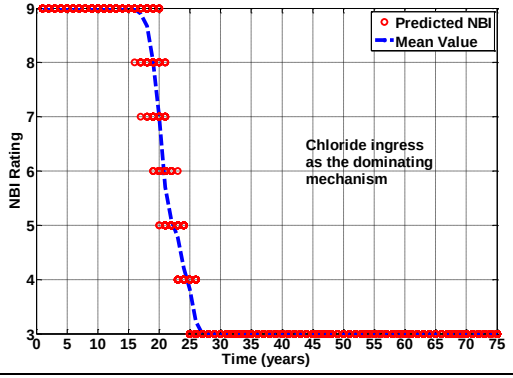	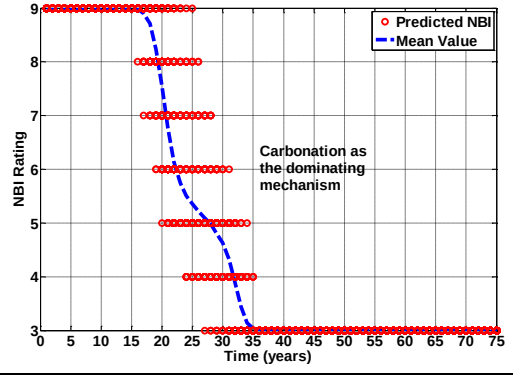	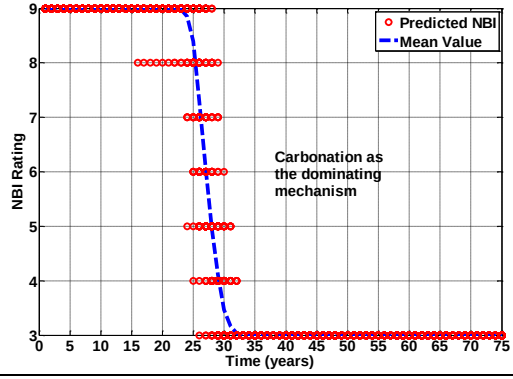

6.3 Discussion

A review on the modeling the carbonation-induced corrosion was presented. A three-phrase process similar to the chloride-induced corrosion was presented and the coupling effect of chloride and carbonation in the diffusion process was investigated. Similar to the modeling of chloride-induced corrosion, appropriate models were selected for carbonation corrosion and implemented into the proposed probabilistic-based framework. The coupling effect of chloride and carbonation effects in the diffusion process was investigated. The prediction of NBI ratings in a given region shows that one of these two corrosion process dominates under different environmental scenarios.

7 CONCLUSIONS AND RECOMMENDATIONS

Service life predictions are very challenging due to uncertainty in the inputs and the inherent complexity of the degradation processes. Further, it should be emphasized that no model is perfect, since they are all based on a set of assumptions. By selecting mechanistic models from the literature, the probabilistic-based framework developed in this report shows that it is feasible to estimate the service condition of RC decks due to the effects of chloride induced corrosion. Predicted degradation curves, defined as condition rating as a function of deck age, were developed and compared with inspection data at the project and network levels. Based on the analysis results, the following conclusions can be drawn.

1. Three major causes of deterioration of RC deck were recognized, including chloride induced corrosion, carbonation and freeze thaw. Existing analytical models for these three mechanisms were studied and compared. A review of commercial programs developed for concrete durability modeling was conducted and their advantages and disadvantages were summarized. From this review, perceived limitations were identified in order to choose suitable models and to improve the accuracy of service life prediction.

2. The selection of appropriate deterministic models from the most recent published literature improves on the noted shortcomings of existing analytical solutions and commercial software for service life prediction. The complete cracking process due to chloride induced corrosion at the deck level was described as a three-phase process. In particular, the propagation phase was estimated by a model on the basis of fracture mechanics and strain energy. Based on the summary of key parameters in the noted phases, a flow chart for numerically implementing the model was presented. The selected models were able to provide time-dependent information on important parameters and features of the degradation process due to chloride ingress.

3. At the deck level, a probabilistic-based framework was used by employing Monte Carlo Simulations (MCS). Key parameters were considered as random variables and appropriate probability distributions were assigned to capture the random nature of the model outputs. Through this approach the predicted damage severity of the deck could be predicted based on a probabilistic approach and represented as contour plots of time to cracking and crack width.

4. The predicted severity of deck damage through the MCS was mapped to the National Bridge Inventory (NBI) rating scale by using the predicted percentage of damaged cells on the deck. A

series of investigation were carried out for validating the proposed mechanistic-based framework. Recommendations were given to define the number of representative cells for adequate accuracy and computational efficiency. At the project level, the observed ratings of 10 decks were matched to the predicted NBI ratings. At the network level, generalized degradation curves obtained by the MCS were used to represent decks in in different regions. It was found that the bounds to the prediction have a reasonable range that brackets most of the archived inspection data.

5. A parametric study was presented to investigate the influence of key parameters on deck degradation. The results showed that the use of ECR, concrete compressive strength and concrete cover are the top three factors that affect deck degradation. Three environmental data (temperature, humidity and surface chloride concentration) also have notable effect. The change of bar diameter did not significantly change the prediction of condition ratings. Based on these parametric studies six tables (36 reference charts) were established for facilitate use of the developed model. Results from the parametric study are thought to offer particular benefit as a guideline for future design and practice.
6. Finally, deck deterioration due to the multi-mechanism was discussed. It was noted that chloride corrosion is the major cause for deck degradation. Carbonation was considered as another effect due to its similarity to chloride induced corrosion and the availability of local mechanistic models that could be readily implemented into the proposed probabilistic framework for global level degradation modeling. The effects of freeze-thaw were not incorporated into the mechanistic model since this mechanism is controlled by microstructure parameters not considered in the current modeling scheme and the existing methods to evaluate damage from freeze-thaw effects are not directly applicable to the proposed global level modeling. The coupling effect of chloride and carbonation in the diffusion process was investigated by decoupling the processes and identifying the controlling degradation mechanism. The prediction of NBI rating at a given region shows that one of these two corrosion process will dominate depending on the environmental scenarios.

Although all the discussion in this report only concerned bridge decks in Michigan, the proposed probabilistic framework can be applied in general for service-life prediction when dealing with the up-scaling of local-level mechanistic-based deterministic models to global-level degradation modeling of large size structural elements and systems. The success of this statistics-based framework could assist

highway agencies in identifying appropriate maintenance timings and optimal deck design options. A user-interface in the Matlab GUI environment was developed with the hope that it can facilitate and promote use of the developed degradation model. Detailed description about this interface can be found in the Appendix.

For the improvement of the proposed framework for future prediction modeling, it is highly recommended that:

1. At the cell level, the deterministic models need more accurate simulation of the entire corrosion process, especially the diffusion process. In addition, the deterioration due to multi-mechanisms should be taken into account. Ideally, models to update the concrete microstructure as a function of time should be developed and implemented. In this way, deterministic model can provide a better simulation of the actual conditions of the deck. Meanwhile, models to predict the time to cracking at the cell level need to improve in accuracy compared to the one used in this work.

2. At the deck level, it is better to define all the model input based on actual material and environmental data. In particular, project-level predictions can be improved with actual material test data and exposure information. In order to improve the accuracy of the MCS, other key parameters should also be considered as random inputs, such as the material properties of the steel and rust. Clearly, more iteration can also be run to achieve better accuracy.

   For model validation, the descriptors for the service life (i.e., NBI ratings) should be improved with more specific information (i.e., crack width). At the same time, inspection error should be minimized with use of advanced technology so that the severity of the deck can be more accurately measures for improve mapping relations between inspection records and quantitative results from mechanics-based modes as the ones used in this work.

APPENDIX: MECHANISTIC-DECK 1.1 USER'S MANUAL

Nan Hu, Rigoberto Burgueño and Syed W. Haider
Michigan State University

A.1 Introduction

Mechanistic-Deck (Mechanistic 1.1) is a program developed by Michigan State University for the Michigan Department of Transportation (MDOT) as part of a research project to model the degradation of highway bridge decks due to multi-mechanism, including chloride-induced corrosion, carbonation and freeze-thaw cycle. Mechanistic-Deck is a stand-alone executable compiled from Matlab (Mathworks 2012) codes using a graphic user interface (GUI).

Mechanistic-Deck provides a framework to implement a statistical-based model for predicting deck degradation in Michigan. The methodology in this program is a two-level strategy. At a local (unit cell) level, a three-phase corrosion process was modeled by employing mechanistic models [1] that can predict the time for reinforcement bar corrosion to manifest in surface cracking. At a global (bridge deck) level, a Monte Carlo Simulation (MCS) approach was implemented on a representative number of cells from the deck domain. Material and environmental properties at the local/cell level were varied based on probability distributions. A cumulative damage index (CDI) curve of the deck was calculated based on the predicted time to surface cracking from all the cells. Finally, the damage severity of the deck was mapped to the National Bridge Inventory (NBI) rating, a conventional bridge rating system used by highway agencies. Bridges from different regions in Michigan were used to validate the prediction model. The validation results show a good match between observed and predicted bridge ratings.

Overall, this program provides an approach to model bridge deck conditions utilizing a statistical based framework. It can assist the MDOT on future design and maintenance of bridge deck. It is noted however, that the prediction by this program is not 'perfect', because all the mechanistic models are based on a set of assumptions. The models were chosen with consideration of ease of implementation in a framework for life-time prediction and durability modeling. Also, its accuracy is affected by the selection of the model input data. For that, it is better to define all the key inputs based on real data of a specific deck.

A.2 Installation

A.2.1 Copy CD files to destination folder

Copy the files in the CD to the location where Mechanistic-Deck is to be executed.

A.2.2. Set up MCRInstaller.

Install the Matlab Component Runtime (MCR) through the MCRInstaller. MCRInstaller is required before running all the Matlab stand-alone application, because it contains the toolboxes that the application needs. You need to have administrative rights in the computer/account in order to do this installation. Double click to open MCRInstaller and follow the InstallShield Wizard instructions, as shown through Figure A-1 to Figure A-5. After finishing the installation, the MCRInstaller file may be deleted.

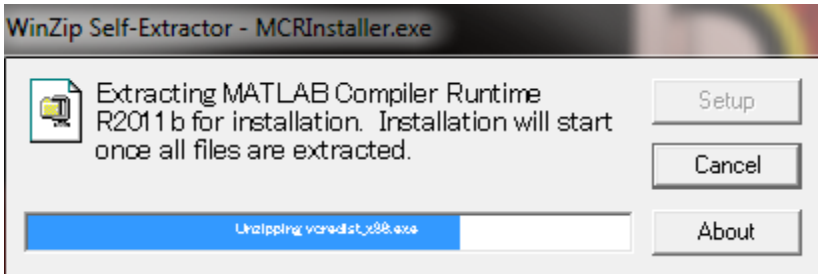

Figure A-1 Run the MCRInstaller.exe

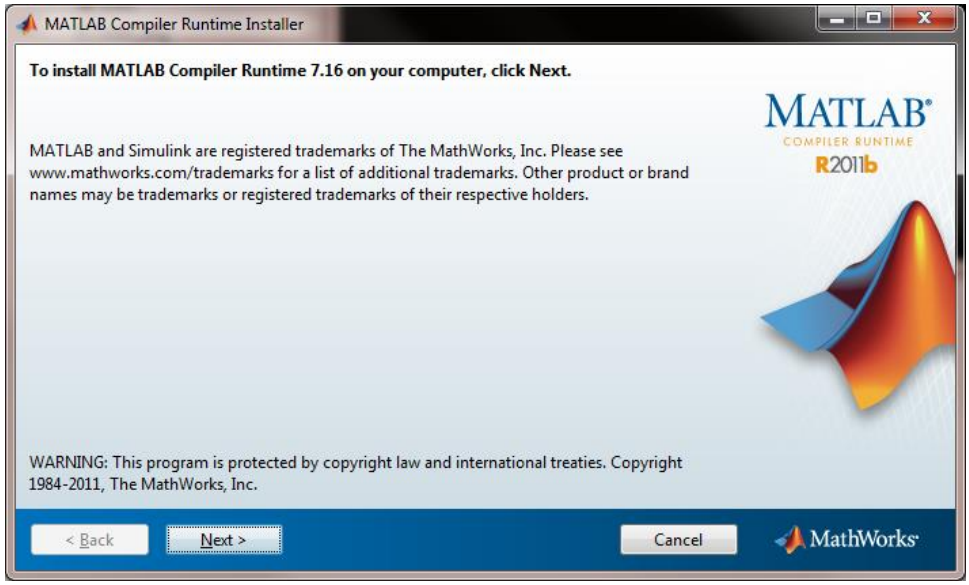

Figure A-2 Matlab Complier Runtime Installer

The Matlab Complier Runtime Installer will start. Click ‘Next’.

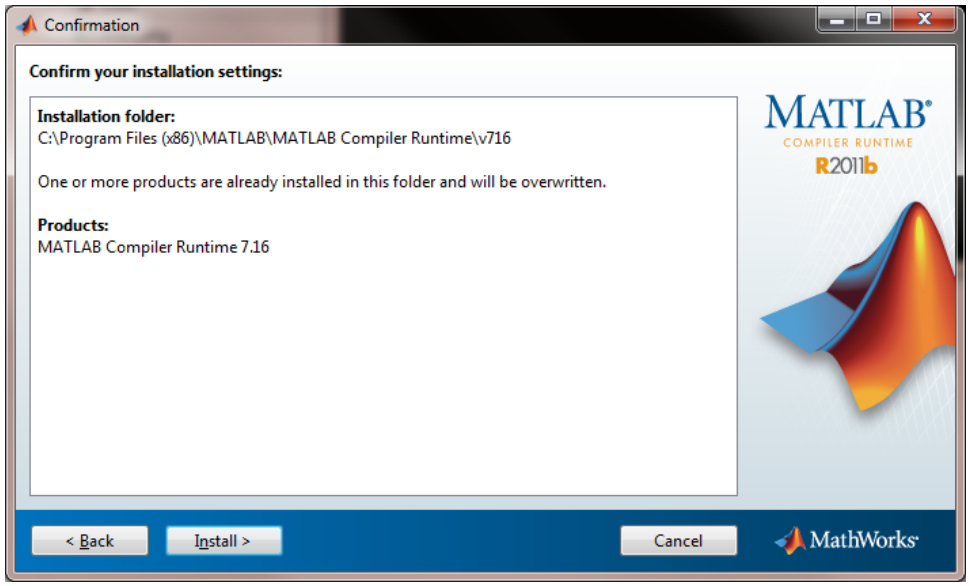

Figure A-3 the installation setting of Matlab Complier Runtime

Click ‘Install’.

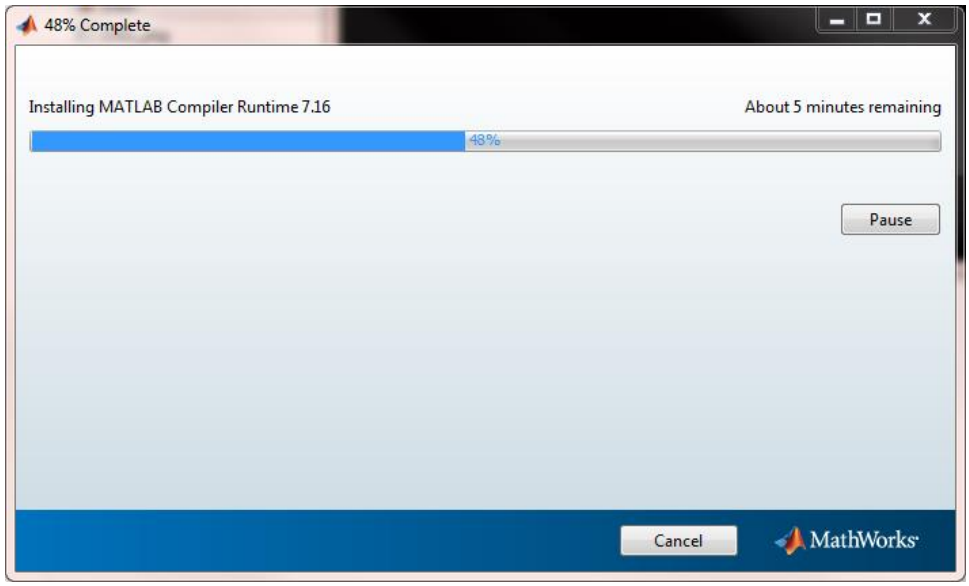

Figure A-4 the installation process of Matlab Complier Runtime

The program should now be installing.

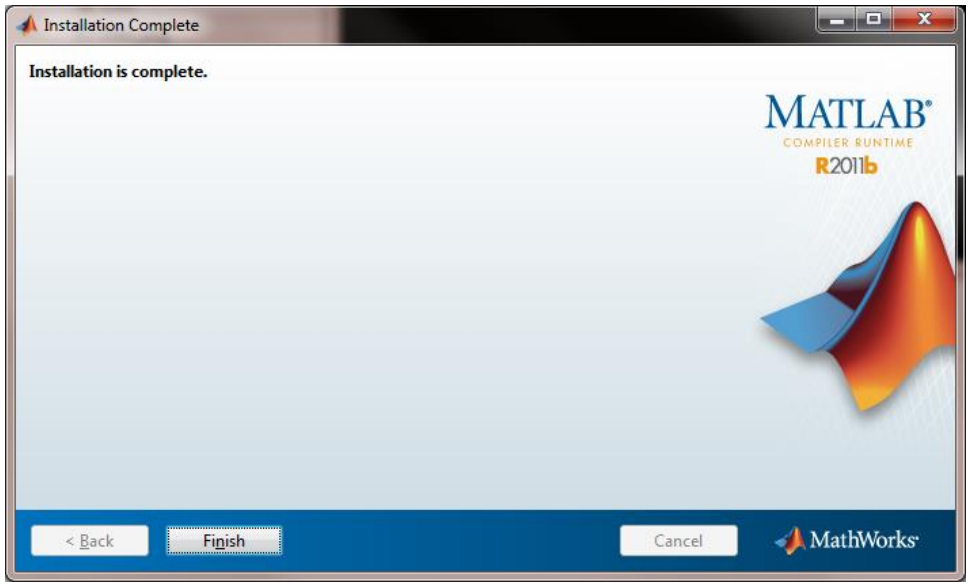

Figure A-5 the completion of installation process

After installation, click ‘Finish’.

A.2.3. Install Mechanistic-Deck_pkg.

Mechanistic-Deck 1.1 and a readme file will be given once the users double-click the ‘Mechanistic-Deck_pkg’.

A.2.4. Execute Mechanistic-Deck 1.1

Mechanistic-Deck 1.1 can be run after the installation of MCR by double-clicking the ‘Mechanistic-Deck 1.1’.

A.3 User Interface

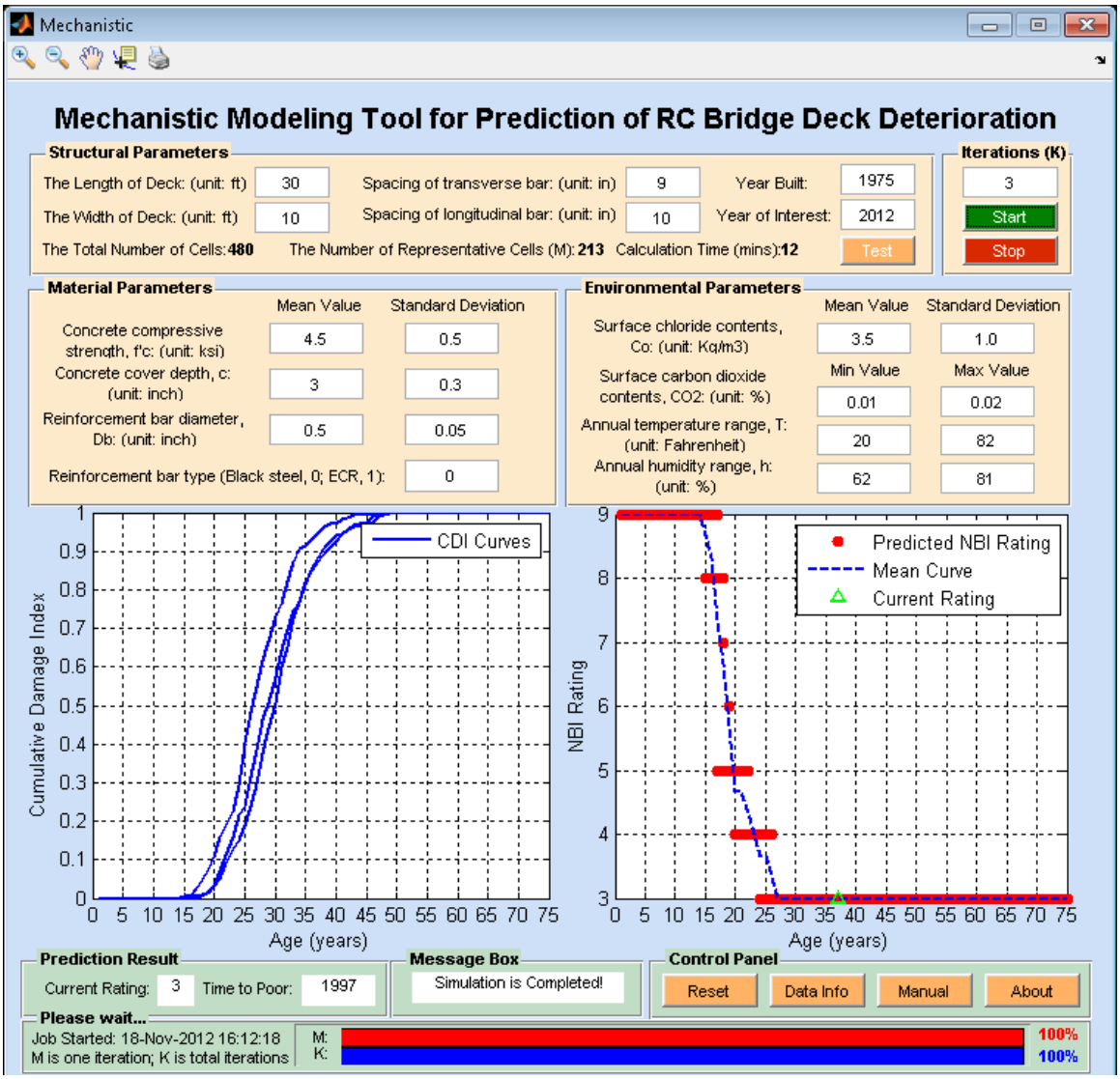

Figure A-6 Interface of Mechanistic 1.1

The user interface of Mechanistic-Deck program is shown in Figure A-6. It contains three main zones: model input, plotting and model output.

A.3.1. Model input

Model input of this program contains structural parameters, material parameters, environmental parameters and iterations of Monte Carlo simulation, as shown in Figure A-7. Default values are given to all the model input.

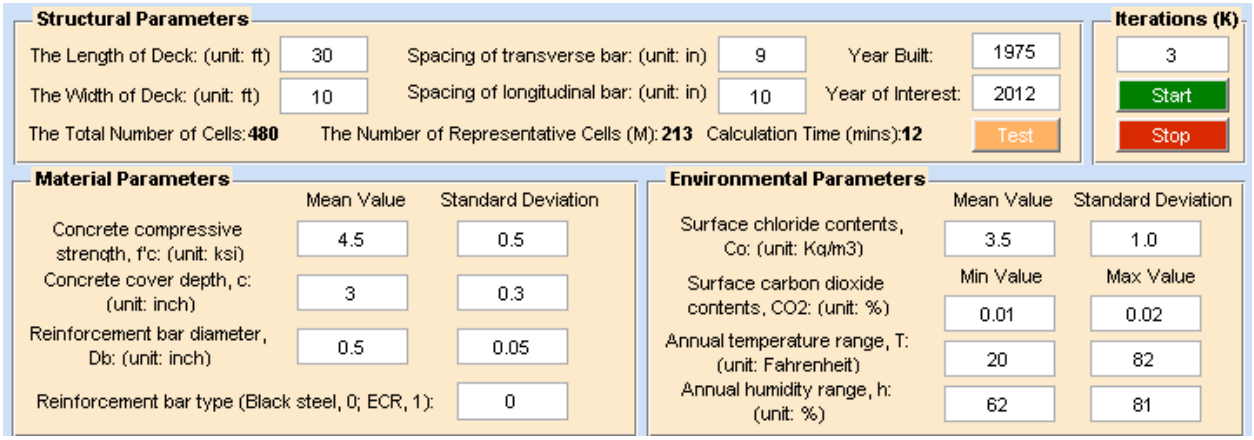

Figure A-7 Model input of Mechanistic 1.1

A.3.2. Structural parameters and the number of iteration

Structural parameters are used to estimate a total number of concrete cells at the entire bridge deck domain. The first step is modifying all these default values in structural parameters and the number of iterations for a specific deck, as shown in Figure A-8.

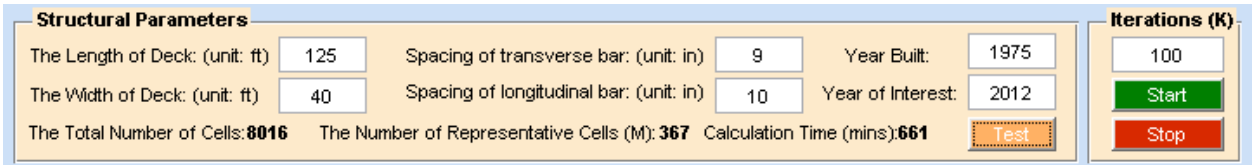

(a)

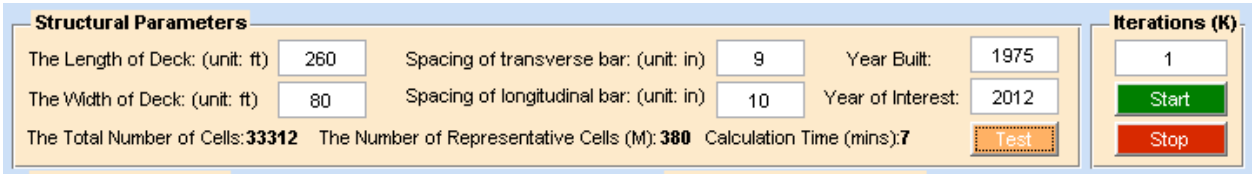

(b)

Figure A-8 Structural parameters and iterations (K)

At the local/cell level, deterministic analysis is performed on a cross-section of a cubic block, which contains a thick-wall concrete ring with a concentric reinforcing bar that can predict the time for reinforcement bar corrosion to manifest in surface cracking. Due to the requirement of one bar per cell, the total number of cells on the deck domain is dependent on the bar spacing on the transverse and longitudinal directions. Choosing random samples spatially represents the whole population of cells on the deck to achieve an acceptable prediction. Three constraints while estimating the appropriate representative cells size are listed as follow:

1. Mechanistic model (one bar per cell);
2. Equal probability of damage on the entire deck;
3. The resolution according to the NBI rating (e.g. 2% damaged area for Grade 7);

The first constraint is the prerequisite for the cell-level deterministic model. As mentioned previously, the cracking process in this model just considers one bar per cell. The dimension of the cell is equal to the spacing of the transverse bar.

The second constraint represents an equal probability of damage. Given that the deterioration of the RC deck is only associated with the environmental conditions, the probability of damage in each cell should be similar. However, there is no set percentage that is accurate for every RC deck. It would be inefficient, if too many cells are chosen with no significant improvement in the accuracy of prediction. The equation in Figure A-9 is chosen to determine the sample size (Watson, 2001).

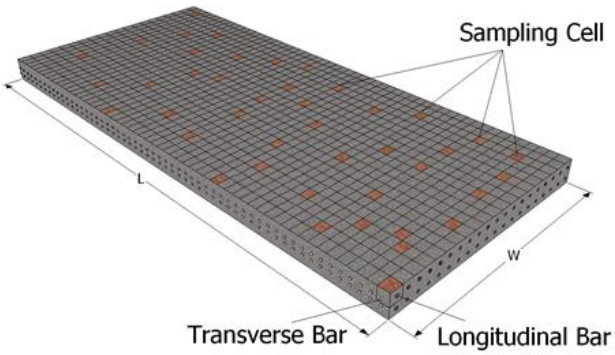

$$n = \frac{P \cdot (1 - P)}{A^2/Z^2 + P \cdot (1 - P)/N}$$

- n = sample size required;
- P = estimated variance in population 50%
- A = desired precision 5%
- Z = Based on confidence level 95%
- N = number of cell population on deck

Figure A-9 Representative cells on the deck domain

In this program, the prediction assumes a 95% confidence level, 50% variance (P) and five percent margin of error (A). N is the total number of cells on the entire deck obtained by the bar spacing. It is estimated that 394 cells are required for a total number of 25000.

The third constraint is about the resolution of the deterioration on the deck. After estimating the T3 in each cell, the number of damaged cells in a given time can be determined. This number of cells must be enough to catch the damaged area that is required by the NBI.

Another important input at this step is the number of iterations. The calculation time is dependent on how many iteration are selected for the Monte Carlo simulation. As shown in Figure 3-3, a larger

number of iterations will take about 661 minutes to complete the whole simulation process while one iteration just takes about 7 minutes. It is noted that the user can run just one iteration to get a degradation curve. But for accuracy of the MCS, 100 iterations are enough to meet the statistical purpose and consider the input data uncertainty. After modifying all the values, the user may click the 'Test' pushbutton. The program will show the total number of cells and the number of representative cells and an estimated calculation time. Based on that, the user may change the number of iterations before starting the simulation.

A.3.3. Material parameters

Based on a series of parametric studies during this research project, it was confirmed that the use of epoxy coating reinforcing (ECR) bars, concrete compressive strength (f'c) and concrete cover (c) are the three key material factors that affected the deck deterioration. The reinforcement bar diameter (Db) did not significantly change the degradation curves.

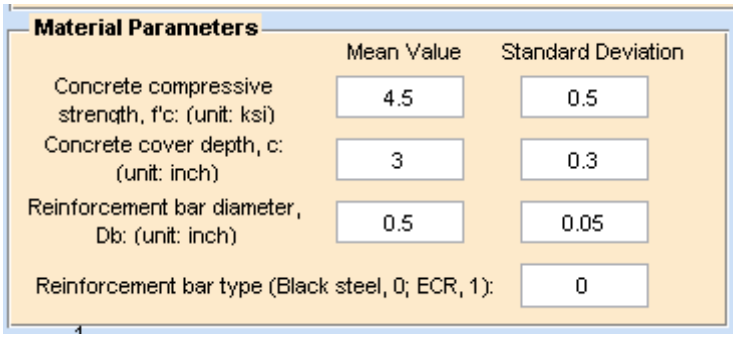

Figure A-10 Material parameters

The three random inputs related to structural design are f'_c, cover and D_b, as shown in Figure A-11. The construction of RC decks in US began in 1930s. The design standards have changed over the years. The enhancement of concrete quality is the most common way to improve the durability of RC decks. In this program, a value of 31.5 MPa at 28 days (4.5 ksi) is used for the default of f'_c. The requirement of minimum cover depth is another way to reduce the deterioration of decks. In older decks, the cover depth of 38.1mm (1.5 in.) was used. Later, many states have increased the minimum cover to 63.5 mm (2.5 in.). According to Michigan DOT's standard bridge slab design guides, the minimum clear cover for transverse bars is 76.2 mm (3 in.). Thus, the default of concrete cover has a mean value of 76.2 mm and a standard deviation 11mm due to construction variability. As for the D_b, the typical size for a

transverse bar is 15.875mm (No.5 bar). Similar to cover depth, a 10% deviation ($\pm$ 1.5mm) is considered to account for construction variability. These three parameters are considered to be normally distributed. Finally, the selection of rebar type is used to define a threshold value of chloride content to initiate the corrosion (C_{th}). In this program, the C_{th} values of 1.2kg/m^3 and 2.2kg/m^3 were used for BS and ECR bar, respectively

A.3.4. Environmental parameters

The main statistical environmental parameters for the MCS in this program include surface chloride concentration (C_0), surface carbon-dioxide concentration (CO_2), temperature and humidity, as shown in Figure A-12. It is noted that the debate on the correctness of model input always existed, since the data were obtained from different labs and fields. The best way to find the information is to look into the MDOT database, for example, all the surface chloride concentration measurements from concrete cores. If those values are not available, at least, an appropriate range must be selected under certain assumptions.

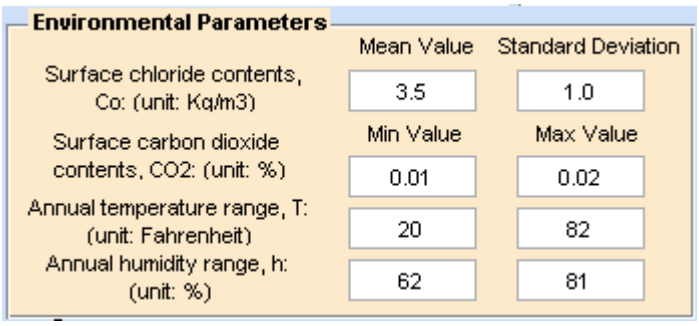

Figure A-11 Environmental parameters

The input C_0 was considered as time-dependent and was accumulated with time, because over time concrete deck could cyclically expose to deicing salts. However, a generally accepted knowledge is that C_0 reaches a maximum value at a certain concrete depth (typically 12.7 mm), so that it may be assumed quasi-constant after exposure (Fanous and Wu 2005). Typical range reported in the literature is between 1.2 to 8.2 kg/m^3 in US (Vu and Steward 2000). In most of the previous studies (Stewart and Rosowsky 1998, Vu and Stewart 2000, Stewart and Mullard 2007) concerning probabilistic analysis, C_0 is a commonly regarded as a lognormal distribution with mean value of 3.5 kg/m^{3}and coefficient of variance of 0.5. Therefore, these values are selected as default for the program. The other values are listed in Table A-1.

Table A-1. The statistical value for Cth in the literature (kg/m^3)

Literature	Mean or Range	COV	Distribution	Notes
Stewart and Rosowsky (1998)	0.9	0.19	Uniform	0.6-1.2
Lounis (2003)	1.35	0.1	Lognormal	
Stewart et al. (2004)	1.4	0.125	Normal	0.4% weight
Stewart and Mullard (2007)	2.4	0.2	Normal	
Lu et al. (2011)	0.4-1.0	0.247	Uniform	

The difference between Cl- and CO_2 concentration is that Cl- content was varied for each cell while $C0_2$ content was the same for the entire deck. A simplifying assumption in the modeling process is that the corrosion process due to carbonation is independent to that of chloride-induced corrosion. The dominating mechanism in each cell was determined after calculating the corrosion time at the rebar surface for both processes. If the corrosion time of chloride-induced corrosion is larger than the corrosion time of carbonation, then carbonation-induced corrosion was considered critical for that cell, and vice versa. The measurement in different conditions is shown in Table A-2. The surface CO_2 was considered as a uniform distribution with the following ranges: 0.01-0.02%, 0.03-0.04%, 0.05-0.06% for open county, city center and industrial zone, respectively. Again, it is better to measure the real data for input.

Table A-2. Concentration of CO2 measured in different types of environment

No.	Sample from	CO_2 [μV s]	CO_2 concentration [% vol.]
1	Open country	2293	0.015
2	City center	5469	0.036
3	Industrial zone	6814	0.045
4	Well-aired stable	6880	0.046
5	Stable	11,217	0.075
6	Motor car exhaust	2,513,424	16.690
7	Human breath	545,152	3.62

According to the MDOT region offices and transportation service centers (listed in Table A-3), the temperature and humidity of those cities in Michigan was collected from an online climate database, as shown in Table A-4. It should be emphasized that all these values are the monthly mean and not the maximum or minimum ones.

Table A-3: MDOT offices by regions

Region	Region Office	Transportation Service Center
1-Superior	Escanaba	Crystal Falls, Ishpeming, Newberry
2-North	Gaylord	Alpena, Cadillac, Traverse City
3-Grand	Grand Rapid	Muskegon
4-Bay	Saginaw	Bay City, Davison, Mt. Pleasant
5-Southwest	Kalamazoo	Coloma, Marshall
6-University	Jackson	Brighton, Lansing
7-Metro	Southfield	Detroit, Oakland, Macomb/St. Clair, Taylor

Table A-4: the mean temperature and humidity of major cities in Michigan

Region		Humidity Max (%)	Humidity Min (%)	Avg. Tmax °C	Avg. Tmin °C
1-Superior	Escanaba	76	68	18	-12
	Crystal Falls	83	73	18	-12
	Ishpeming	82	68	19	-10
	Newberry	84	67	18	-9
	Average	**81.3**	**69.0**	**18.3**	**-10.8**
2-North	Gaylord	83	64	20	-8
	Alpena	79	67	15	-11
	Cadillac	84	67	20	-7
	Traverse City	78	66	21	-6
	Average	**81.0**	**66.0**	**19.0**	**-8.0**
3-Grand	Grand Rapids	79	65	23	-4
	Muskegon	78	65	22	-3
	Average	**78.5**	**65.0**	**22.5**	**-3.5**
4-Bay	Saginaw	79	65	22	-5
	Bay City	79	67	22	-5
	Davison	79	66	22	-6
	Mt. Pleasant	83	65	22	-6
	Average	**80.0**	**65.8**	**22.0**	**-5.5**
5-Southwest	Kalamazoo	82	69	23	-3
	Coloma	80	71	23	-3
	Marshall	81	65	22	-6
	Average	**81.0**	**68.3**	**22.7**	**-4.0**
6-University	Jackson	81	68	22	-4
	Brighton	81	64	22	-5
	Lansing	80	68	22	-4
	Average	**80.7**	**66.7**	**22.0**	**-4.3**
7-Metro	Southfield	75	56	22	-5
	Detroit	74	61	23	-3
	Oakland	80	68	22	-5
	Macomb/St. Clair	78	68	22	-4
	Taylor	76	64	23	-3
	Average	**76.6**	**63.4**	**22.4**	**-4.0**

The user may click the ‘Info’ pushbutton for this information, as shown in Figure A-12. The user can also click ‘Data’ for further instruction on data selection, as shown in Figure A-13.

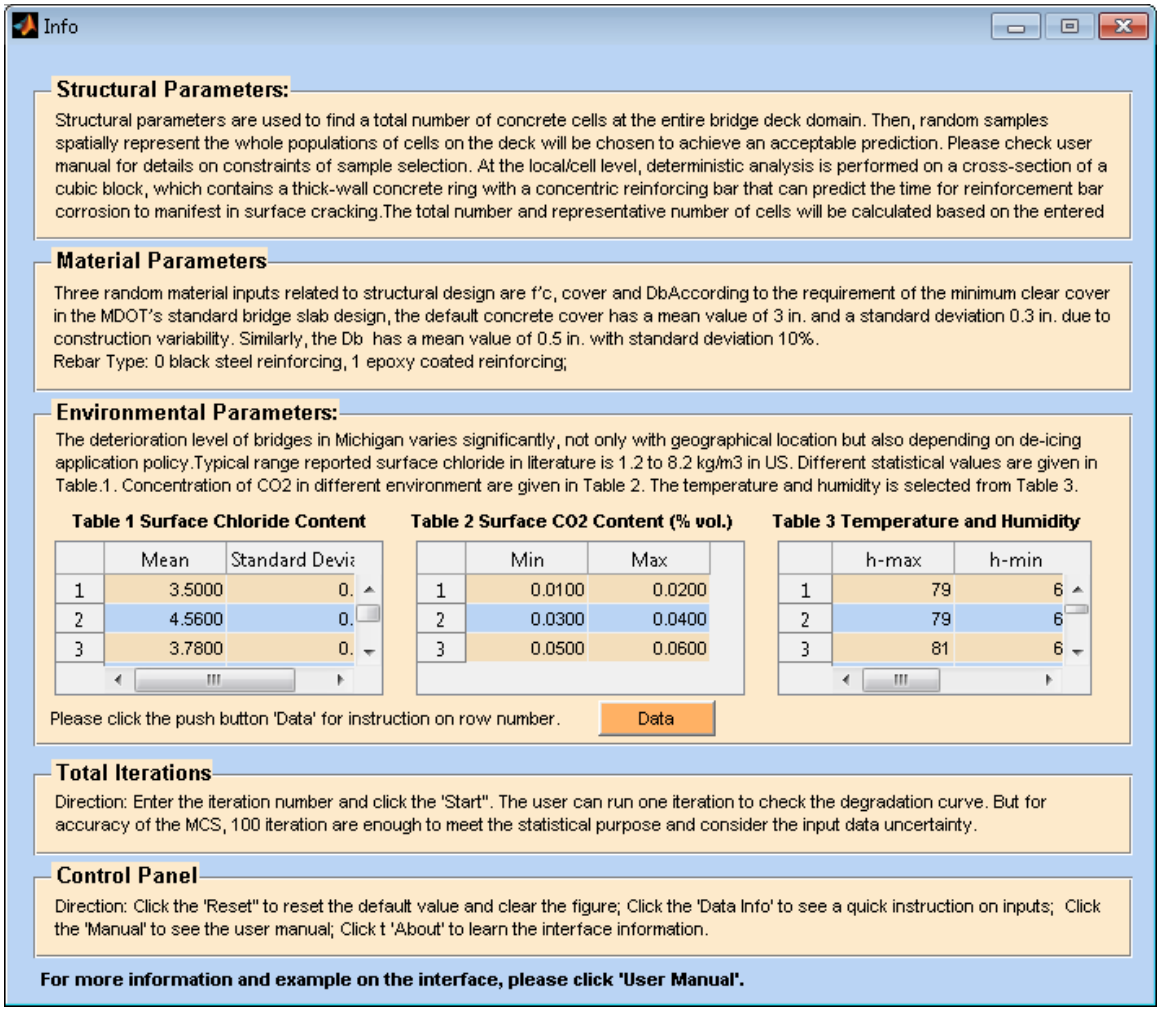

Figure A-12 Info window for a quick instruction on model input

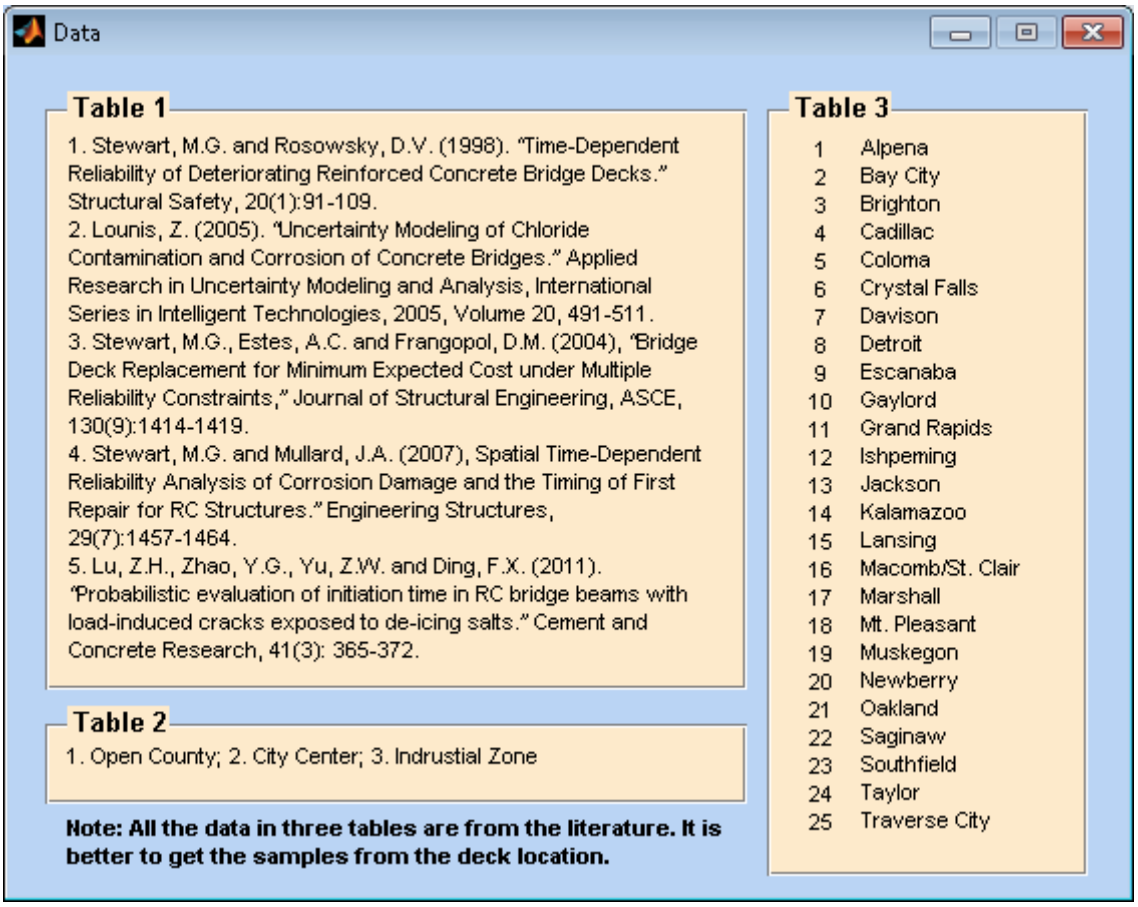

Figure A-13 Data window for a further instruction on model input

A.4. Modeling Process

To account for the uncertainty of model input and statistical analyses, Monte Carlo simulations are adopted into the prediction of deck service life. Cumulative damage of the deck is calculated based on the predicted time to surface cracking from all the cells. Then, the damage severity of the deck is mapped to the National Bridge Inventory (NBI) rating.

After clicking the 'Start' pushbutton, the whole modeling process will start. At the bottom of the interface, there is a 'Please wait…' panel which shows the time the job started and a bar graph showing 100% complete, as shown in Figure A-14. The first bar (red) indicates how many cells have been calculated according to the total number of representative cells on the deck domain. The second bar (blue) shows how many iterations of Monte Carlo simulation have been done according to the user-defined number 'K'. In the example case, K is equal to 3. It can be seen from Figure A-14 (a) that the

model is running in the first iteration, while Figure A-14 (b) indicates that simulation is running in the second interation. Figure A-14 (c) shows that simulation is completed.

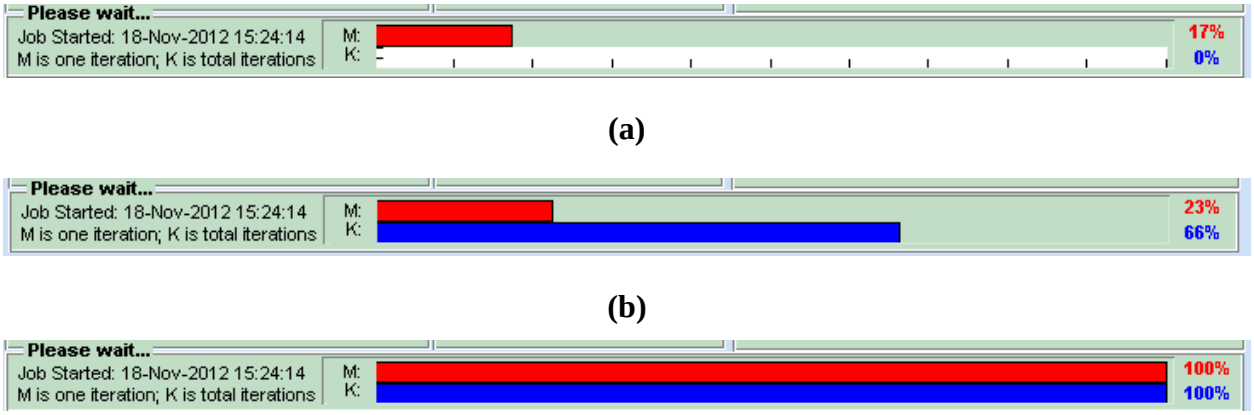

Figure A-14 the wait bar of modeling process

A.5. Model Output

Two figures are plotted as the model output, i.e. the cumulative damage index curve and predicted NBI ratings bound. As shown in Figure A-15, these two plots are updated when each iteration is done. It can be seen that two iterations is done in this example.

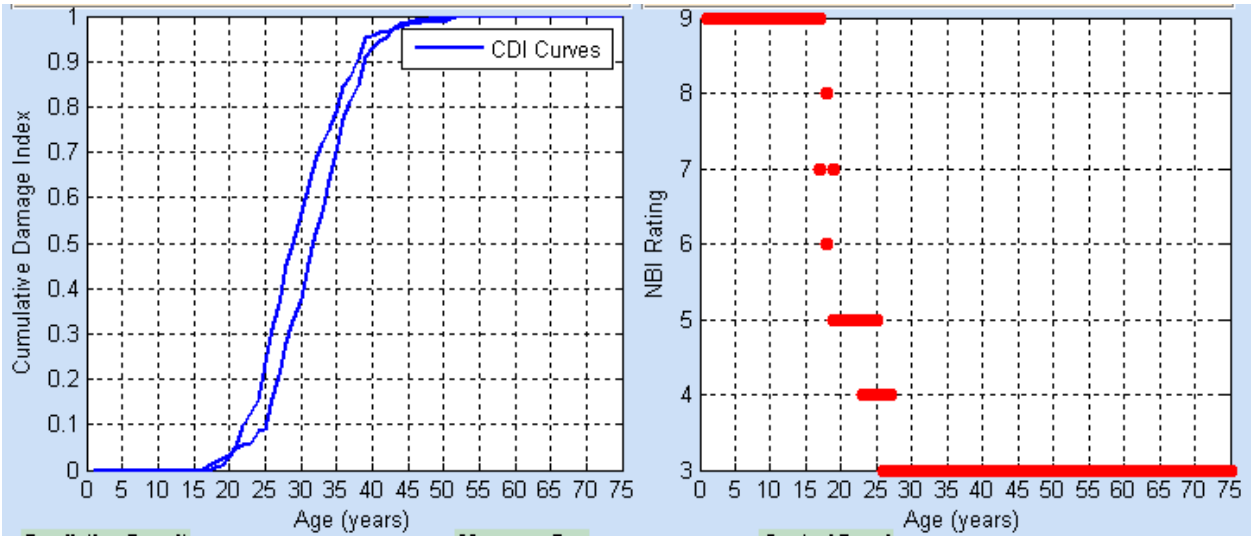

Figure A-15 Data window for a further instruction on model input

Once the whole simulation is completed, the NBI mean value curves will be calculated. Current rating and the time to poor (i.e. NBI rating reaches 4) will be found on this mean curve according to the given year of interest by user, as shown in Figure A-16 and Figure A-17. After simulation is done, the user can click 'Reset' button in the control panel to reset all the figures and data, as shown in Figure A-118. Every time the simulation is done, there is a text file that is saved in the same folder of the program, named 'NBI.txt', which contain the values of NBI mean curve ratings.

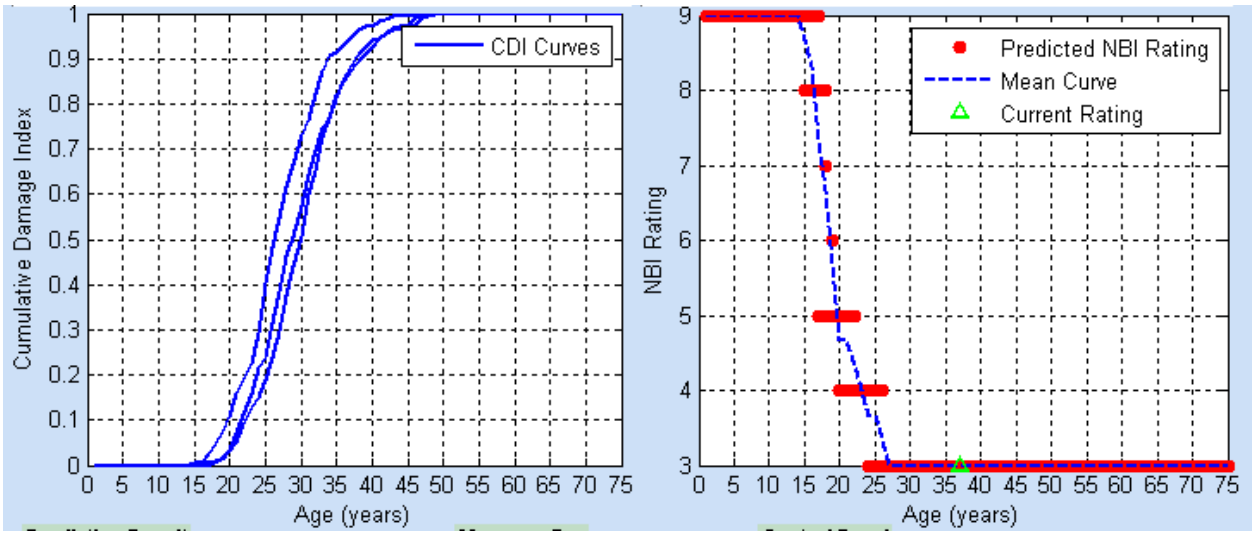

Figure A-16 Cumulative damage curve and NBI rating bound

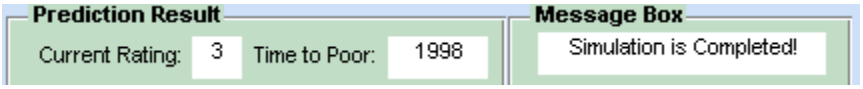

Figure A-17 Model output box and message box

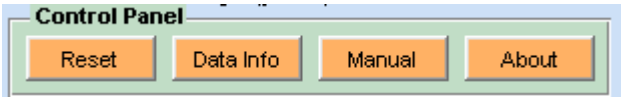

Figure A-18 Control panel output box and message box

Finally, the ‘About’ button may be clicked to find the information about the program , as shown in Figure A-19.

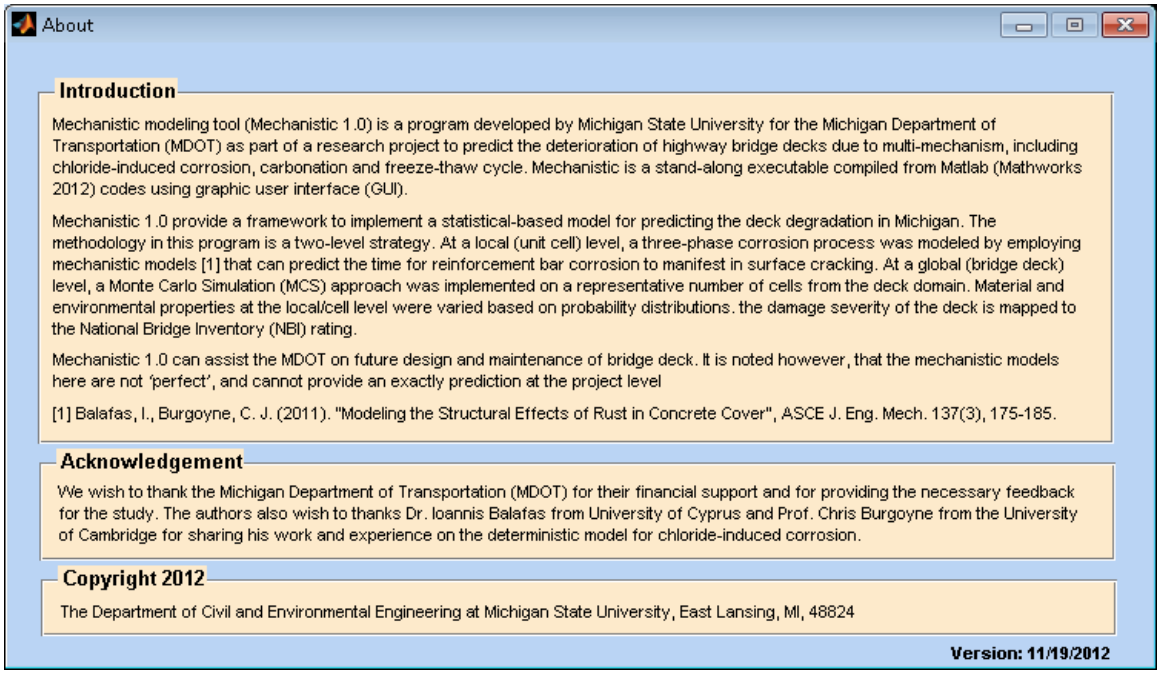

Figure A-19 ‘About’ pushbutton for interface information

REFERENCES

Amini, B. and Tehrani, S. (2011). ”Combined Effects of Saltwater and Water Flow on Deterioration of Concrete under Freeze–Thaw Cycles.” *Journal of Cold Regions Engineering*, 25(4), 145–161.

Balafas, I., Burgoyne, C. J. (2010). “Environmental effects on cover cracking due to corrosion.” *Cem. Concr. Res*., 40(9), 1429–1440.

Balafas, I., Burgoyne, C. J. (2011). "Modeling the Structural Effects of Rust in Concrete Cover", J. Eng. Mech. 137(3), 175-185.

Bazant, Z.P. (1979). "Physical model for steel corrosion in concrete sea structures-theory", ASCE J. Struct. Div., 105: 1137–1153

Basheer, P.A.M., Chidiact S.E., and Long A.E. (1996). “Predictive models for deterioration of concrete structures”, Construction and building materials, 10 (1), 27-37.

Basheer L., and Cleland D.J. (2006). “Freeze-thaw resistance of concretes treated with pore liners.” *Construction and Building Materials*, 20 (10), 990-998.

Bastidas-Arteaga, E., Bressolette, P., Chateauneuf, A., and Sánchez-Silva, M. (2009). "Probabilistic lifetime assessment of RC structures under coupled corrosion–fatigue deterioration processes." Structural Safety, 31(1), 84–96.

Bažant, Z. P., Chern, J. C., Rosenberg, A. M., Gaidis, J. M. (1988). “Mathematical model for freeze–thaw durability of concrete.” *J Am Ceram Soc*, 71 (9), 776–783.

Bertolini, L., Elsener, B., Pedeferri, P., and Polder, R. B. (2004).“Corrosion of Steel in Concrete, Prevention, Diagnosis, Repair”, John Wiley & Sons, 2004.

Boddy, A., Bentz, E., Thomas M. D. A., and Hooton, R.D. (1999). “An overview and sensitivity study of a multimechanistic chloride transport model”, Cement and concrete research 29, 827-837.

Chernin, L., Val, D.V., Volokh, K. (2010). "Analytical modeling of concrete cover cracking caused by corrosion of reinforcement", *Mater. and Structures*, 43(4): 543-556.

Chernin, L., Val, D.V., and Stewart, M.G. (2012). “Prediction of cover crack propagation in RC structures caused by corrosion.” *Magazine of Concrete Research*, 64(2): 95 –111.

Chi, J.M., Huang, R., and Yang, C.C. (2002). “Effects of carbonation on mechanical properties and durability of concrete using accelerated testing method.” *Journal of Marine Science and Technology*, 10(1), 14–20.

Cho, T. (2007). “Prediction of cyclic freeze-thaw damage in concrete structures based on response surface method.” *Construction and Building Materials*, 21 (12), 2031-2040.

Choo, C.C. and Harik, E. I. (2006). “Inspection and Evaluation of a Bridge Deck Reinforced with Carbon Fiber Reinforced Polymer (CFRP) Bars.” Kentucky Transportation Center, College of Engineering, University of Kentucky, 26 p.

Chung C. W., Shon C. S., and Kim Y. S. (2010). “Chloride ion diffusivity of fly ash and silica fume concretes exposed to freeze-thaw cycles.” *Construction and Building Materials*, 24(9), 1739-1745.

Enright, M. and Frangopol, D. (1998). ”Service-Life Prediction of Deteriorating Concrete Bridges.” J. Struct. Eng., 124(3), 309–317.

Ervin, B. L. (2007). “Monitoring corrosion of rebar embedded in mortar using guided ultrasonic waves,” Diss. University of Illinois at Urbana-Champaign, 2007. 3290229.

Estes, A. C. and Frangopol, D. M. (2003). “Updating Bridge Reliability Based on Bridge Management Systems Visual Inspection Results.” ASCE J. Bridge Eng. 8(1): 374-382.

Estes A. C., and Frangopol D. M. (2001). “Minimum expected cost-oriented optimal maintenance planning for deteriorating structures: Application to concrete bridge decks.” Reliability Engineering and System Safety, 73 (3): 281-291.

Fabbri, A., Coussy, O., Fen-Chong, T., and Monteiro, P. (2008). ”Are Deicing Salts Necessary to Promote Scaling in Concrete?.” *J. Eng. Mech.*, 134(7), 589–598.

Fagerlund, G. (1995). “Frost resistance of high performance concrete-some theoretical considerations.” PRO 1: International RILEM Workshop on Durability of High Performance Concrete, RILEM proceedings ed. by Sommer, H. 112-130.

Fanous, F. and Wu, H. (2005). “Performance of Coated Reinforcing Bars in Cracked Bridge Decks” *ASCE J. Bridge Eng.* 10(3), 255-261.

Firouzi, A. and Rahai, A. R. (2011). “Prediction of extent and likelihood of corrosion-induced cracking in reinforced concrete bridge deck.” International Journal of Civil Engineering, 9(3), 184-192.

Frangopol D.M., Kallen M.J., van Noortwijk J.M. (2004). "Probabilistic models for life-cycle performance of deteriorating structures: Review and future directions", Progress in Structural Engineering and Materials, 6 (4), pp. 197-212.

Frangopol D.M. and Akgul, F. (2005). "Lifetime Performance Analysis of Existing Reinforced Concrete Bridges. II: Application. " J. Infrastruct. Syst. 11(2): 129-141.

Frangopol D.M., Lin, K.Y. and Estes, A.C. (1997). "Life-Cycle Cost Design of Deteriorating Structures." ASCE J. Struct. Eng. 123(10): 1390-1401.

Fu, Y., Cai, L., and Yonggen, W. (2011). "Freeze-thaw cycle test and damage mechanics models of alkali-activated slag concrete." *Construction and Building Materials*, 25 (7), 3144-3148.

Ghafoori, N. and Mathis, R. (1995). "Prediction of freezing and thawing durability of concrete paving blocks." *ASCE Journal of Materials in Civil Engineering*, 10(1), 45-51.

Helene, P.R.L., and Castro-Borges, P. (2009). " A novel method to predict concrete carbonation." *Concreto y Cemento*: investigación y desarrollo, 1, 25-35.

Isgor, O.B., Razaqpur, A.G. (2004). "Finite element modelling of coupled heat transfer, moisture transport and carbonation processes in concrete structures." Cement and Concrete Composites, 26: 57-73.

Jacobsen S., and Sellevold E.J. (1996). "Self-healing of high strength concrete after deterioration by freeze/thaw." *Cement and Concrete Research*, 26 (1), 55-62.

Janssen, D. and Snyder, M. (1994). "Resistance of concrete to freezing and thawing." Report SHRP-C-391, Strategic Highway Research Program, National Research Council, Washington, D.C.

Jia, C, Ji, S. Z., and Zhang, F. (2010). "Study on the stability of concrete bay bridge pier under freeze-thaw action." *Journal of Sichuan University (Engineering)*, 42(3), 7-13. (In Chinese)

Kassir, M. K. and Ghosn, M. (2002). "Chloride-Induced Corrosion of Reinforced Concrete Bridge Decks", Cement and Concrete Research, 32 (1), 139-143.

Karakoça M. B., Demirboğab, R., Türkmen, I., and Can, I. (2011). "Modeling with ANN and effect of pumice aggregate and air entrainment on the freeze–thaw durability of HSC." *Construction and Building Materials*, 25(11), 4241–4249.

Kelly, B. and Murphy, P. (2010). “Prediction of Freeze-thaw Resistance of Concrete.” Project, presented to University College Dublin, in partial fulfillment of the requirements for the degree of Bachelor of Engineering.

Keller, W.J. (2004). “Effect of Environmental Conditions and Structural Design on Linear Cracking in Virginia Bridge Decks.” M.S Thesis, Virginia Polytechnic Institute and State University, 179 p.

Kirkpatrick, T.J., Weyers, R.E., Anderson-Cook, C.M., Sprinkel, M.M. (2002). “Probabilistic model for the chloride-induced corrosion service life of bridge decks”, Cement and Concrete Research, 32 (12), pp. 1943-1960.

Krauss, P. D., Lawler, J. S., and Steiner, K. A., (2009). "Guidelines for Selection of Bridge Deck Overlays, Sealers and Treatments," NCHRP Project 20-07, Task 234, Transportation Research Board, Washington DC, May 2009.

Lin, Ga., Liu, Y. H., Xiang, Z. H., (2010). “Numerical modeling for predicting service life of reinforced concrete structures exposed to chloride environments”, Cement and concrete composites 32, 571-579.

Lounis, Z. (2005). “Uncertainty Modeling of Chloride Contamination and Corrosion of Concrete Bridges.” Applied Research in Uncertainty Modeling and Analysis, International Series in Intelligent Technologies, 2005, Volume 20, 491-511

Lounis, Z. and Daigle, L. (2008), “Reliability-based decision support tool for life cycle design and management of highway bridge decks.” in Annual Conference of the Transportation Association of Canada, Toronto , 19 pp.

Li, C.Q., Melchers, R.E., and Zheng, J. (2006). “Analytical model for corrosion-induced crack width in reinforced concrete structures.” ACI Structural Journal, 103 (4): 479–487.

Li, C.Q., Yang, Y. and Melchers, R.E. (2008). “Prediction of reinforcement corrosion in concrete and its effects on concrete cracking and strength reduction”, *ACI materials journal* 105: 3-10.

Liu, T., and Weyers, R. W. (1998a). “Modeling the dynamic corrosion process in chloride contaminated concrete structures.” Cem. Concr. Res. , 28 (3), 365–379.

Liu, T, and Weyers, R.W. (1998b). “Modeling the time-to-corrosion cracking of the cover concrete in chloride contaminated reinforced concrete structures.” ACI Mater. J, 95: 675–81.

Liu, M. H., and Wang, Y. F. (2012). “Damage Constitutive Model of Fly Ash Concrete under Freeze-thaw Cycles.” *ASCE Journal of Materials in Civil Engineering*, in press.

Lu, Z.H., Zhao, Y.G., Yu, Z.W. and Ding, F.X. (2011). “Probabilistic evaluation of initiation time in RC bridge beams with load-induced cracks exposed to de-icing salts.” Cement and Concrete Research, 41(3): 365-372.

Macinnis, C. and Whiting, J. D. (1979). “The frost resistance of concrete subject to a deicing agent.” Cem. Concr. Res., 9(3), 325–336.

Malumbela, G., Alexander, M., Moyo, P. (2011). "Model for cover cracking of RC beams due to partial surface steel corrosion", *Construction and Building Materials*, 25(2): 987-991.

Mangat P. S., and Molloy B. T. (1994). “Prediction of long term chloride concentration in concrete”, Materials and structures, 27, 338-346.

Marchand J., and Samson E. (2009). “Predicting the service-life of concrete structures – limitations of simplified models”, Cement and concrete composites 31, 515-521.

Marques P.F., and Costa A. (2010). “Service life of RC structures: Carbonation induced corrosion. Prescriptive vs. performance-based methodologies.” Construction and Building Mater., 24 (3), 258-65.

Marsh, P. S. and Frangopol, D. M. (2008) "Reinforced Concrete Bridge Deck Reliability Model Incorporating Temporal and Spatial Variations of Probabilistic Corrosion Rate Sensor Data," Reliability Engineering & System Safety, 93(3), 394-409.

MathWorks. (2011). Matlab version 7.12 R2011a. The MathWorks Inc. www.mathworks.com.

Michigan Department of Transportation (MDOT). (2001). “Bridge Design Guides: 6.41.01, Standard Bridge Slabs (Load Factor Design).” Michigan, USA.

Michigan Department of Transportation (MDOT), (2009). “Michigan structure inventory and appraisal coding guide.” Michigan Department of Transportation, Lansing, MI.

Mu, R., Miao C., Luo X., and Sun W. (2002). “Interaction between loading, freeze-thaw cycles, and chloride salt attack of concrete with and without steel fiber reinforcement.” *Cement and Concrete Research*, 32 (7), 1061-1066.

Otieno, M., Beushausen, H., Alexander, M. (2011). "Prediction of corrosion rate in reinforced concrete structures – a critical review and preliminary results", *Materials and Corrosion*, 62: 1-13.

Pantazopoulou, S. J. and Papoulia, K. D. (2001). "Modeling Cover-Cracking due to Reinforcement Corrosion in RC Structures", *J. Eng. Mech.* 127(4): 342-351.

Papadakis, V.G, Fardis, M.N, Vayenas, C.G. (1992). "Effect of composition, environmental factors and cement-lime mortar coating on concrete carbonation." *Mater and Struct*, 25, 293–304.

Penttala V. (2006). "Surface and internal deterioration of concrete due to saline and non-saline freeze-thaw loads." *Cement and Concrete Research*, 36 (5), 921-928.

Poulsen, E., and Mejlbro, L. (2006). "Diffusion of Chloride in Concrete-Theory and Application; Volume 14 of Modern Concrete Technology." Taylor & Francis, 1-60.

Que, N. S. (2007). "History and development of predictions models of time-to-initiate-corrosion in reinforced concrete structures in marine environment." Philippine Engineering Journal 28(2): pp. 29-44.

Rahim, A., Jansen, D. and Abo-Shadi, N. (2006). "Concrete Bridge Deck Crack Sealing: An Overview of Research." Submitted to California Department of Transportation, 96 p.

Rønning, T. F. (2001). "Freeze thaw resistance of concrete-Effect of curing condition, moisture exchange and materials." Thesis, presented to Norwegian Institute of Technology, in partial fulfillment of the requirements for the degree of Doctor of Philosophy.

Russell, H. G. (2004). Concrete bridge deck performance, NCHRP Synthesis Report Volume 333, Transportation Research Board, Washington D.C.

Sabir, B.B. (1997). "Mechanical properties and frost resistance of silica fume concrete." *Cement and Concrete Composites*, 19(4), 285-294.

Saetta A.V., Vitaliani R.V. (2004). "Experimental investigation and numerical modeling of carbonation process in reinforced concrete structures Part I: Theoretical formulation." *Cement and Concrete Research*, 34 (4), 571-579.

Saetta A.V., Vitaliani R.V. (2005). "Experimental investigation and numerical modeling of carbonation process in reinforced concrete structures: Part II. Practical applications." *Cement and Concrete Research*, 35 (5), 958-967.

Shang H. S., Song Y. P., and Ou J. P. (2009). "Behavior of air-entrained concrete after freeze-thaw cycles." *Acta Mechanica Solida Sinica*, 22 (3), 261-266.

Shang H.S., and Song Y.P. (2008). “Behavior of air-entrained concrete under the compression with constant confined stress after freeze-thaw cycles.” *Cement and Concrete Composites*, 30 (9), 854-860.

Song, H. W., Kwon, S. J., Byun, K. J. and Park, C.K. (2006)."Predicting carbonation in early-aged cracked concrete." Cement and Concrete Research, 36 (5), 394-409.

Song, H.W., Shim H.B., Petcherdchoo A., Pack, S.W. (2009). “Service life prediction of repaired concrete structures under chloride environment using finite difference method”, Cement and concrete composites 31, 120-127.

Song, H.W., Pack, S.W., Ann, K.Y. (2009). “Probabilistic assessment to predict the time to corrosion of steel in reinforced concrete tunnel box exposed to sea water.” Construction and Building Materials, 23(10):3270-3278.

Stewart, M.G., Estes, A.C. and Frangopol, D.M. (2004), “Bridge Deck Replacement for Minimum Expected Cost under Multiple Reliability Constraints,” Journal of Structural Engineering, ASCE, 130(9):1414-1419.

Stewart, M.G. and Rosowsky, D.V. (1998). “Time-Dependent Reliability of Deteriorating Reinforced Concrete Bridge Decks.” Structural Safety, 20(1):91-109.

Stewart, M.G. (2001), “Reliability-based assessment of ageing bridges using risk ranking and life cycle cost decision analyses.” Reliability Engineering and System Safety, 74(3):263-273.

Stewart, M.G. and Mullard, J.A. (2007), Spatial Time-Dependent Reliability Analysis of Corrosion Damage and the Timing of First Repair for RC Structures.” Engineering Structures, 29(7):1457-1464.

Stewart M.G., Wang X., Nguyen M.N. (2011). “Climate change impact and risks of concrete infrastructure deterioration.” *Engineering Structures*, 33 (4), pp. 1326-1337.

Suwito, C. and Xi, Y., (2008). “The effect of chloride-induced steel corrosion on service life of reinforced concrete structures”, *Structure and infrastructure engineering*, 4 (3), 177-192.

Sun W., Mu R., Luo X., and Miao C. (2002). “Effect of chloride salt, freeze-thaw cycling and externally applied load on the performance of the concrete.” *Cement and Concrete Research*, 32 (12), 1859-1864.

Talukdar, S., Banthia, N., and Grace, J.R. (2012). “Carbonation in concrete infrastructure in the context of global climate change: Part 1, experimental results and model development.” *Cem Concr Compos*, 34 (8), 924–930.

Tanesi, J. and Meininger, R. (2006). “Freeze-Thaw Resistance of Concrete With Marginal Air Content.” Publication No. FHWA-HRT-06-117, MeLean, VA.

Transportation Research Board (TRB). (2006). “Control of Cracking in Concrete: State of the Art.” TRB’s Transportation Research Circular E-C107: 56 p.

Vu, K., and Stewart, M.G. (2000). "Structural reliability of concrete bridges including improved chloride-induced corrosion models", Struct Saf, 22(4), 313–333.

Wang, H. L. and Song, Y. P. (2010). “Reliability models and service life estimation of concrete structure under freeze-thaw action.” Proceedings of the Twentieth International Offshore and Polar Engineering Conference, Beijing, China, 51-54.

Watson, J. (2001). How to Determine a Sample Size: Tipsheet #60, University Park, PA: Penn State Cooperative Extension.

Winn, E.K. (2011). “Artificial neural network models for the prediction of bridge deck condition ratings.” M.S Thesis, Civil and Environmental Engineering, Michigan State University, 195 p.

Winn, E.K. and Burgueño, R. (2012). “Development and Validation of Deterioration Models for Concrete Bridge Decks – Phase 1: Artificial Intelligence Models and Bridge Management System,” Research Report CEE-RR – 2012/2 – Department of Civil and Environmental Engineering, Michigan State University, East Lansing, Michigan, 152 p.

Yoon, I.S., Copuroglu, O., and Park, K.B. (2007). “Effect of global climate change on carbonation progress of concrete.” *Atmos. Environ*., 41(34). 7274–7285.

Zhou, K. (2005). “Models for predicting corrosion-induced cracking, spalling, delamination of rehabilitated RC bridge decks” Diss. University of Ottawa. MR11480.

Zemajtis, J. (1998). “Modeling the Time to Corrosion Initiation for Concretes with Mineral Admixtures and/or Corrosion Inhibitors in Chloride-Laden Environments.” Ph.D. Dissertation, Virginia State University, Blacksburg, Virginia, 140 p.

Zaharieva R., Buyle-Bodin F., and Wirquin E. (2004). “Frost resistance of recycled aggregate concrete.” *Cement and Concrete Research*, 34 (10), 1927-1932.

Zhao, Y.X, Yu, J, Hu, B.Y., Jin, W. L. (2012). "Crack shape and rust distribution in corrosion-induced cracking concrete", *Corrosion Science*, 55: 385-393.

Zhong, J., Gardoni, P., Rosowsky, D. (2010). "Stiffness degradation and time to cracking of cover concrete in reinforced concrete structures subject to corrosion", *J Eng Mech, ASCE*, 136(2): 209–219.